STUDIES ON MODERATELY THICK COMPOSITE SECTOR PLATES

A thesis submitted by

Ashish Sharma

in fulfillment of the requirement for the degree of

Doctor of Philosophy

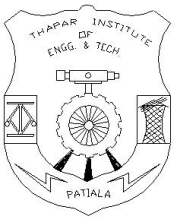

MECHANICAL ENGINEERING DEPARTMENT
THAPAR INSTITUTE OF ENGINEERING AND TECHNOLOGY
(Deemed University)
PATIALA
INDIA, PIN-147004
OCTOBER 2005

CERTIFICATE

This is to certify that the thesis entitled " **Studies on moderately thick composite sector plates** " being submitted by **Mr. Ashish Sharma** for the award of the Doctor of Philosophy, to the **Thapar Institute of Engineering and Technology (Deemed University), Patiala**, is a record of bonafide research work carried out by him. The thesis in our opinion has reached the requisite standard fulfilling the requirement of Doctor of Philosophy Degree.

The research report and the results presented in this thesis have not been submitted in parts or in full to any other University or Institute for the award of any Degree or Diploma.

(H.B. Sharda)
Principal,
Shaheed Bhagat Singh College
of Engineering and Technology,
Ferozepur 152001, India

(Y. Nath)
Professor,
Applied Mechanics Department,
Indian Institute of Technology,
New Delhi 110016, India

ACKNOWLEDGEMENT

I take this opportunity to express my deep sense of gratitude to my supervisors Dr. H.B. Sharda, Principal, Shaheed Bhagat Singh College of Engineering and Technology, Ferozepur, and, Dr. Y. Nath, Professor, Applied Mechanics Department, I.I.T. Delhi for their most invaluable guidance, encouragement and thoughtful discussions during the course of my work. My association with Dr. Sharda and Dr. Nath has been most fruitful both in terms of technical understanding as well as the understanding of the efforts made by the researching community.

I express my gratitude to Dr. H.N. Chandrawat, Dr. R.G. Tathgir, Dr. N.K. Nayar and Dr. S.K. Mohapatra, successive Heads of the Mechanical Engineering Department at TIET, Patiala for their continuous support and encouragement during this research work. I am also thankful to Dr. S.C. Saxena, Director, TIET, Patiala, for taking keen interest in the research work of the faculty members.

I pay my respect to the Russian mathematician Pafnuty Lvovich Chebyshev for giving Chebyshev Polynomials to this world and to Dr. Y. Nath for introducing me to Chebyshev Polynomials. This research work would not have been possible without the easy availability of computational power provided by the Linux operating system. I am indebted to Mr. Sanjeev Guleria, System Analyst at TIET, Patiala, for introducing me to Linux. I further pay my gratitude to the Linux community for providing the free operating system along with the compiler 'gcc,' the plot program 'gnuplot,' the graphics package 'xfig,' the text processing system Latex and several

other tools without which this research work would not have been possible.

I thank my wife Madhu and my son Anagh for allowing me long working hours during the course of writing this thesis.

Ashish Sharma

ABSTRACT

Rapid advancements made in materials science and manufacturing technologies has lead to the application of composite materials in various areas of engineering applications like aerospace industries, marine structures, automobiles, power plant systems etc. The composite materials are often subjected to severe operating conditions with respect to kinds of loadings, temperature variations, vibration, shocks etc. The structural configurations could be in various shapes, the most common being in the form of plates and shells. The plates can be of rectangular, circular, sectoral or of any other shape. There are different kinds of important and complicated phenomena like bending, buckling, vibration etc. associated with these structural elements. Therefore, it is necessary to study adequately these aspects for accurate design estimates.

The models studied could be linear for small deformation analysis in linearly elastic range. For large deformation analysis or for non-linear constitutive relationships, the model is non-linear. The stringent operating conditions often lead to deformations comparable to plate thickness. This necessitates the application of geometrically non-linear formulations. The computational effort is reduced by reducing the general three dimensional problem to planar problem with the use of different kinds of plate theories. The formulation analyzed in this thesis applies the FSDT and takes in to account von-Kármán type of non-linearities.

The differential equations governing the behavior of sector plates are more complicated as compared to other geometrical configurations. The present thesis attempts

to study the behavior of laminated plates in sectoral domain using fast converging Chebyshev polynomials.

The linear eigenvalue problems of buckling and free vibration of isotropic and laminated composite plates are studied. The non-linear algebraic equations generated from the static large deformation analysis are solved using an incremental iterative scheme based on Newton-Raphson technique. For the study of transient large deformation response, the temporal discretization is done with the help of Houbolt implicit time marching method and the non-linearity is handled with the help of quadratic extrapolation along with fixed point iteration. Spatial and temporal convergence studies have been carried out. Results are validated for sector plates and square plates. The variations of response with a wide range of boundary conditions are studied. The effects of various geometrical parameters like sector angle, thickness ratio and annularity (ratio of inside to outside radii), and of material parameters like orthotropy and lamination schemes have been studied. Piezolaminated sector plates subjected to piezothermomechanical loadings are also studied.

Keywords: *Mindlin sector plate, Chebyshev polynomials, Buckling, Free Vibration, Cylindrical orthotropy, Laminated Composite plates, von-Kármán type non-linearity, large deformation, Non-linear transient response, piezothermomechanical response.*

Following papers have been prepared from the present thesis:

1. Y. Nath, H.B. Sharda and Ashish Sharma, "Stability and Vibration of Mindlin Sector Plates: An analytical approach," *AIAA Journal*, Vol. 43 no. 5, 2005, pp. 1–1452.

2. Ashish Sharma, H.B. Sharda and Y. Nath, "Stability and vibration of thick laminated composite sector plates," *Journal of Sound and Vibration*, Vol. 287, nos. 1–2, 2005, pp. 1–23.

3. Y. Nath, H.B. Sharda and Ashish Sharma, "Non-linear analysis of moderately thick sector plates," *Communications in Non-linear Science and Numerical Simulation*, Vol. 10, no. 7 , 2005, pp. 765–778.

4. Ashish Sharma, Y. Nath and H.B. Sharda, "Large deflection of moderately thick laminated composite sector plates," *LAJSS (Communicated).*

5. Ashish Sharma, Y. Nath and H.B. Sharda, "Non-linear transient analysis of moderately thick laminated composite sector plates," *Communications in Non-linear Science and Numerical Simulation (Revision requested).*

6. Ashish Sharma, Y. Nath and H.B. Sharda, "Non-linear piezothermoelastic static response of moderately thick laminated composite sector plates," *AIAA Journal (Communicated).*

7. S. Singh, B.P. Patel, A. Sharma, K.K. Shukla and Y. Nath, "Non-linear dynamics and stability of laminated composite plates and shells," *The Seventh International Conference on Vibration Problems (ICOVP-2005)*, ISIK University, Istanbul, Turkey, 05-09 September, 2005. url: http://icovp.isikun.edu.tr

Contents

List of Figures

List of Tables

NOMENCLATURE

A_{ij}, B_{ij}, D_{ij}	Extensional stiffnesses, bending-extension coupling stiffnesses and bending stiffnesses of the laminated plate, $(i, j = 1, 2, 6)$
A_{ij}	Transverse shear stiffnesses of the laminated plate, $(i, j = 4, 5)$
C	Symbol for denoting clamped edge condition
C	Symbol for denoting a layer with circumferential orientation of fiber
$d_{31}^{(k)}$, $d_{32}^{(k)}$	Piezoelectric constants
$E_r^{(k)}$, $E_\theta^{(k)}$	Elastic moduli in respective directions for the kth layer
E_0	Reference elastic moduli for non-dimensionalization, $E_0 = E_\theta$ for an orthotropic layer with fiber orientation in radial direction
$E_z^{(k)}$	Potential gradient across the kth layer
F	Symbol for denoting free edge condition
$G_{r\theta}^{(k)}$, $G_{\theta z}^{(k)}$, $G_{zr}^{(k)}$	Moduli of rigidity in respective planes for the kth layer
I_0	Normal inertia
I_1	Coupled normal-rotary inertia
I_2	Rotary inertia
k^2	Shear correction factor, (5/6)
M, N	Highest degrees in r and θ dimensions in the Chebyshev series expansions
M_r, M_θ, $M_{r\theta}$	Moment resultants

M'_r, M'_θ, $M'_{r\theta}$	Non-dimensional moment resultants, $M'_r = \frac{M_r(1-\mu)^2 r_0^2}{E_0 h^4}$, etc.
n	Number of layers
N_r, N_θ, $N_{r\theta}$	In-plane force resultants
N'_r, N'_θ, $N'_{r\theta}$	Non-dimensional in-plane force resultants, $N'_r = \frac{N_r(1-\mu)^2 r_0^2}{E_0 h^3}$, etc.
q	Uniform transverse load
q'	Non-dimensional uniform transverse load used for isotropic plates, $\frac{q r_0^4}{E h^4}$
Q	Non-dimensional uniform transverse load used for laminated plates, $\frac{q(1-\mu)^4 r_0^4}{E_0 h^4}$
$Q_{ij}^{(k)}$	Plane stress reduced stiffnesses for the kth layer, $(i, j = 1, 2, 6)$
$Q_{ij}^{(k)}$	Transverse shear reduced stiffnesses for the kth layer, $(i, j = 4, 5)$
Q_r, Q_θ	Transverse shear stress resultants
R	Symbol for denoting a layer with radial orientation of fiber
r_i, r_o, h	Internal and external radii and total thickness of the laminated sector plate
r^*	Radial coordinate
r	Non-dimensional radial coordinate, $\frac{r^* - r_i}{r_o - r_i}$
S	Symbol for denoting simply supported edge condition
T_0, T_n	Temperature increase at the top and bottom surfaces
t	Time
u^*, v^*, w^*	Linear displacement components in r, θ, z directions
u, v, w	Linear displacement components of a point on the plane $z = 0$ in r, θ, z directions

u', v', w'	Non-dimensional linear displacement components of a point on the plane $z = 0$ in r, θ, z directions, $u' = u/h$, $v = v/h$, $w, = w/h$
u_{ij}, v_{ij}, w_{ij}	Coefficients in Chebyshev series expansions of linear displacement components u, v, w
z	Coordinate in transverse direction

Greek Letters

$\alpha_r^{(k)}$, $\alpha_\theta^{(k)}$	Thermal expansion coefficients in respective directions for the kth layer
ϵ_r, ϵ_θ, ϵ_z	Linear strain components in respective directions
$\epsilon_r^{(0)}$, $\epsilon_\theta^{(0)}$	Linear strain components in respective directions at $z = 0$ plane
$\gamma_{\theta z}$, γ_{rz}, $\gamma_{r\theta}$	Shear strains between respective directions
$\gamma_{r\theta}^{(0)}$	Shear strains between r and θ directions at $z = 0$ plane
κ	Thermal conductivity of a layer in thickness direction
$\kappa_r^{(0)}$, $\kappa_\theta^{(0)}$, $\kappa_{r\theta}^{(0)}$	Curvatures of the $z = 0$ plane
λ	Thickness ratio (h/r_o)
μ	Annularity (r_i/r_o)
$\nu_{r\theta}^{(k)}$	Poisson's ratio in $r\theta$ plane for the kth layer
ϕ_r, ϕ_θ	Angular displacements in rz and θz planes
$\phi_{r,ij}$, $\phi_{\theta,ij}$	Coefficients in Chebyshev series expansions of angular displacement components ϕ_r and ϕ_θ
θ^*	Angular coordinate

θ Non-dimensional angular coordinate (θ^*/Θ)

Θ Total included sector angle

τ Non-dimensional time $\tau = t\sqrt{\dfrac{4A_{22}}{I_0(1-\mu)^2 r_o^2}}$

Subscripts

dof Degree of freedom; u, v, w, ϕ_r and ϕ_θ

ij Indices in the coefficients of Chebyshev series expansions

$,r$ First derivative with respect to r

$,rr$ Second derivative with respect to r

$,r\theta$ Mixed derivative with respect to r and θ

$,tt$ Second derivative with respect to t

$,\theta$ First derivative with respect to θ

$,\theta\theta$ Second derivative with respect to θ

Superscripts

(0) $z = 0$ plane

(k) kth layer in a laminated plate

$'$ Non-dimensionalized quantity

INTRODUCTION

The advancements made in material science and manufacturing capabilities has lead to rapid increase in the application of composite materials in modern engineering industries. Composite materials, in the form of single or multiple layer laminated plates, are increasingly being used in various structural and machine elements needed in modern engineering systems like aircrafts, space vehicles, satellites, ships, submarines, turbines, bridges, automobiles etc. The study of the behavior of laminated composite plates in terms of bending, vibration and buckling is necessary to meet the design challenges.

The subject of elastic plates is very vast and enormous amount of literature exists dealing various aspects like shape (rectangular, polygonal, circular or sector), material (isotropic, anisotropic), thickness (thin, thick plates), deflections (small, large), loadings (static or dynamic, mechanical, thermal, hydrostatic etc.), boundary conditions (Clamped, Simply supported or Free) etc.

Analytical methods based on Fourier expansion and domain discretization methods like Finite Difference method, Finite Element Method, Boundary Element Method, and Differential Quadrature Method are most commonly used for the analysis. The analytical methods are limited to a specific set of boundary conditions and domain geometry in comparison to the domain discretization based methods. Analytical solutions are mostly for one-dimensional problems of beams and axisymmetric circular plates and shells, and for the two-dimensional problems in rectangular domain. Both

linear as well as non-linear formulations have been employed. The studies are aimed at analyzing the static deflection, vibration and buckling of laminated composite plates.

The Classical Laminated Plate Theory (CLPT) which ignores transverse shear deformation is limited to thin plates. It breaks down when the ratio of in-plane modulus to transverse shear modulus is high and for determining the higher modes of vibration. The design estimates of modern structural elements demand the usage of theories which allow transverse shear deformation of plates. First order Shear Deformation Theory (FSDT) and Third order Shear Deformation Theory (ASST) are most commonly employed.

With operational conditions becoming more severe, the plates as structural elements are often subjected to large deformations comparable to their thickness that leads to the interaction between bending and stretching, and makes the governing equations non-linear which are not amenable to exact solution. It is obvious from the literature that very little attention has been devoted to the study of laminated composite sector plate configuration. A few studies pertaining to linear and non-linear static analysis of isotropic and symmetrically laminated (with rectilinear orthotropic layers) sector plates are available.

The laminated sector plates consisting of multiple layers of fiber reinforced materials are extensively employed and their applications will continue to grow as load bearing structural and machine elements in modern sophisticated engineering systems. Therefore, a need was felt to have a simple, efficient, and robust methodology for accurate estimation and understanding of response and stability characteristics of

sector plates. Present work is an effort in this direction.

Considering the first order shear deformation theory and von-Kármán type geometric non-linearity, equations of motion are derived using Hamilton's principle and solved analytically along with appropriate boundary conditions using two-dimensional Chebyshev polynomials. The influence of material features like orthotropy and lamination scheme, and, geometrical features like boundary conditions, annularity and the total included sector angle on large deflection static and dynamic response of moderately thick sector plates subjected to uniformly distributed load is investigated. Eigenvalue analyses for free vibration and stability of composite sector plates are carried out.

The ever-growing application of surface bonded and embedded piezoelectric layers in composite laminated structures has drawn the attention of many researchers for active vibration control, damage identification, mechatronic devices etc. The methodology developed in this thesis is further consolidated by analyzing the large deflection response of laminated composite sector plates to piezothermomechanical loads.

In Chapter 1, the governing equations of layered moderately thick sector plates undergoing moderately large deflection are developed based on First order shear deformation theory and von-Kármán type non-linearity.

The solution methodology employing fast converging Chebyshev polynomials is discussed in Chapter 2. The procedure to eliminate the redundancy arising out of the application of individual edge conditions is discussed and the details are presented.

Convergence studies and validation of the results have been carried out for all the

cases dealt with in the thesis and the details are given in respective chapters.

In Chapter 3, the eigenvalue problems of free-vibration and buckling analyses of isotropic Mindlin sector plates are analyzed. Effects of boundary conditions, plate thickness, and annularity on natural frequencies and critical buckling loads are investigated.

The free vibration and buckling analysis of laminated composite sector plates is carried out in Chapter 4. Effects of geometrical parameters, lamination schemes and orthotropy are studied.

Chapter 5 presents the results pertaining to the large deflection static analysis of isotropic moderately thick sector plates. The results have been compared with those given in the literature. The effects of annularity, thickness ratio, sector angle and boundary conditions on static deflection and moment resultants are investigated.

The large deformation static analysis of laminated composite sector plates is carried out in Chapter 6. Effects of geometrical parameters, lamination schemes and elastic constants are studied.

Chapter 7 deals with the dynamic response of moderately thick laminated composite sector plates undergoing moderately large deflection. Uniformly distributed step and sinusoidal loadings are considered. Influence of boundary conditions, moduli ratio, lamination scheme, sector angle and annularity on the deflection response are analyzed.

The non-linear static response of shear-deformable laminated sector plates having cylindrically orthotropic and piezoelectric layers is analyzed in Chapter 8. Temperature distribution across the thickness obtained by solving the heat conduction

equation for a prescribed uniform surface temperatures is employed for the piezothermomechanical analysis.

Finally, in Chapter 9 the conclusions derived from the thesis are summarized. The scope of future work in the context of mechanics of composite sector plates is discussed.

CHAPTER 1
MATHEMATICAL FORMULATION

1.1 Introduction

This thesis analyzes some of the problems of static and dynamic large deflection response of moderately thick laminated sector plates subjected to uniformly distributed transverse loading. As an extension of the developed methodology, piezothermomechanical response of piezolaminated plates are also analyzed. This chapter is aimed at developing the governing differential equations of equilibrium (static as well as dynamic) and corresponding domain boundary conditions.

The studies on elastic behavior of plates started with the Kirchhoff's plate theory (Timoshenko and Woinowsky-Krieger, 1970). This theory, also known as thin plate theory or CLPT, ignores the transverse shear deformation. This implies that a straight line normal to the plates mid-plane remains straight, normal to the mid-plane and undeformed. This theory is restricted to thin isotropic plates having the typical in-plane dimension to thickness ratio larger than 25. The CLPT is also inadequate for higher modes of vibration and for higher Young's modulus to Shear modulus ratio. Recent researches are now more directed towards the analysis of non-homogeneous plates (Reddy, 1997; Vinson, 1999, 2001; Oh et al., 2003; Qatu, 2002; Wang et al., 2004).

In order to to overcome this limitation of the thin plate theory, several compu-

tational models allowing transverse shear deformation have been proposed. Noor and Burton (1989) presented an assessment of different shear deformation theories for multi-layered composite plates. A few other published works have also reviewed and compared various plate theories (Kapania and Raciti, 1989; Reddy and Robbins Jr. , 1994; Noor et al., 1996; Varadan and Bhaskar, 1997). These theories permit the transverse shear deformation by assuming the displacement field in thickness direction to be some polynomial function of the thickness coordinate (z). The First order Shear Deformation Theory (FSDT) assumes a linear variation in the thickens direction. It is thus the simplest approximation and has been found to be a good compromise between computational accuracy and efficiency.

In this chapter, considering the FSDT due to Reissner (1945) and Mindlin (1951), the differential equations governing the large deformation behavior of moderately thick laminated sector plates made up of cylindrically orthotropic and piezoelectric layers are developed employing the Hamilton's principle. The external loads are in the form of uniformly distributed lateral pressure, specified surface temperatures and uniform electric potential gradient applied across the piezoelectric layers.

1.2 Strain Displacement Relations

Figure 1.1 shows the geometry of the sector plate. Each lamina is considered to be cylindrically orthotropic with the fiber orientation being either in the radial or circumferential direction. The layers are assumed to be perfectly bonded. Considering the first order shear deformation theory, the displacement fields are expressed as

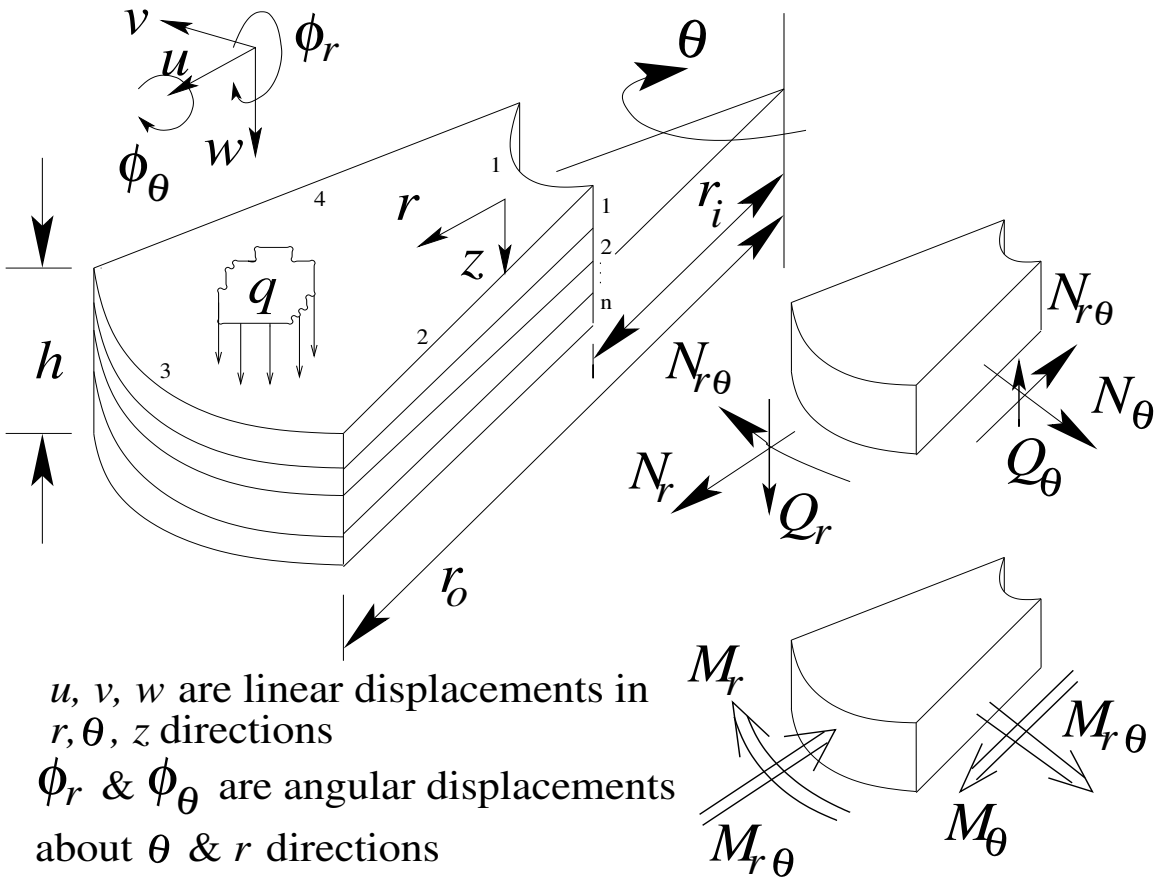

Fig. 1.1 Geometry of the problem.

follows.

$$u^*(r,\theta,z,t) = u(r,\theta,t) + z\phi_r(r,\theta,t) \tag{1.1a}$$

$$v^*(r,\theta,z,t) = v(r,\theta,t) + z\phi_\theta(r,\theta,t) \tag{1.1b}$$

$$w^*(r,\theta,z,t) = w(r,\theta,t) \tag{1.1c}$$

The following quantities are introduced,

$$r = r^*/(r_o - r_i) \tag{1.2a}$$

$$\theta = \theta^*/\Theta \tag{1.2b}$$

$$\mu = r_i/r_o \tag{1.2c}$$

$$\zeta = \{r(1-\mu) + \mu\} \tag{1.2d}$$

$$\zeta' = \zeta_{,r} \tag{1.2e}$$

With the displacement field considered here, $\epsilon_{zz} = \frac{\partial w}{\partial z} = 0$. Including von-Kármán type non-linearity, other strain displacement relations can be expressed as follows.

In-plane strains at the mid-plane are:

$$\epsilon_r^{(0)} = \frac{1}{r_0}\frac{u_{,r}}{\zeta'} + 0.5\left(\frac{1}{r_0}\frac{w_{,r}}{\zeta'}\right)^2 \tag{1.3a}$$

$$\epsilon_\theta^{(0)} = \frac{1}{r_0\zeta}\left(u + \frac{v_{,\theta}}{\Theta}\right) + \frac{0.5}{r_0^2\zeta^2}\left(\frac{w_{,\theta}}{\Theta}\right)^2 \tag{1.3b}$$

$$\gamma_{r\theta}^{(0)} = \frac{1}{r_0\zeta}\frac{u_{,\theta}}{\Theta} + \frac{1}{r_0}\frac{v_{,r}}{\zeta'} - \frac{v}{r_0\zeta} + \frac{1}{r_0\zeta}\frac{1}{r_0}\left(\frac{w_{,r}}{\zeta'}\frac{w_{,\theta}}{\Theta}\right) \tag{1.3c}$$

The curvatures of mid-plane are:

$$\kappa_r^{(0)} = \frac{1}{r_0}\frac{\phi_{r,r}}{\zeta'} \tag{1.4a}$$

$$\kappa_\theta^{(0)} = \frac{1}{r_0\zeta}\left(\phi_r + \frac{\phi_{\theta,\theta}}{\Theta}\right) \tag{1.4b}$$

$$\kappa_{r\theta}^{(0)} = \frac{1}{r_0\zeta}\frac{\phi_{r,\theta}}{\Theta} + \frac{1}{r_0}\frac{\phi_{\theta,r}}{\zeta'} - \frac{\phi_\theta}{r_0\zeta} \tag{1.4c}$$

The shear strains in rz and θz planes are:

$$\gamma_{rz} = \phi_r + \frac{1}{r_0}\frac{w_{,r}}{\zeta'} \tag{1.5a}$$

$$\gamma_{\theta z} = \phi_\theta + \frac{1}{r_0\zeta}\frac{w_{,\theta}}{\Theta} \tag{1.5b}$$

The strain components at any point can thus be expressed as,

$$\begin{Bmatrix} \epsilon_r \\ \epsilon_\theta \\ \gamma_{\theta z} \\ \gamma_{rz} \\ \gamma_{r\theta} \end{Bmatrix} = \begin{Bmatrix} \epsilon_r^{(0)} \\ \epsilon_\theta^{(0)} \\ \gamma_{\theta z} \\ \gamma_{rz} \\ \gamma_{r\theta}^{(0)} \end{Bmatrix} + z \begin{Bmatrix} \kappa_r^{(0)} \\ \kappa_\theta^{(0)} \\ 0 \\ 0 \\ \kappa_{r\theta}^{(0)} \end{Bmatrix} \tag{1.6}$$

1.3 Constitutive Equations

In this study, fiber orientation in a composite laminate (polar orthotropic) is either radial (R) or circumferential (C) so that the material axes coincide with the geometrical axes. The piezoelectric lamina is subjected to an electric field in z-direction only and exhibits symmetry of an orthorhombic crystal of class mm2 with poling in direction z, perpendicular to the plate (Kapuria et al., 1997). The stress-strain relations are thus obtained as follows for an orthotropic piezoelectric lamina (Reddy (1997), pp. 122-123).

$$\begin{Bmatrix} \sigma_{rr} \\ \sigma_{\theta\theta} \\ \sigma_{r\theta} \end{Bmatrix} = \begin{bmatrix} Q_{11} & Q_{12} & 0 \\ Q_{12} & Q_{22} & 0 \\ 0 & 0 & Q_{66} \end{bmatrix} \begin{Bmatrix} \epsilon_{rr} - \alpha_1\Delta T \\ \epsilon_{\theta\theta} - \alpha_2\Delta T \\ \gamma_{r\theta} \end{Bmatrix} - E_z \begin{Bmatrix} e_{31} \\ e_{32} \\ 0 \end{Bmatrix} \tag{1.7}$$

$$\begin{Bmatrix} \sigma_{\theta z} \\ \sigma_{rz} \end{Bmatrix} = \begin{bmatrix} Q_{44} & Q_{45} \\ Q_{45} & Q_{55} \end{bmatrix} \begin{Bmatrix} \gamma_{\theta z} \\ \gamma_{rz} \end{Bmatrix} \tag{1.8}$$

The stiffness constants Q_{ij} for a lamina are,

$$\begin{aligned} Q_{11} &= \frac{E_r}{[1-\nu_{r\theta}{}^2(E_\theta/E_r)]},\ Q_{22} = \frac{E_\theta}{[1-\nu_{r\theta}{}^2(E_\theta/E_r)]}, \\ Q_{12} &= \frac{\nu_{r\theta}E_\theta}{[1-\nu_{r\theta}{}^2(E_\theta/E_r)]},\ Q_{66} = G_{r\theta},\ Q_{44} = G_{\theta z},\ Q_{55} = G_{rz},\ Q_{45} = 0 \end{aligned} \tag{1.9}$$

1.4 Equations of Motion

The necessary equations of motion can be derived using the Hamilton's principle (Reddy (1997), pp. 158-163),

$$0 = \int_{t_1}^{t_2} (\delta U + \delta V - \delta K) dt \tag{1.10}$$

in which δU is the virtual strain energy, δK is the virtual kinetic energy and δV is the virtual work done by the applied forces. These energies can be evaluated as,

$$\delta U = \int_A \left[\int_{-h/2}^{h/2} (\sigma_{rr}\delta\epsilon_{rr} + \sigma_{\theta\theta}\delta\epsilon_{\theta\theta} + \sigma_{\theta z}\delta\gamma_{\theta z} + \sigma_{rz}\delta\gamma_{rz} + \sigma_{r\theta}\delta\gamma_{r\theta}) dz \right] dA \tag{1.11}$$

$$\delta V = -\int_A (q\delta w) dA \tag{1.12}$$

$$\delta K = \int_A \left[\int_{-h/2}^{h/2} \rho(\dot{u}\delta\dot{u} + \dot{v}\delta\dot{v} + \dot{v}\delta\dot{v}) dz \right] dA \tag{1.13}$$

Equations of motion in terms of stress resultants and non-dimensional coordinates can thus be derived as (Salehi and Shahidi, 1994),

$$\frac{1}{r_0}\frac{N_{r,r}}{\zeta'} + \frac{1}{r_0\zeta}\left(\frac{N_{r\theta,\theta}}{\Theta} + N_r - N_\theta\right) = I_0 u_{,tt} + I_1 \phi_{r,tt} \tag{1.14}$$

$$\frac{1}{r_0}\frac{N_{r\theta,r}}{\zeta'} + \frac{1}{r_0\zeta}\left(\frac{N_{\theta,\theta}}{\Theta} + 2N_{r\theta}\right) = I_0 v_{,tt} + I_1 \phi_{\theta,tt} \tag{1.15}$$

$$\frac{1}{r_0}\frac{Q_{r,r}}{\zeta'}+\frac{1}{r_0\zeta}\left(\frac{Q_{r,\theta}}{\Theta}+Q_r\right)+\frac{\mathcal{N}(w)}{r_0\zeta}+q(t)=I_0w_{,tt} \tag{1.16}$$

$$\frac{1}{r_0}\frac{M_{r,r}}{\zeta'}+\frac{1}{r_0\zeta}\left(\frac{M_{r\theta,\theta}}{\Theta}+M_r-M_\theta\right)-Q_r=I_1u_{,tt}+I_2\phi_{r,tt} \tag{1.17}$$

$$\frac{1}{r_0}\frac{M_{r\theta,r}}{\zeta'}+\frac{1}{r_0\zeta}\left(\frac{M_{\theta,\theta}}{\Theta}+2M_{r\theta}\right)-Q_\theta=I_1v_{,tt}+I_2\phi_{\theta,tt} \tag{1.18}$$

where

$$\begin{aligned}\mathcal{N}(w)=&\frac{1}{r_0\zeta'}\frac{\partial}{\partial r}\left(N_r\zeta\frac{w_{,r}}{\zeta'}+N_{r\theta}\frac{w_{,\theta}}{\Theta}\right)\\&+\frac{1}{r_0\zeta\Theta}\frac{\partial}{\partial\theta}\left(N_{r\theta}\zeta\frac{w_{,r}}{\zeta'}+N_\theta\frac{w_{,\theta}}{\Theta}\right)\end{aligned} \tag{1.19}$$

The inertias are defined as follows.

$$(I_0,I_1,I_2)=\sum_{k=1}^{n}\int_{z_k}^{z_{k+1}}\rho^{(k)}(1,z,z^2)dz \tag{1.20}$$

with the index k representing one of the n number of layers.

The in-plane force resultants, the moment resultants and the shear force resultants are as follows (Reddy, 1997).

$$\begin{Bmatrix}N_r\\N_\theta\\N_{r\theta}\end{Bmatrix}=\begin{bmatrix}A_{11}&A_{12}&A_{16}\\A_{12}&A_{22}&A_{26}\\A_{16}&A_{26}&A_{66}\end{bmatrix}\begin{Bmatrix}\epsilon_r^{(0)}\\\epsilon_\theta^{(0)}\\\epsilon_{r\theta}^{(0)}\end{Bmatrix}+\begin{bmatrix}B_{11}&B_{12}&B_{16}\\B_{12}&B_{22}&B_{26}\\B_{16}&B_{26}&B_{66}\end{bmatrix}\begin{Bmatrix}\kappa_r^{(0)}\\\kappa_\theta^{(0)}\\\kappa_{r\theta}^{(0)}\end{Bmatrix}-\begin{Bmatrix}N_r^T\\N_\theta^T\\N_{r\theta}^T\end{Bmatrix}-\begin{Bmatrix}N_r^P\\N_\theta^P\\N_{r\theta}^P\end{Bmatrix} \tag{1.21}$$

$$\begin{Bmatrix}M_r\\M_\theta\\M_{r\theta}\end{Bmatrix}=\begin{bmatrix}B_{11}&B_{12}&B_{16}\\B_{12}&B_{22}&B_{26}\\B_{16}&B_{26}&B_{66}\end{bmatrix}\begin{Bmatrix}\epsilon_r^{(0)}\\\epsilon_\theta^{(0)}\\\epsilon_{r\theta}^{(0)}\end{Bmatrix}+\begin{bmatrix}D_{11}&D_{12}&D_{16}\\D_{12}&D_{22}&D_{26}\\D_{16}&D_{26}&D_{66}\end{bmatrix}\begin{Bmatrix}\kappa_r^{(0)}\\\kappa_\theta^{(0)}\\\kappa_{r\theta}^{(0)}\end{Bmatrix}-\begin{Bmatrix}M_r^T\\M_\theta^T\\M_{r\theta}^T\end{Bmatrix}-\begin{Bmatrix}M_r^P\\M_\theta^P\\M_{r\theta}^P\end{Bmatrix} \tag{1.22}$$

$$\begin{Bmatrix}Q_\theta\\Q_r\end{Bmatrix}=k^2\begin{bmatrix}A_{44}&A_{45}\\A_{45}&A_{55}\end{bmatrix}\begin{Bmatrix}e_{\theta z}\\e_{rz}\end{Bmatrix} \tag{1.23}$$

Where, $k^2(=5/6)$ is the shear correction factor and,

$$\left.\begin{aligned} A_{ij} &= \sum_{k=1}^{n}(z_k - z_{k-1})Q_{ij}^{(k)}, \quad B_{ij} = \frac{1}{2}\sum_{k=1}^{n}(z_k^2 - z_{k-1}^2)Q_{ij}^{(k)}, \\ D_{ij} &= \frac{1}{3}\sum_{k=1}^{n}(z_k^3 - z_{k-1}^3)Q_{ij}^{(k)} \end{aligned}\right\} \forall \quad i,j = 1,2,6 \tag{1.24}$$

$$A_{ij} = \sum_{k=1}^{n}(z_k - z_{k-1})Q_{ij}^{(k)} \quad \forall \quad i,j = 4,5 \tag{1.25}$$

The stiffness constants $Q_{ij}^{(k)}$'s are same as defined in equation-set (1.9) for the kth layer. For the cases of symmetric and unsymmetric laminated plates made up of piezoelectric layers and cylindrically orthotropic layers having fiber orientations either in radial or circumferential directions,

$$A_{16} = A_{26} = 0,\ B_{16} = B_{26} = 0,\ D_{16} = D_{26} = 0,\ A_{45} = 0 \tag{1.26}$$

The non-vanishing thermal and piezoelectric force and moment resultants are,

$$\begin{bmatrix} N_r^T & M_r^T \\ N_\theta^T & M_\theta^T \end{bmatrix} = -\sum_{k=1}^{n}\int_{z_{k-1}}^{z_k} \begin{bmatrix} Q_{11}^{(k)} & Q_{12}^{(k)} \\ Q_{22}^{(k)} & Q_{12}^{(k)} \end{bmatrix} \begin{Bmatrix} \alpha_r \\ \alpha_\theta \end{Bmatrix} \begin{bmatrix} 1 & z \end{bmatrix} T^{(k)}(z)dz \tag{1.27}$$

$$\begin{bmatrix} N_r^P & M_r^P \\ N_\theta^P & M_\theta^P \end{bmatrix} = -\sum_{k=1}^{n} E_z^{(k)} \begin{bmatrix} Q_{11}^{(k)} & Q_{12}^{(k)} \\ Q_{22}^{(k)} & Q_{12}^{(k)} \end{bmatrix} \begin{Bmatrix} d_{31}^{(k)} \\ d_{32}^{(k)} \end{Bmatrix} \begin{bmatrix} (z_k - z_{k-1}) & \frac{1}{2}(z_k^2 - z_{k-1}^2) \end{bmatrix} \tag{1.28}$$

Where, $T^{(k)}(z)$ is the rise in temperature within a layer from the unstrained state. Assuming uniform temperature over any plane parallel to the plate's mid-plane, the temperature is a piecewise linear function of z-coordinate. The temperature at each interface can easily be determined using the heat continuity equations. Thus, thermal actuation is prescribed in terms of temperatures at the top (T_0) and bottom (T_n) surfaces. Electrical actuation is prescribed in terms of potential gradient $E_z^{(k)}$ across piezoelectric layers.

Using equations (1.21)- (1.28) and (1.3a)- (1.6), the equations (1.14)- (1.18) can be expressed in terms of the five displacement components (u, v, w, ϕ_r, ϕ_θ) defined in equation (1.1).

With radial edges being at ($\theta = 0,\ 1$) and circumferential edges being at ($r = 0,\ 1$), the spatial boundary conditions are as follows. Clamped edge boundary condition on any edge is:

$$u = v = w = \phi_r = \phi_\theta = 0 \tag{1.29}$$

Simply supported radial edge condition is:

$$u = v = w = \phi_r = M_\theta = 0 \tag{1.30}$$

Free radial edge requires:

$$N_{r\theta} = N_\theta = Q_\theta = M_{r\theta} = M_\theta = 0 \tag{1.31}$$

Simply supported circumferential edge condition is:

$$u = v = w = M_r = \phi_\theta = 0 \tag{1.32}$$

Free circumferential edge condition is:

$$N_r = N_{r\theta} = Q_r = M_r = M_{r\theta} = 0 \tag{1.33}$$

The initial conditions are,

$$u = v = w = o \tag{1.34a}$$

$$u_{,t} = v_{,t} = w_{,t} = 0 \tag{1.34b}$$

$$\phi_r = \phi_\theta = 0 \tag{1.34c}$$

$$\phi_{r,t} = \phi_{\theta,t} = 0 \tag{1.34d}$$

CHAPTER 2
METHOD OF SOLUTION

2.1 Introduction

This chapter presents the methodology developed for the solution of non-linear partial differential equations. The technique of spatial discretization is presented. The two-dimensional fast converging Chebyshev polynomials is used for generating the algebraic equations from the governing partial differential equations of motion/equilibrium along with appropriate domain boundary conditions. The method of removing redundancy in the application of boundary conditions is explained. This transforms the mathematical model from a system of partial differential equations to a system of algebraic equations. The algebraic equations are solved accordingly for the eigenvalue problems of free vibration and buckling analyses and for the problems of non-linear static and dynamic analyses respectively. The details are discussed in respective chapters.

2.2 Spatial Discretization

The linear and non-linear governing equations of plates are spatially discretized using different techniques like Finite elements, Finite difference, Boundary element, Fourier series and Galerkin method (Noor and Burton, 1989; Kapania and Raciti, 1989; Varadan and Bhaskar, 1997). Recently, Tanriover and Senocak (2004) employed Galerkin method for solving the large deflection problem of thin laminated

rectangular plates. Woo et al. (2003) applied p-version FEM for materially and geometrically non-linear analysis of laminated plates.

Salehi and Shahidi (1994) have analyzed the large deflection behavior of thick isotropic sector plates, Turvey and Salehi (1998) gave the large deflection results for stiffened sector plates and Salehi and Sobhani (2004) presented the non-linear analysis of laminated sector plates with rectilinear orthotropy. In all these studies dynamic relaxation with finite difference discretization was the only technique employed. Liew and Liu (2000) solved the linear free vibration problem of isotropic Mindlin sector plates using Differential Quadrature Method (DQM) for spatial discretization.

Clenshaw and Norton (1963) presented the method for solving non-linear ordinary differential equations using Chebyshev series. Evans and Murphy (1981) demonstrated the application of Chebyshev series to the solution of linear bi-harmonic equation in rectangular domain. Sinha and Butcher (1996) utilized Chebyshev polynomials to solve one-dimensional p^{th} order linear differential equation with periodic coefficients. Park and Kapania (1998) found that Chebyshev polynomials required least CPU time for solving non-linear initial value problems governed by second order differential equations. Nath (1977), Reddy (1980), Jain (1985), Kumar (1997) and Shukla and Nath (2000) used Chebyshev polynomials for the studying the problems of rectangular and axisymmetric plates and shells. All these studies demonstrated the fast converging properties of Chebyshev series.

Fox and Parker (1968) and Rivlin (1974) have presented the detailed analysis of the properties of Chebyshev polynomials. Chebyshev polynomial $T_k(x)$ of degree k

in the range $(-1 \leq x \leq 1)$ is defined as,

$$T_k(x) = \cos k\theta, \cos\theta = x \tag{2.1}$$

Using trigonometric identities, the recurrence relationship for generating the Chebyshev polynomials is obtained as,

$$T_{k+1}(x) = 2xT_k(x) - T_{k-1} \quad \forall \quad k > 1 \tag{2.2}$$

with $T_0(x) = 1$ and $T_1(x) = x$. The n^{th} degree minimax polynomial approximation (Fox and Parker (1968), pp. 3-4) of a function $f(x) \equiv 0$ in the domain $(-1 \leq x \leq 1)$ is some multiple of $T_n(x)$. This capability of efficient approximation of zero by Chebyshev polynomials is made use of in solving differential equations by approximating the dependent field variable in a given problem by a Chebyshev series.

The advantage of using Chebyshev polynomials for spatial discretization of differential equations can further be explained by considering a function $y(x)$ governed by an n^{th} degree differential equation

$$\sum_{i=1}^{n} a_i \frac{\partial^n y}{\partial x^n} + a_0 = 0 \tag{2.3}$$

If this problem is solved by approximating y by an N^{th} degree Chebyshev series $(N > n)$ as,

$$y(x) = \sum_{i=0}^{N} \delta_i b_i T_i(x) \tag{2.4}$$

with

$$\begin{aligned} \delta_i \quad &= 1/2 \quad for \quad i = 0 \\ &= 1 \quad \forall \quad i > 0 \end{aligned} \tag{2.5}$$

then, substituting the approximation in equation (2.4) into the governing equation (2.3), the following equation is obtained on using the relations given later in this section for evaluating the derivatives of Chebyshev series,

$$\sum_{i=0}^{N} \delta_i b_i^* T_i(x) = 0 \tag{2.6}$$

in which, each b_i^* is a linear combination of all the coefficients b_i's in the equation (2.4). A total N number of linear algebraic equations are generated in terms of b_i's by equating all the b_i^*'s to zero. Additional n number of linear algebraic equations are obtained by expressing the same number of boundary conditions of the given problem in terms of the Chebyshev series approximation of the function $y(x)$. These additional n number of equations are accommodated by ignoring the same number of higher order terms in equation (2.6). Thus all the boundary conditions of the given problem are satisfied exactly and the governing equation (2.3) is satisfied with a residual error of $\sum_{i=N-n+1}^{N} \delta_i b_i^* T_i(x)$. The earlier mentioned ability of Chebyshev polynomials to approximate zero ensures that this error is small enough if N is large enough.

These characteristics of Chebyshev polynomials are even more useful in the modeling and analysis of non-linear systems. In this study, the problem domain being sectorial, modified Chebyshev polynomials $T_k^*(x)$ are used. These are defined as, $T_k^*(x) = T_k(2x-1)$ in the range $0 \leq x \leq 1$. For brevity, the asterisk in $T_k^*(x)$ is dropped in further discussions.

A general function $\Psi(r, \theta)$ can be approximated in space domain by a finite degree

double Chebyshev polynomial as:

$$\Psi(r,\theta) = \sum_{i=0}^{M}\sum_{j=0}^{N} \delta_{ij}\Psi_{ij}T_i(r)T_j(\theta) \quad for \quad 0 \le r \le 1, \quad 0 \le \theta \le 1 \tag{2.7}$$

$$\left.\begin{aligned} \delta_{ij} &= 1/2 \quad \forall \quad (i=0, j>0)\ or\ (i>0, j=0) \\ &= 1/4 \quad for \quad (i=0, j=0) \\ &= 1 \quad \text{otherwise} \end{aligned}\right\} \tag{2.8}$$

The spatial derivative of the function can be expressed as:

$$\Psi^{,p,q}(r,\theta) = \sum_{i=0}^{M-p}\sum_{j=0}^{N-q} \delta_{ij}\Psi_{ij}^{pq}T_i(r)T_j(\theta) \tag{2.9}$$

where, p and q are orders of derivative with respect to r and θ respectively. The coefficients Ψ_{ij}^{pq} can be evaluated using the recurrence relation (Fox and Parker (1968), Chapter 3) as:

$$\Psi_{(i-1)j}^{pq} = \Psi_{(i+1)j}^{pq} + 4i\Psi_{ij}^{(p-1)q} \tag{2.10}$$

$$\Psi_{i(j-1)}^{pq} = \Psi_{i(j+1)}^{pq} + 4j\Psi_{ij}^{p(q-1)} \tag{2.11}$$

Non-linearity in the governing equations is due to the product of dependent variables. The product of two double Chebyshev polynomials is expressed as:

$$\begin{aligned} T_i(r)T_j(\theta)T_k(r)T_l(\theta) =& \frac{1}{4}[T_{i+k}(r)T_{j+l}(\theta) + T_{i+k}(r)T_{j-l}(\theta) \\ &+ T_{i-k}(r)T_{j+l}(\theta) + T_{i-k}(r)T_{j-l}(\theta)] \end{aligned} \tag{2.12}$$

2.3 Method of applying Boundary Conditions

The displacement components u, v, w, ϕ_r and ϕ_θ are approximated as,

$$(u,v,w,\phi_r,\phi_\theta) = \sum_{i=0}^{M}\sum_{j=0}^{N} \delta_{ij}(u,v,w,\phi_r,\phi_\theta)_{ij}T_i(r)T_j(\theta) \tag{2.13}$$

Substituting Eq. (2.13) in to the equilibrium Eqs. (1.14)- (1.18) and making use of Eqs. (1.3)- (1.27) and Eqs. (2.7)- (2.12), the equations of equilibrium are discretized in terms of $(u, v, w, \phi_r, \phi_\theta)_{ij}$. Similarly, appropriate boundary conditions are discretized. By equating the coefficients of like terms on either sides of the resulting equations two sets of non-linear algebraic equations are generated - one from the equilibrium Eqs. (1.14)- (1.18) and the other from a total of 20 number of appropriate boundary conditions. Ignoring the coefficients of $T_i(r)T_j(\theta)$ having $(i > M)$ a set of 5(M + 1)(N + 1) number of non-linear equations are generated from equilibrium equations and another set of [10(M + 1) + 10(N + 1)] equations are generated from the boundary conditions. In this manner more algebraic equations are generated than the unknowns. Nath and Kumar (1995) employed the linear regression analysis with least square error norms and obtained the unique solution. In the present work the additional equations are eliminated using the minimax property of Chebyshev polynomials and a linear interpolation scheme.

Expressing the four boundary conditions, two along each of the two dimensions (r and θ), corresponding to each displacement component gives a set of [2(M + 1) + 2(N +1)] number of equations. But, four equations in this set are redundant since each of the four corners is common between two edges. The redundancy is removed by an interpolation scheme and is described as follows.

For example (refer Fig. 2.1), consider the case of clamped or simply supported radial edges with the circumferential edges being clamped, simply supported or free. The four boundary conditions corresponding to, say, the displacement component ϕ_r are expressed as follows.

ϕ_r specified as zero on the radial edges, would give the following algebraic equations.

$$\sum_{j=0}^{N} \delta_{ij}(-1)^j \phi_{r,ij} = 0 \quad \forall \quad 0 \leq i \leq M \quad at\ \theta = 0 \tag{2.14}$$

$$\sum_{j=0}^{N} \delta_{ij} \phi_{r,ij} = 0 \quad \forall \quad 0 \leq i \leq M \quad at\ \theta = 1 \tag{2.15}$$

These two boundary conditions thus contribute total 2(M+1) number of equations. On the circumferential edges, $\phi_r = 0$ for the clamped edge, and $M_r = 0$ for the simply supported edge or the free edge. Thus, for e.g. if the r = 0 edge is clamped, the displacement component ϕ_r along this edge is visualized as,

$$\sum_{j=0}^{N} T_j(\theta) \sum_{i=0}^{M} \delta_{ij}(-1)^i \phi_{r,ij} = (B_1\bar{\phi}_{r,0} + B_2\bar{\phi}_{r,1})T_{N-1}(\theta) + (A_1\bar{\phi}_{r,0} + A_2\bar{\phi}_{r,1})T_N(\theta) \tag{2.16}$$

Where, $\bar{\phi}_{r,0}$ and $\bar{\phi}_{r,1}$ are the values of ϕ_r at the corner points (r = 0, θ = 0) and (r =0, θ = 1), respectively, and have already been prescribed as zero by virtue of Eqs. (2.14) and (2.15). A_1, A_2, B_1 and B_2 are interpolation constants.

In order to avoid redundancy in the application of boundary conditions to have non-singular system of equations, the corresponding clamped boundary condition is applied as,

$$\sum_{i=0}^{M} \delta_{ij}(-1)^i \phi_{r,ij} = 0 \quad \forall \quad 0 \leq j \leq (N-2) \tag{2.17}$$

The above set of (N-1) equations simply skips the equations corresponding to coefficients of the two highest order terms in Eq. (2.16). Thus, if ϕ_r is specified as zero on all the four edges it would contribute a total $[2(M+1)+2(N-1) = 2(M+N)]$ number of equations. To accommodate these $2(M+N)$ number of equations, coefficients of $T_i(r)T_j(\theta)$ for $(i > M-2)$ and $(j > N-2)$ are considered negligible and thus ignored.

The basis of this approach is in the minimax property of the Chebyshev polynomials (refer section 2.2). On the other hand, if the two circumferential edges are simply supported or free, one needs to specify $(M_r = 0)$ on these edges. The quantity $(r^2 M_r)$ can be expressed as follows using the appropriate constitutive equations.

$$r^2 M_r = \sum_{i=0}^{M} \sum_{j=0}^{N} \delta_{ij} F_{r^2 M_r, ij}(u, v, w, \phi_r, \phi_\theta)_{i'j'} T_i(r) T_j(\theta), \quad 0 \leq i' \leq M,\ 0 \leq j' \leq N \tag{2.18}$$

Here, $F_{r^2 M_r, ij}$'s are coefficients in the Chebyshev series expansion of $(r^2 M_r)$. Each of these $F_{r^2 M_r, ij}$'s is a non-linear function of the coefficients $(u, v, w, \phi_r, \phi_\theta)_{i'j'}$ of the Chebyshev series expansion of the five displacement components. Thus, the boundary condition $(M_r = 0)$ is applied as,

$$\sum_{i=0}^{M} \delta_{ij} (-1)^i F_{r^2 M_r, ij} = 0 \quad \forall \quad 0 \leq j \leq (N-2) \quad at\ r = 0 \tag{2.19}$$

$$\sum_{i=0}^{M} \delta_{ij} F_{r^2 M_r, ij} = 0 \quad \forall \quad 0 \leq j \leq (N-2) \quad at\ r = 1 \tag{2.20}$$

The basis of ignoring equations for $(j > N-2)$ also lies in the minimax property of the Chebyshev polynomials. In this manner, the application of boundary conditions $(\phi_r = 0)$ on the radial edges and $(Mr = 0)$ on the circumferential edges contributes a total $[2(M+1)+2(N-1) = 2(M+N)]$ number of equations. Similarly, application of various combinations of force and displacement boundary conditions corresponding to each of the five displacement components contributes a total $2(M+N)$ number of algebraic equations. These are then accommodated into the overall system of equations by ignoring the same number of higher order coefficients in the respective equilibrium equations. This generates the complete system of $5(M+1)(N+1)$ number of algebraic equations in terms of the $5(M+1)(N+1)$ number of unknown coefficients.

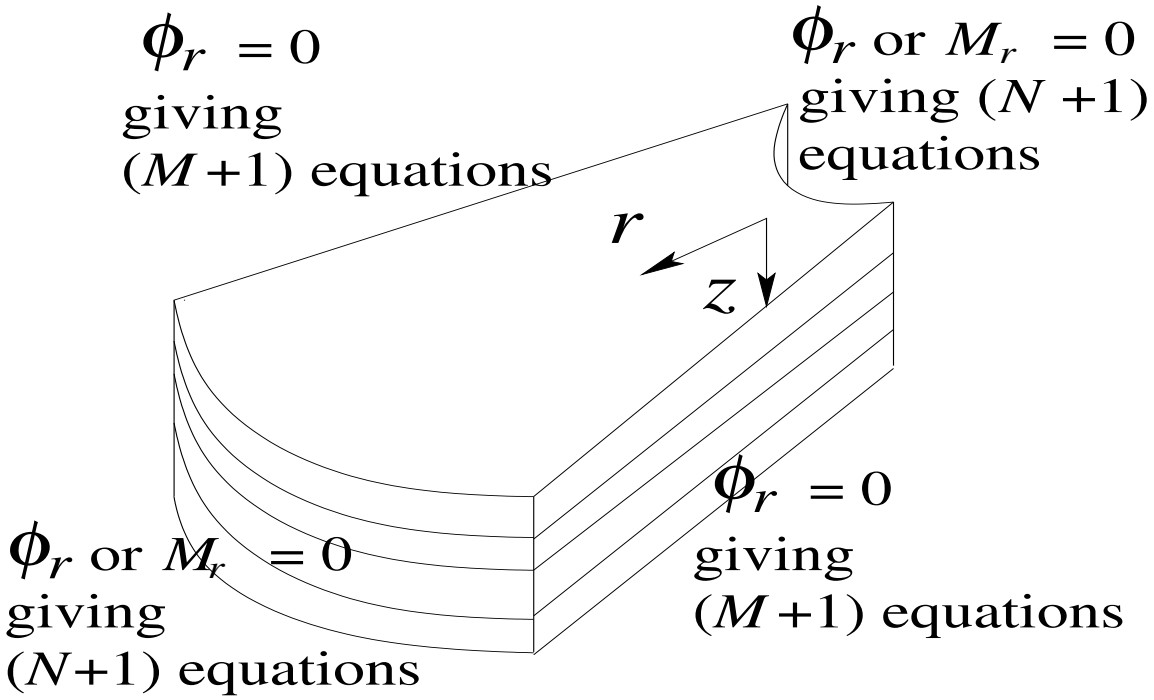

Fig. 2.1 Generation of redundancy in the application of boundary conditions.

CHAPTER 3
LINEAR VIBRATION AND BUCKLING OF ISOTROPIC SECTOR PLATES

3.1 Introduction

This Chapter presents a simple analytical formulation for the eigenvalue problems of buckling and free-vibration analysis of isotropic moderately thick (Reissner-Mindlin) sector plates. The non-axisymmetric formulation in cylindrical coordinates is discretized in the space domain in terms of two-dimensional Chebyshev polynomials. The formulation facilitates application of several combinations of simply supported, clamped, and free-edge conditions. Convergence study has been carried out, and the obtained results are compared with those available in the literature. The critical buckling loads and the natural frequencies are presented. Effects of boundary conditions, plate thickness, and annularity are studied.

Many papers dealing with buckling and vibration analysis of plates of various shapes and subjected to various combinations of edge conditions have been published. Initially (Ben-Amoz, 1959; Yonezawa, 1962; Ramakrishnan and Kunukkasseril, 1973; Irie et al., 1979; Kim and Dickinson, 1989; Liew and Lam, 1993), the research on sector plates was based on the linear Kirchhoff plate model, which ignored the transverse shear effect. The effect becomes significant for moderately thick plates and even for materials having higher ratio of Young's modulus to shear modulus. Further, this effect gets pronounced for higher modes of thin plates. Reissner (1945) and Mindlin

(1951) proposed a more refined model for the analysis of plates which accounts for first order shear effect.

Free vibration problems of annular Mindlin sector plates have been solved earlier by using the finite element method (Rao et al., 1977; Guruswamy and Yang, 1979), the boundary element method (Srinivasan and Thiruvenkatachari, 1985), the finite strip method (Benson and Hinton, 1976; Cheung and Chan, 1981) and the Rayleigh-Ritz method Xiang et al. (1993).

Buckling behaviors of rectangular and circular plates have been studied extensively. Wang et al. (1994) had derived an exact relationship between Mindlin plate and Kirchhoff plate buckling loads for polygonal plates with simply supported edges and for circular plates with either clamped or simply supported edges. Recently, Ozakca et al. (2003a,b) presented a finite element formulation for the buckling analysis and shape optimization of Mindlin circular and annular plates.

Buckling of thin sector plates has been studied by Rubin (1978) and Harik (1985). Wang and Xiang (1999) proposed a method for deducing buckling loads of Mindlin sector plates from the Kirchhoff plate results. They gave an exact relationship between buckling loads of Mindlin model and of Kirchhoff model applied to complete sector plates having simply supported radial and circumferential edges.

McGee et al. (1995) presented exact solutions for free vibration analysis of sector plates having simply supported radial edges and all possible combinations of free, simply supported and clamped boundary conditions on circumferential edges. Liew and Liu (2000) used differential quadrature method for vibration analysis of shear deformable sector plates.

It is clear from literature that there is a need for an analytical solution that handles several kinds of boundary conditions. The present study is an effort in this direction. Considering the first order shear deformation theory, the vibration and stability analyses of moderately thick sector plates are carried out analytically using Chebyshev polynomials. The influence of boundary conditions, thickness ratio λ, annularity μ and rotary inertia on the frequency and critical loads are investigated. The eigenvalue problem is formulated by discretizing the governing equilibrium equations and boundary conditions with the help of two-dimensional Chebyshev polynomials and then solved using the procedure given by Wilkinson and Reinsch (1971) for non-symmetric matrices. The eigenvalues and the corresponding mode shapes are obtained.

3.2 Governing Equations

For isotropic plates, there is no bending-stretching coupling. Thus, only three displacement components (w, ϕ_r, ϕ_θ), refer equation (1.1), are required for analyzing the bending modes of vibrations. The equations of motion for free vibration analysis of isotropic sector plates are obtained from equations (1.16)- (1.18) by using equations (1.3)– (1.6) and (1.21)– (1.26). After ignoring the non-linear terms and piezothermal effects, the equations of motion for isotropic plates in terms of displacement components are obtained as,

$$
\begin{aligned}
&-\left[0.5\left(1-\nu\right)\left(\frac{k^2}{\lambda^2}\right)\right]\zeta^2\frac{w'_{,r}}{\zeta'}+\left(\frac{1}{12\lambda}\right)\left[\zeta^2\frac{\phi_{r,rr}}{\zeta'^2}+\zeta\frac{\phi_{r,r}}{\zeta'}-\phi_r\right]\\
&+\left[\frac{0.5\left(1-\nu\right)}{12\lambda}\right]\frac{\phi_{r,\theta\theta}}{\Theta^2}-\zeta^2\left[0.5\left(1-\nu\right)\left(\frac{k^2}{\lambda^3}\right)\right]\phi_r\\
&+\left[\frac{0.5\left(1+\nu\right)}{12\lambda}\right]\zeta\frac{\phi_{\theta,r\theta}}{\zeta'\Theta}-\left[\frac{0.5\left(3-\nu\right)}{12\lambda}\right]\frac{\phi_{\theta,\theta}}{\Theta}
\end{aligned}
$$

$$= \left(\frac{\zeta^2\lambda}{12}\right)\frac{12r_o^4\rho(1-\nu^2)}{Eh^2}\phi_{r,tt} \tag{3.1}$$

$$\begin{aligned}
&-\left[0.5\,(1-\nu)\left(\frac{k^2}{\lambda^2}\right)\right]\zeta\frac{w'_{,\theta}}{\Theta}+\left[\frac{0.5\,(1+\nu)}{12\lambda}\right]\zeta\frac{\phi_{r,r\theta}}{\zeta'\Theta}\\
&+\left[\frac{0.5\,(3-\nu)}{12\lambda}\right]\frac{\phi_{r,\theta}}{\Theta}+\left[\frac{0.5\,(1-\nu)}{12\lambda}\right]\left[\zeta^2\frac{\phi_{\theta,rr}}{\zeta'^2}+\zeta\frac{\phi_{\theta,r}}{\zeta'}-\phi_\theta\right]\\
&+\left[\frac{1}{12\lambda}\right]\frac{\phi_{\theta,\theta\theta}}{\Theta^2}-\zeta^2\left[0.5\,(1-\nu)\left(\frac{k^2}{\lambda^3}\right)\right]\phi_\theta\\
&=\left(\frac{\zeta^2\lambda}{12}\right)\frac{12r_o^4\rho(1-\nu^2)}{Eh^2}\phi_{\theta,tt}
\end{aligned} \tag{3.2}$$

$$\begin{aligned}
&\left[0.5\,(1-\nu)\left(\frac{k^2}{\lambda^2}\right)\right]\left[\zeta^2\frac{w'_{,rr}}{\zeta'^2}+\zeta\frac{w'_{,r}}{\zeta'}+\frac{w'_{,\theta\theta}}{\Theta^2}\right]+\zeta\left[0.5\,(1-\nu)\left(\frac{k^2}{\lambda^3}\right)\right]\\
&\times\left[\zeta\frac{\phi_{r,r}}{\zeta'}+\phi_r+\frac{\phi_{\theta,\theta}}{\Theta}\right]=\left(\frac{\zeta^2}{12}\right)\frac{12r_o^4\rho(1-\nu^2)}{Eh^2}w'_{,tt}
\end{aligned} \tag{3.3}$$

For the buckling problem, the right hand sides in equations (3.1) and (3.1) are zero whereas the right hand side of (3.3) is replaced by

$$\left(\frac{1}{12}\right)N'_{ip}\left[\zeta^2\frac{w'_{,rr}}{\zeta'^2}+\zeta\frac{w'_{,r}}{\zeta'}+\frac{w'_{,\theta\theta}}{\Theta^2}\right]$$

where, the non-dimensionalized quantities are defined as,

$$w'=\left(\frac{w}{h}\right),\ N'_{ip}=\frac{N_{ip}}{\left(\frac{D}{r_o^2}\right)},\ \omega'=\frac{\omega}{\frac{1}{r_o^2}\left(\frac{D}{\rho h}\right)^{\frac{1}{2}}},\ N'_{cr}=\frac{N_{cr}}{\left(\frac{D}{r_o^2}\right)} \tag{3.4}$$

3.3 Method of solution

Chebyshev series expansions of (u, ϕ_r and ϕ_θ) are substituted in to each of these three equations. The set of $(M+1)(N+1)$ number of algebraic equations thus obtained form

each of the equations (3.1)– (3.3) along with the appropriate boundary conditions. These equations in terms of the $3(M+1)(N+1)$ number of coefficients and the eigenvalue η are arranged as,

$$A'_{dof}\{X\} - \eta B'_{dof}\{X\} = 0,\ dof = w',\ \phi_r,\ \phi_\theta \tag{3.5}$$

Here,

$$\{X\} = \begin{Bmatrix} W' \\ \Phi_r \\ \Phi_\theta \end{Bmatrix} \tag{3.6}$$

A'_{dof} and B'_{dof} are rectangular matrices of dimension $(M+1)(N+1)$ by $3(M+1)(N+1)$. Using the methodology of section 2.3, the redundancy in the application of boundary conditions is eliminated appropriately. The algebraic equations obtained from boundary conditions are included by having the lowest $2(M+N)$ rows of B'_{dof} as null vectors and those of A'_{dof} obtained from left-hand sides of the boundary condition equations (1.29)- (1.33).

Assembling the three matrix equations obtained from equation (3.5), we get the following eigenvalue problem.

$$A^{-1}B\{X\} = \left(\frac{1}{\eta}\right)\{X\} \tag{3.7}$$

A and B are square matrices given by,

$$A = \begin{bmatrix} A'_w \\ A'_{\phi_r} \\ A'_{\phi_\theta} \end{bmatrix},\ B = \begin{bmatrix} B'_w \\ B'_{\phi_r} \\ B'_{\phi_\theta} \end{bmatrix} \tag{3.8}$$

The eigenvalue problem in (3.7) is solved using the procedure given by Wilkinson and Reinsch (1971).

3.4 Results and Discussions

The section gives the solutions of the eigenvalue problems resulting from buckling and free vibration analyses of moderately thick isotropic sector plates. The effects of annularity (μ), thickness ratio (λ), sector angle (Θ) rotary inertia and boundary conditions are studied. The boundary conditions considered here are various combinations of simply supported (S), clamped (C) and free (F) edges. The combinations are named in the order shown in Figure 1.1.

Table 3.1 Convergence results for buckling analysis with respect to number of terms in series expansion, $\mu = 0$, $\lambda = 0.2$, $\Theta = \pi/3$

$(M+1)$	N'_{cr}	
$\times(N+1)$	$CCCC$	$SSSS$
48	49.61979	27.17685
80	47.58639	27.05869
120	47.56319	27.05877
168	47.56293	27.05877
224	47.56293	27.05877

Results for convergence with respect to the degrees M and N of the series expansions are given in Tables 3.1 and 3.2 in terms of critical buckling loads and natural frequencies respectively. Two more terms were used in r-dimension than the θ-dimension since the equilibrium equations were multiplied with ζ^2 – refer equation (1.2) – in order to remove ζ from the denominators of various terms. Convergence of critical buckling loads to seven significant digits is achieved in Table 3.1 with ($M = 13$, $N = 11$). Table 3.2 shows the convergence of the lowest ten frequencies for the vibration problem. Convergence to six significant digits is attained with ($M = 17$, $N = 15$) for the boundary condition $SSSS$. For $FSFS$ edge condition, better convergence is achieved for higher modes. Only two significant digits are

converged for the lowest mode. This could be attributed to the approximation in application of free edge boundary condition. In the present study total 168 terms ($M = 13$, $N = 11$) gave satisfactory results for all the combinations of various parameters - (λ, μ and Θ). These values of M and N would be used in subsequent analysis.

Table 3.3, for $\mu = 0$, presents the comparison of critical buckling loads obtained by the present analysis with those obtained by Wang and Xiang (1999) for $SSSS$ and $SSCS$ boundary conditions. It can be seen that the difference is less than 2% for most of the results. Maximum difference is 9.7%, obtained for $\lambda = 0.1$ and $\Theta = \pi$.This difference is because of the fact that all these results are obtained with ($M = 13$, $N = 11$) whereas with increasing span with respect to Θ convergence occurs at ($M = 15$, $N = 13$). The critical loads can be seen to be lowering with increasing span with respect to Θ. The decrease in non-dimensional critical load N'_{cr} with increasing λ (i.e. plate thickness) is because of the non-dimensional factor being function of λ^2.

Table 3.4 gives the effect of (Θ, μ and λ) on the critical buckling loads of plates for the edge conditions $CCCC$, $CCSS$, $SSCS$ and $SSSS$. The critical loads are lowered with increasing span with respect to Θ. As the annularity μ increases the critical load also increases, only marginally for smaller Θ but substantially for larger Θ. With respect to λ, it can be noticed the non-dimensional critical load decreases considerably with increasing λ, this decrease being much larger for the $CCCC$ edge condition in comparison to the $SSSS$ edge condition. In fact, critical load increases with increasing thickness and the opposite trend is stated above in terms of non-

dimensional critical load. The critical load is also much larger for the stiffer boundary condition of $CCCC$ in comparison to the edge condition $SSSS$.

Considering three values each of the parameters λ and Θ, and two values of μ the free vibration analysis has been done and the results are depicted in Tables 3.5–3.8 for $SSSS$, $CCCC$, $CSCS$ and $CFCF$. The results obtained by Liew and Liu (2000) using Differential Quadrature Method (DQM) are also shown for comparison. It can be seen that the difference is less than 5% in all the cases except for a few results for thin plates having $\lambda = 0.01$ and $\Theta = 2\pi/3$. In Table mytabch3omscfcf, the results with $\Theta = 2\pi/3$ and $\mu = 0.5$ show large difference after first mode. This difference can be attributed to the presence of a pair of closely spaced two lowest frequencies in the results obtained by Liew and Liu (2000). There is decrease in natural frequencies with increasing thickness parameter λ. It can be noticed that there is significant reduction in natural frequencies when the edge conditions are changed from all clamped ($CCCC$) to all simply supported ($SSSS$). Comparison of results for $CSCS$ and $CFCF$ edge conditions also shows a decrease in natural frequencies when the two radial edges are made free in place of being simply supported.

Table 3.9 gives the results for the edge condition $FSFS$ and compares them with the results obtained by Xiang et al. (1993) using Rayleigh-Ritz procedure. Here also, the maximum difference is about 5%.

Figure 3.1 shows the effect of neglecting the rotary inertia. These results were obtained by making the right hand sides of equations (3.1) and (3.2) zero. The system matrix could thus be reduced to size $(M+1)(N+1)$ from $3(M+1)(N+1)$. Excluding the rotary inertia raises most of the frequencies by about 5% and the rest

by less than 10% among the six lowest natural frequencies shown here.

The effects of λ and Θ (as shown in Table 3.5) on the first six frequencies are summarized in Figs. 3.2 and 3.3 for the $SSSS$ plates. It can be seen that frequency reduces with λ as well as Θ. The difference between lower modes is smaller. Figs. 3.4 and 3.5 show first four mode shapes in terms of w' along the radial center-line at $\theta = 0.5$ and along the arc at $r = 0.5$ for two typical problems. Number of nodal points are increasing with mode-number. In Fig. 3.4, the entire radial line remains undisplaced at the third mode ω_3'.

3.5 Concluding Remarks

The eigenvalue problem of free vibration and buckling of moderately thick sector plates has been solved using Chebyshev polynomials. The formulation facilitates a simple and efficient solution in the sense that an expansion of 14 terms in r-dimensions and 12 terms in θ-dimension was found satisfactory for most of the given results. For the larger span of $\Theta = \pi$, convergence of some results was observed at (16×14) size of expansion. The methodology developed proved to be robust and efficient for all combinations of clamped and simply supported edge conditions and also gives correct free vibration results for two opposite edges being free and the other two either simply supported or clamped. The results are found to be in good agreement with those given in the literature.

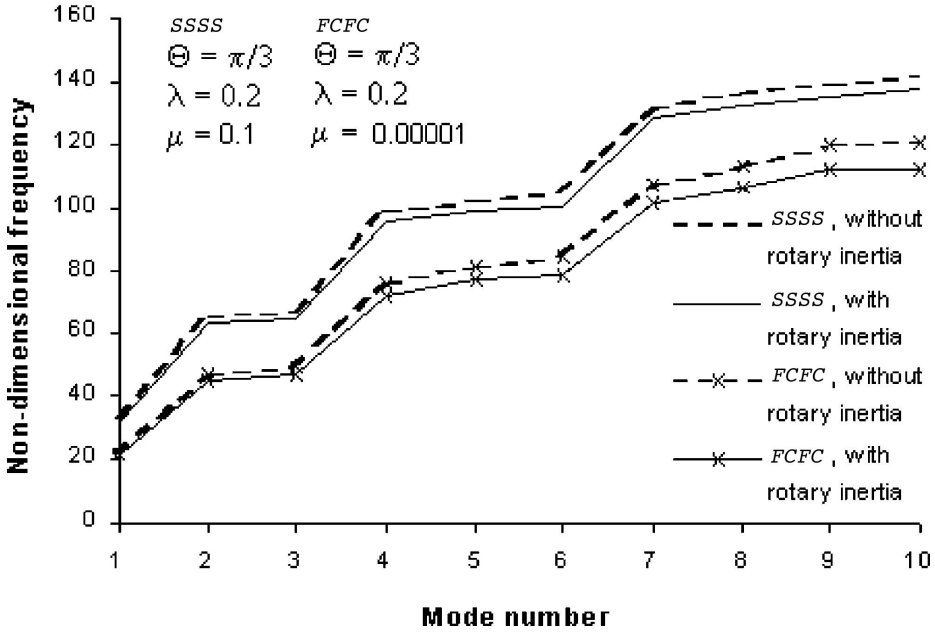

Fig. 3.1 Effect of rotary inertia on frequencies for two sets of boundary conditions

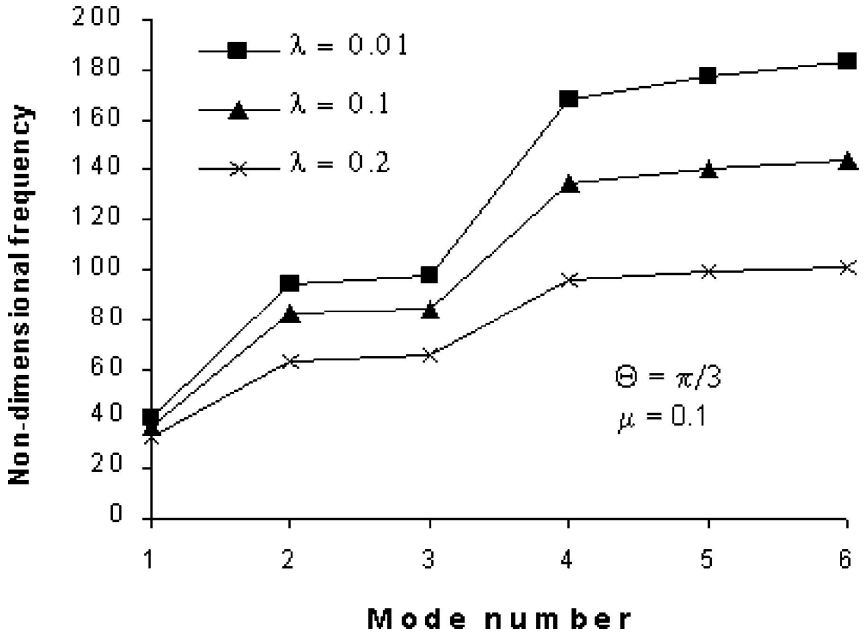

Fig. 3.2 Effect of thickness ratio λ on frequencies of $SSSS$ plates

Table 3.2 Convergence results in terms of ω' for vibration analysis with respect to number of terms in series expansion, $\mu = 0$, $\lambda = 0.2$, $\Theta = \pi/3$, boundary conditions being $SSSS$ and $FSFS$

$(M+1)$	Mode frequency number									
$\times(N+1)$	1	2	3	4	5	6	7	8	9	10
$SSSS$										
80	22.0057	42.8025	50.4331	67.5365	75.9140	81.4357	97.5026	103.6425	109.0922	113.8396
120	22.0058	42.7949	50.4326	64.9324	75.8882	81.3553	87.8665	100.9717	108.7587	113.0122
168	22.0058	42.7945	50.4326	64.8850	75.8875	81.3541	87.3593	100.9226	108.7509	110.6430
224	22.0058	42.7945	50.4326	64.8844	75.8875	81.3541	87.3416	100.9221	108.7510	109.8115
288	22.0058	42.7945	50.4326	64.8844	75.8875	81.3541	87.3418	100.9221	108.7510	109.7819
360	22.0058	42.7945	50.4326	64.8844	75.8875	81.3541	87.3418	100.9221	108.7510	109.7817
$FSFS$										
80	5.0028	18.7471	28.7354	39.0994	51.6996	57.8687	67.6514	77.8634	84.1064	88.9693
120	5.0149	18.7380	28.7253	36.3901	51.6801	56.4881	57.8625	75.2721	84.0712	88.4670
168	5.0305	18.7467	28.7204	36.3373	51.6749	55.8704	57.8634	75.2180	77.1002	84.0685
224	5.0445	18.7587	28.7177	36.3439	51.6725	55.8451	57.8637	75.2140	76.2645	84.0683
288	5.0559	18.7696	28.7161	36.3530	51.6711	55.8496	57.8639	75.2121	76.2321	84.0681
360	5.0650	18.7788	28.7150	36.3613	51.6702	55.8550	57.8640	75.2108	76.2332	84.0680

Table 3.3 Comparison of critical buckling loads N'_{cr} for simply supported radial and circumferential edges, $\mu = 0$

		N'_{cr}			
		SSSS		*SSCS*	
			Wang and Xiang		Wang and Xiang
Θ	λ	Present	[1999]	Present	[1999]
$\pi/6$	0.1	76.09	75.90	89.36	88.89
$\pi/6$	0.2	46.05	45.98	49.73	49.24
$\pi/4$	0.1	48.33	48.09	62.14	62.05
$\pi/4$	0.2	34.16	34.05	39.69	39.69
$\pi/3$	0.1	35.24	34.97	48.81	48.97
$\pi/3$	0.2	27.06	26.90	33.70	33.88
$\pi/2$	0.1	23.21	22.90	36.12	36.10
$\pi/2$	0.2	19.35	19.14	27.08	27.14
$3\pi/4$	0.1	16.03	15.70	28.22	28.23
$3\pi/4$	0.2	14.08	13.84	22.38	22.41
π	0.1	13.44	12.25	25.79	24.21
π	0.2	11.87	11.0	20.64	19.78

Table 3.4 Variation of critical buckling loads N'_{cr} with edge conditions, Θ, μ and λ

			N'_{cr}			
Θ	μ	λ	*CCCC*	*CCSS*	*SSCS*	*SSSS*
$\pi/6$	0.1	0.01	278.341	148.794	122.437	96.984
		0.1	150.717	101.151	89.276	76.097
		0.2	64.890	52.392	49.720	46.049
	0.5	0.01	280.508	154.102	137.393	102.719
		0.1	152.191	103.772	96.555	79.565
		0.2	65.526	53.449	51.725	47.287
$\pi/3$	0.1	0.01	110.873	55.717	57.598	39.194
		0.1	82.579	47.275	48.883	35.270
		0.2	47.565	32.689	33.727	27.070
	0.5	0.01	159.973	86.731	97.735	56.119
		0.1	107.061	67.152	75.070	48.369
		0.2	54.832	40.988	44.456	34.119
$2\pi/3$	0.1	0.01	56.248	26.757	37.848	20.435
		0.1	47.946	24.318	33.547	19.153
		0.2	33.544	19.628	25.422	16.303
	0.5	0.01	150.544	77.347	91.325	44.646
		0.1	100.962	61.233	71.783	39.562
		0.2	52.034	37.984	43.666	29.424

Table 3.5 Comparison of first six natural frequencies for the boundary condition $SSSS$

Θ	μ	λ	ω_1'	ω_2'	ω_3'	ω_4'	ω_5'	ω_6'
$\pi/6$	0.1	0.01†	97.819	183.328	276.702	286.906	409.793	428.145
		‡	97.817	183.322	276.687	286.881	409.124	428.095
		0.1	84.550	144.166	200.212	205.901	269.137	278.139
			84.440	143.881	199.711	205.375	268.226	277.275
		0.2	64.884	100.922	132.049	135.108	166.975	168.297
			64.693	100.536	131.473	134.512	165.947	167.443
	0.5	0.01	103.240	227.694	276.971	423.966	435.455	534.935
			103.238	227.683	276.957	423.932	435.419	534.834
		0.1	88.606	171.622	200.361	275.943	281.573	326.426
			88.486	171.234	199.860	275.089	280.693	325.311
		0.2	67.442	116.302	132.128	171.598	174.693	174.762
			67.237	115.823	131.552	170.760	173.780	173.836
$\pi/3$	0.1	0.01	39.947	94.554	97.819	168.896	177.052	183.328
			39.948	94.539	97.817	168.874	177.030	183.322
		0.1	37.390	82.044	84.550	134.686	140.094	144.166
			37.366	81.937	84.440	134.424	139.820	143.881
		0.2	32.150	63.257	64.884	95.407	98.578	100.922
			32.092	63.072	64.693	95.050	98.205	100.536
	0.5	0.01	55.898	103.240	175.444	178.428	227.694	277.096
			55.898	103.238	175.437	178.407	227.683	276.956
		0.1	51.026	88.606	138.868	140.979	171.622	200.419
			50.982	88.486	138.598	140.702	171.234	199.860
		0.2	42.090	67.442	97.690	99.080	116.302	132.150
			41.996	67.237	97.320	98.704	115.823	131.552
$2\pi/3$	0.1	0.01	20.502	39.947	62.767	66.141	94.554	97.857
			20.492	39.948	62.727	66.136	94.539	97.817
		0.1	19.689	37.390	56.532	59.594	82.044	84.576
			19.675	37.366	56.463	59.535	81.937	84.440
		0.2	17.887	32.150	45.840	48.246	63.257	64.898
			17.862	32.092	45.724	48.129	63.072	64.693
	0.5	0.01	43.961	55.898	75.792	103.270	140.910	162.484
			43.961	55.898	75.788	103.238	137.650	162.478
		0.1	40.808	51.026	67.346	88.626	114.906	130.298
			40.778	50.982	67.272	88.486	113.335	130.056
		0.2	34.563	42.090	53.480	67.452	83.533	92.676
			34.494	41.996	53.340	67.237	82.604	92.334

†: Present ‡: Liew and Liu (2000)

Table 3.6 Comparison of first six natural frequencies for the boundary condition $CCCC$

Θ	μ	λ	ω_1'	ω_2'	ω_3'	ω_4'	ω_5'	ω_6'
$\pi/6$	0.1	0.01†	187.069	297.341	412.541	424.695	572.040	590.354
		‡	187.056	297.335	412.551	424.333	569.715	590.374
		0.1	128.698	183.999	235.345	240.971	299.337	305.280
			128.289	183.331	234.414	240.017	297.884	303.995
		0.2	81.585	111.263	137.310	142.265	172.778	174.854
			81.177	110.699	136.614	141.531	171.828	173.966
	0.5	0.01	190.950	338.680	412.704	562.705	595.343	714.797
			190.942	338.662	412.663	562.649	595.274	714.458
		0.1	131.787	206.519	235.513	301.282	308.754	351.220
			131.375	205.763	234.581	300.052	307.465	349.689
		0.2	83.875	123.782	137.478	174.624	177.207	199.408
			83.457	123.157	136.780	173.724	176.299	198.360
$\pi/3$	0.1	0.01	75.446	144.535	148.168	232.609	241.981	249.047
			75.445	144.531	148.163	232.571	241.913	249.029
		0.1	62.528	108.630	111.010	159.963	165.055	168.299
			62.412	108.355	110.727	159.482	164.547	167.779
		0.2	45.626	72.893	74.286	102.082	104.975	106.345
			45.452	72.576	73.962	101.611	104.487	105.855
	0.5	0.01	105.752	158.638	244.380	261.876	314.714	356.592
			105.750	158.636	244.320	261.859	314.706	356.056
		0.1	82.358	116.931	166.237	170.200	198.807	222.455
			82.164	116.624	165.724	169.620	198.127	221.583
		0.2	56.839	77.703	104.312	105.637	121.749	135.978
			56.594	77.357	103.806	105.145	121.160	135.295
$2\pi/3$	0.1	0.01	38.012	62.713	89.381	94.465	126.441	131.603
			38.009	62.712	89.369	94.448	126.422	131.473
		0.1	34.256	54.054	73.832	77.539	99.820	102.837
			34.218	53.974	73.698	77.387	99.601	102.533
		0.2	27.680	41.137	53.606	56.086	69.667	71.425
			27.602	41.001	53.406	55.878	69.392	71.118
	0.5	0.01	91.939	101.566	119.265	145.865	190.312	245.765
			91.936	101.564	119.268	145.796	180.886	224.242
		0.1	72.487	79.332	91.980	110.293	135.514	162.456
			72.317	79.149	91.761	109.959	132.549	158.272
		0.2	50.006	54.905	63.516	75.172	89.695	99.395
			49.788	54.674	63.253	74.838	88.418	98.91

†: Present ‡: Liew and Liu (2000)

Table 3.7 Comparison of first six natural frequencies for the boundary condition $CSCS$

Θ	μ	λ	ω_1'	ω_2'	ω_3'	ω_4'	ω_5'	ω_6'
$\pi/6$	0.1	0.01†	113.916	205.174	302.087	313.937	442.254	459.651
		‡	113.912	205.158	302.082	313.934	441.102	459.708
		0.1	93.615	153.002	207.485	213.706	275.690	284.143
			93.450	152.635	206.900	213.083	274.652	283.188
		0.2	68.170	102.981	133.466	136.232	166.975	168.683
			67.933	102.556	132.862	135.609	165.947	167.818
	0.5	0.01	135.050	298.004	303.815	482.125	534.046	568.899
			135.047	297.984	303.798	482.085	533.976	568.787
		0.1	103.913	192.218	207.865	289.448	294.305	331.518
			103.682	191.593	207.276	288.449	293.159	330.323
		0.2	72.430	119.969	133.585	172.907	174.762	175.606
			72.152	119.412	132.981	172.041	173.780	174.731
$\pi/3$	0.1	0.01	51.153	111.805	113.916	193.011	197.912	205.174
			51.149	111.796	113.912	192.926	197.884	205.158
		0.1	45.890	91.925	93.615	144.610	148.483	153.002
			45.840	91.764	93.450	144.269	148.134	152.635
		0.2	36.885	66.891	68.170	97.834	100.728	102.981
			36.787	66.656	67.933	97.433	100.317	102.556
	0.5	0.01	98.589	135.050	204.838	257.277	298.004	303.944
			98.586	135.047	204.817	257.257	297.984	303.798
		0.1	77.082	103.913	150.782	167.893	192.218	207.924
			76.902	103.682	150.413	167.327	191.593	207.276
		0.2	53.321	72.430	101.527	103.517	119.969	133.610
			53.099	72.152	101.108	103.024	119.412	132.981
$2\pi/3$	0.1	0.01	31.739	51.153	79.760	83.069	111.805	113.958
			31.730	51.149	79.752	83.049	111.796	113.912
		0.1	28.598	45.890	68.589	68.880	91.925	93.643
			28.570	45.840	68.489	68.764	91.764	93.450
		0.2	23.733	36.885	51.148	52.250	66.891	68.185
			23.678	36.787	50.975	52.087	66.656	67.933
	0.5	0.01	91.201	98.589	112.754	135.075	168.877	213.429
			91.198	98.586	112.749	135.047	165.879	204.813
		0.1	71.900	77.082	87.538	103.932	126.735	155.797
			71.730	76.902	87.339	103.682	125.174	150.412
		0.2	49.513	53.321	61.052	72.442	86.898	99.284
			49.296	53.099	60.813	72.152	85.948	98.802

†: Present ‡: Liew and Liu (2000)

Table 3.8 Comparison of first six natural frequencies for the boundary condition $CFCF$

Θ	μ	λ	ω_1'	ω_2'	ω_3'	ω_4'	ω_5'	ω_6'
$\pi/6$	0.1	0.01†	26.177	58.147	73.560	132.549	145.599	215.000
		‡	25.208	57.687	71.714	134.539	142.769	214.384
		0.1	23.716	45.815	60.991	96.174	109.986	148.521
			22.899	44.274	59.550	96.968	107.901	152.784
		0.2	19.356	33.055	44.385	64.848	74.338	93.018
			18.907	30.786	43.501	62.626	73.053	93.078
	0.5	0.01	88.392	110.811	226.756	243.429	274.934	418.069
			87.768	113.532	225.328	241.877	280.166	414.370
		0.1	70.013	82.451	158.406	160.074	175.759	249.381
			69.340	83.530	157.007	159.210	177.555	247.316
		0.2	48.326	55.218	97.214	105.626	109.058	151.085
			47.924	55.145	96.171	105.689	109.390	150.750
$\pi/3$	0.1	0.01	26.592	37.757	74.253	87.349	93.044	146.472
			25.948	37.927	73.138	87.650	94.937	144.922
		0.1	23.995	32.923	61.414	73.212	74.853	110.507
			23.333	32.377	60.356	73.172	75.670	109.074
		0.2	19.523	26.288	44.537	54.201	55.054	74.517
			19.111	25.558	43.790	54.719	54.829	73.532
	0.5	0.01	88.857	92.936	122.985	173.775	243.558	252.807
			88.299	95.342	122.393	176.818	242.992	252.931
		0.1	70.213	73.121	92.612	129.057	160.050	163.269
			69.744	73.872	91.885	129.168	158.774	164.194
		0.2	48.430	50.401	63.225	87.597	97.536	100.783
			48.080	50.551	62.967	87.122	96.732	100.911
$2\pi/3$	0.1	0.01	26.824	29.893	42.973	67.810	75.419	98.062
			26.607	29.742	43.782	68.445	74.154	80.196
		0.1	24.717	25.270	38.789	58.764	61.602	66.633
			23.917	26.425	38.813	58.885	61.216	65.904
		0.2	19.899	21.011	31.285	44.693	45.213	48.753
			19.426	21.569	31.362	44.309	45.102	48.653
	0.5§	0.01	89.135	96.952	107.198	127.603	156.414	204.405
			88.596	90.300	96.821	109.012	128.056	155.011
		0.1	70.432	75.678	83.102	97.568	116.068	144.340
			69.969	70.954	75.206	83.556	97.139	116.047
		0.2	48.543	51.940	57.641	67.356	79.566	95.996
			48.176	48.823	51.613	57.522	67.088	79.603

†: Present ‡: Liew and Liu (2000) §: Large differences after first mode

Table 3.9 Comparison of first six natural frequencies for the boundary condition $FSFS$, $\mu = 0.00001$

Θ	λ	ω_1'	ω_2'	ω_3'	ω_4'	ω_5'	ω_6'
$\pi/6$	0.1†	42.949	101.638	137.065	160.702	222.313	225.700
	‡	43.493	101.415	137.540	160.460	222.073	225.456
	0.2	36.337	75.217	97.021	109.375	141.402	144.275
		36.449	74.991	96.897	109.170	141.174	144.092
$\pi/3$	0.1	11.811	42.949	48.257	86.160	94.660	101.638
		12.220	43.493	48.012	86.722	94.404	101.415
	0.2	11.239	36.337	40.044	65.980	71.067	75.217
		11.397	36.449	39.802	65.977	70.854	74.991
$\pi/2$	0.1	5.033	20.522	33.057	42.951	64.954	70.750
		5.387	20.991	32.775	43.495	64.722	71.305
	0.2	5.031	18.747	28.720	36.337	51.675	55.870
		5.183	18.905	28.457	36.449	51.442	55.892

†Present; ‡Xiang et al. (1993)

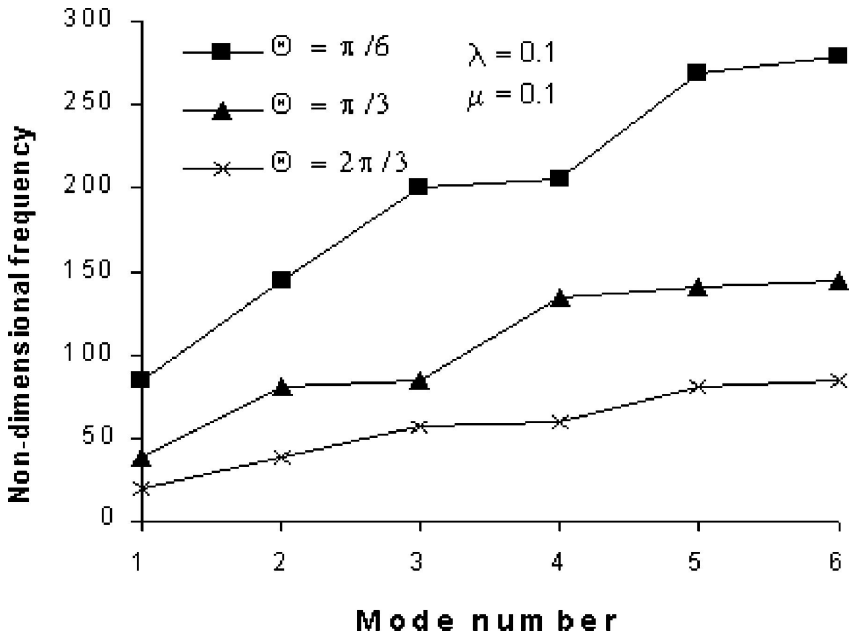

Fig. 3.3 Effect of sector angle Θ on frequencies of $SSSS$ plates

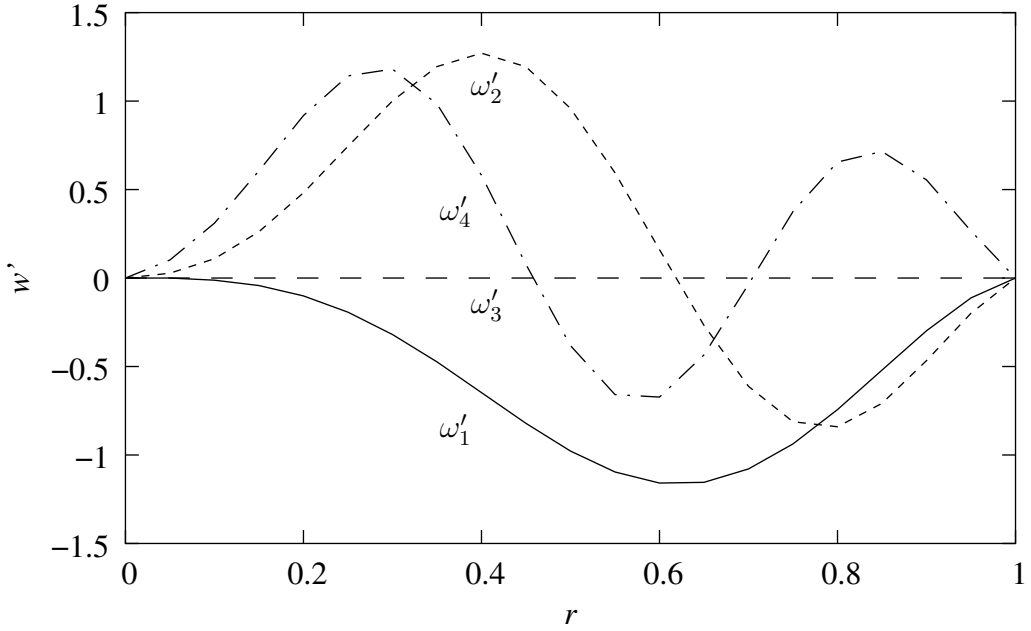

Fig. 3.4 Mode shapes along the radial line at $\theta = 0.5$ of $CCCC$ plates, $\Theta = \pi/3$, $\mu = 0.1$, $\lambda = 0.1$

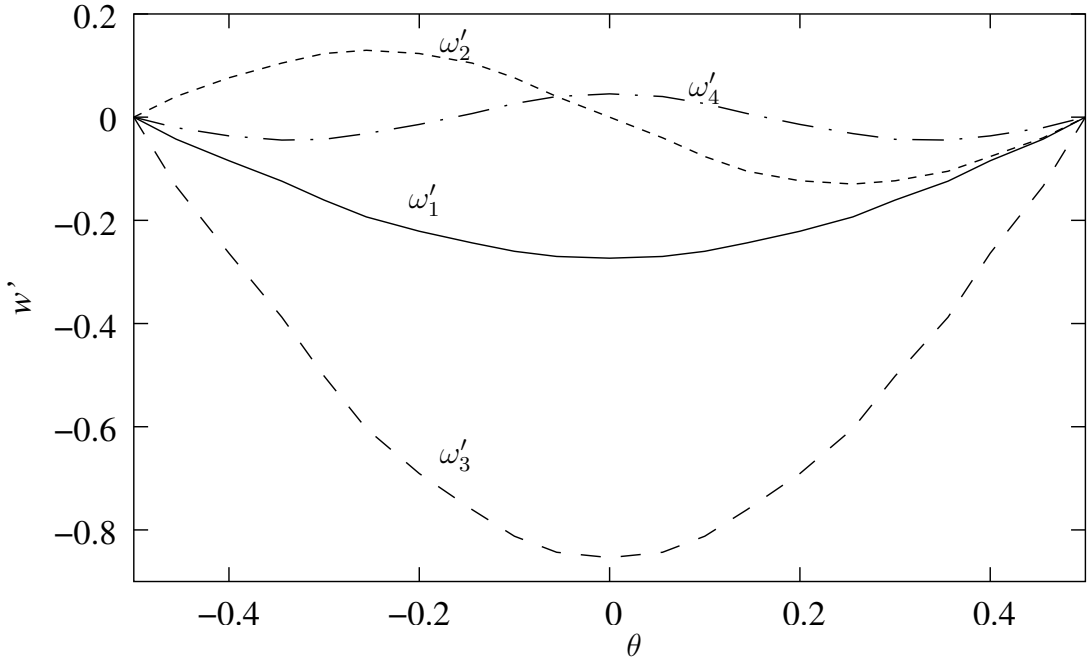

Fig. 3.5 Mode shapes along the arc at $r = 0.5$ of $FSFS$ plates, $\Theta = \pi/2$, $\mu = 0.00001$, $\lambda = 0.1$

CHAPTER 4
LINEAR VIBRATION AND BUCKLING OF LAMINATED COMPOSITE SECTOR PLATES

4.1 Introduction

The methodology developed in Chapter 4 for the linear eigenvalue problem of buckling and free vibration analysis of shear deformable isotropic plates is extended here to laminated sector plates made up of cylindrically orthotropic layers. Several combinations of simply supported, clamped and free edge conditions are considered. Convergence study has been carried out and the obtained results are compared with the results of laminated square plates and isotropic sector plates available in literature. Effects of boundary conditions, number of layers, moduli ratio, rotary and in-plane inertia, plate thickness, sector angle and annularity on free vibration and stability are studied.

Vibration analyses of both isotropic as well as anisotropic and non-homogeneous rectangular plates have been carried out extensively (Yamada and Irie, 1987; Khdeir and Librescu, 1988; Tauchert, 1991; Reddy, 1997; Auricchio and Sacco, 1999). Both linear formulations involving different kinds of complicating effects (Khdeir, 1989; Xiang and Wei, 2002) as well as non-linear (Sathyamoorthy, 1987; Nath and Shukla, 2001b,a) studies are being reported.

Nath and Kumar (1998, 2000) have presented non-linear analysis of laminated axisymmetric shells. Rubin (1978) studied the stability of orthotropic sector plates.

Turvey and Marshall (1995) has given a comprehensive monograph for buckling analysis of composite plates. It is clear from literature that there is a need for an analytical solution that handles several kinds of boundary conditions as well as non-isotropy and non-homogeneity of the material in the free vibration and buckling analysis of sector plates. The present chapter is devoted to the vibration and stability of laminated composite sector plates comprising cylindrically orthotropic layers. The presence of material coupling makes the governing equations coupled, and hence, the formulation is more involved.

The eigenvalue problem is formulated by discretizing the governing equilibrium equations and boundary conditions with the help of two-dimensional Chebyshev polynomials (Nath and Kumar, 1995) and then solved using the procedure given by Wilkinson and Reinsch (1971) for non-symmetric matrices.

4.2 Governing Equations

The equations of motion for linear free vibration analysis of laminated sector plates are obtained from equations (1.14)- (1.18) after ignoring the non-linear terms and piezothermal effects. After making use of equations (1.3)– (1.6) and (1.21)– (1.26), the equations of motion in terms of displacement components become,

$$
\begin{aligned}
&A_{11}\frac{\zeta^2}{\zeta'^2}u_{,rr}+2A_{16}\frac{\zeta}{\zeta'\Theta}u_{,r\theta}+A_{66}\frac{1}{\Theta^2}u_{,\theta\theta}+A_{11}\frac{\zeta}{\zeta'}u_{,r}-A_{22}u\\
&+A_{16}\frac{\zeta^2}{\zeta'^2}v_{,rr}+(A_{12}+A_{66})\frac{\zeta}{\zeta'\Theta}v_{,r\theta}+A_{26}\frac{1}{\Theta^2}v_{,\theta\theta}-A_{26}\frac{\zeta}{\zeta'}v_{,r}\\
&-(A_{22}+A_{66})\frac{1}{\Theta}v_{,\theta}-A_{26}v+B_{11}\frac{\zeta^2}{\zeta'^2}\phi_{r,rr}+2B_{16}\frac{\zeta}{\zeta'\Theta}\phi_{r,r\theta}\\
&+B_{66}\frac{1}{\Theta^2}\phi_{r,\theta\theta}+B_{11}\frac{\zeta}{\zeta'}\phi_{r,r}-B_{22}\phi_r+B_{16}\frac{\zeta^2}{\zeta'^2}\phi_{\theta,rr}\\
&+(B_{12}+B_{66})\frac{\zeta}{\zeta'\Theta}\phi_{\theta,r\theta}+B_{26}\frac{1}{\Theta^2}\phi_{\theta,\theta\theta}-B_{26}\frac{\zeta}{\zeta'}\phi_{\theta,r}
\end{aligned}
$$

$$-\left(B_{22}+B_{66}\right)\frac{1}{\Theta}\phi_{\theta,\theta}-B_{26}\phi_{\theta}=\zeta^2 r_o^2\left(I_0\frac{d^2u}{dt^2}+I_1\frac{d^2\phi_r}{dt^2}\right) \tag{4.1}$$

$$\begin{aligned}
&A_{16}\frac{\zeta^2}{\zeta'^2}u_{,rr}+\left(A_{12}+A_{66}\right)\frac{\zeta}{\zeta'\Theta}u_{,r\theta}+A_{26}\frac{1}{\Theta^2}u_{,\theta\theta}+\left(2A_{16}+A_{26}\right)\frac{\zeta}{\zeta'}u_{,r}\\
&+\left(A_{22}+A_{66}\right)\frac{1}{\Theta}u_{,\theta}-A_{26}u+A_{66}\frac{\zeta^2}{\zeta'^2}v_{,rr}+2A_{26}\frac{\zeta}{\zeta'\Theta}v_{,r\theta}+A_{22}\frac{1}{\Theta^2}v_{,\theta\theta}\\
&-A_{66}\frac{\zeta}{\zeta'}v_{,r}-A_{66}v+B_{16}\frac{\zeta^2}{\zeta'^2}\phi_{r,rr}+\left(B_{12}+B_{66}\right)\frac{\zeta}{\zeta'\Theta}\phi_{r,r\theta}+B_{26}\frac{1}{\Theta^2}\phi_{r,\theta\theta}\\
&+\left(2B_{16}+B_{26}\right)\frac{\zeta}{\zeta'}\phi_{r,r}+\left(B_{22}+B_{66}\right)\frac{1}{\Theta}\phi_{r,\theta}-B_{26}\phi_r+B_{66}\frac{\zeta^2}{\zeta'^2}\phi_{\theta,rr}\\
&+2B_{26}\frac{\zeta}{\zeta'\Theta}\phi_{\theta,r\theta}+B_{22}\frac{1}{\Theta^2}\phi_{\theta,\theta\theta}-B_{66}\frac{\zeta}{\zeta'}\phi_{\theta,r}-B_{66}\phi_{\theta}\\
&=\zeta^2 r_o^2\left(I_0\frac{d^2u}{dt^2}+I_1\frac{d^2\phi_r}{dt^2}\right)
\end{aligned} \tag{4.2}$$

$$\begin{aligned}
&k^2A_{55}\frac{\zeta^2}{\zeta'^2}w_{,rr}+2k^2A_{45}\zeta' w_{,r\theta}+k^2A_{44}\frac{1}{\Theta^2}\frac{\partial^2 w}{\partial\theta^2}+k^2A_{55}\frac{\zeta}{\zeta'}w_{,r}\\
&+k^2A_{55}\frac{\zeta^2 r_o}{\zeta'}\phi_{r,r}+k^2A_{45}\frac{\zeta r_o}{\Theta}\phi_{r,\theta}+k^2A_{55}\zeta r_o\phi_r\\
&+k^2A_{45}\frac{\zeta^2 r_o}{\zeta'}\phi_{\theta,r}+k^2A_{45}\frac{\zeta r_o}{\Theta}\phi_{\theta,\theta}+k^2A_{44}\zeta r_o\phi_{\theta}\\
&+N_{ip}\left[\left(\frac{\zeta^2}{\zeta'^2}w_{,rr}\right)+\left(\frac{\zeta}{\zeta'}w_{,r}\right)+\frac{1}{\Theta^2}\frac{\partial^2 w}{\partial\theta^2}\right]=\zeta^2 r_o^2 I_0\frac{d^2w}{dt^2}
\end{aligned} \tag{4.3}$$

$$\begin{aligned}
&B_{11}\frac{\zeta^2}{\zeta'^2}u_{,rr}+2B_{16}\frac{\zeta}{\zeta'\Theta}u_{,r\theta}+B_{66}\frac{1}{\Theta^2}u_{,\theta\theta}+B_{11}\frac{\zeta}{\zeta'}u_{,r}-B_{22}u\\
&+B_{16}\frac{\zeta^2}{\zeta'^2}v_{,rr}+\left(B_{12}+B_{66}\right)\frac{\zeta}{\zeta'\Theta}v_{,r\theta}+B_{26}\frac{1}{\Theta^2}v_{,\theta\theta}-B_{26}\frac{\zeta}{\zeta'}v_{,r}\\
&-\left(B_{22}+B_{66}\right)\frac{1}{\Theta}v_{,\theta}-B_{26}v-k^2A_{55}\frac{\zeta^2 r_o}{\zeta'}w_{,r}-k^2A_{45}\frac{\zeta r_o}{\Theta}w_{,\theta}\\
&+D_{11}\frac{\zeta^2}{\zeta'^2}\phi_{r,rr}+2D_{16}\frac{\zeta}{\zeta'\Theta}\phi_{r,r\theta}+D_{66}\frac{1}{\Theta^2}\phi_{r,\theta\theta}+D_{11}\frac{\zeta}{\zeta'}\phi_{r,r}-D_{22}\phi_r\\
&-k^2A_{55}\zeta^2 r_o^2\phi_r+D_{16}\frac{\zeta^2}{\zeta'^2}\phi_{\theta,rr}+\left(D_{12}+D_{66}\right)\frac{\zeta}{\zeta'\Theta}\phi_{\theta,r\theta}\\
&+D_{26}\frac{1}{\Theta^2}\phi_{\theta,\theta\theta}-D_{26}\frac{\zeta}{\zeta'}\phi_{\theta,r}-\left(D_{22}+D_{66}\right)\frac{1}{\Theta}\phi_{\theta,\theta}-D_{26}\phi_{\theta}\\
&-k^2A_{45}\zeta^2 r_o^2\phi_{\theta}=\zeta^2 r_o^2\left(I_2\frac{d^2\phi_r}{dt^2}+I_1\frac{d^2u}{dt^2}\right)
\end{aligned} \tag{4.4}$$

$$B_{16}\frac{\zeta^2}{\zeta'^2}u_{,rr}+\left(B_{12}+B_{66}\right)\frac{\zeta}{\zeta'\Theta}u_{,r\theta}+B_{26}\frac{1}{\Theta^2}u_{,\theta\theta}+\left(2B_{16}+B_{26}\right)\frac{\zeta}{\zeta'}u_{,r}$$

$$
\begin{aligned}
&+(B_{22}+B_{66})\frac{1}{\Theta}u_{,\theta}-B_{26}u+b_{66}\frac{\zeta^2}{\zeta'^2}v_{,rr}+2B_{26}\frac{\zeta}{\zeta'\Theta}v_{,r\theta}+B_{22}\frac{1}{\Theta^2}v_{,\theta\theta}\\
&-B_{66}\frac{\zeta}{\zeta'}v_{,r}-B_{66}v-k^2A_{45}\frac{\zeta^2 r_o}{\zeta'}w_{,r}-k^2A_{55}\frac{\zeta r_o}{\Theta}w_{,\theta}+D_{16}\frac{\zeta^2}{\zeta'^2}\phi_{r,rr}\\
&+(D_{12}+D_{66})\frac{\zeta}{\zeta'\Theta}\phi_{r,r\theta}+D_{26}\frac{1}{\Theta^2}\phi_{r,\theta\theta}+(2D_{16}+D_{26})\frac{\zeta}{\zeta'}\phi_{r,r}\\
&+(D_{22}+D_{66})\frac{1}{\Theta}\phi_{r,\theta}-D_{26}\phi_r-k^2A_{45}\zeta^2r_o^2\phi_r+D_{66}\frac{\zeta^2}{\zeta'^2}\phi_{\theta,rr}\\
&+2D_{26}\frac{\zeta}{\zeta'\Theta}\phi_{\theta,r\theta}+D_{22}\frac{1}{\Theta^2}\phi_{\theta,\theta\theta}-D_{66}\frac{\zeta}{\zeta'}\phi_{\theta,r}-D_{66}\phi_\theta-k^2A_{44}\zeta^2r_o^2\phi_\theta\\
&=\zeta^2r_o^2\left(I_2\frac{d^2\phi_r}{dt^2}+I_1\frac{d^2u}{dt^2}\right)
\end{aligned}
\tag{4.5}
$$

For free vibration problems, inplane load $N_{ip}=0$. In the buckling analysis, the inertia terms in above equations (4.1)- (4.5) are ignored. The appropraite boundary conditions in equations (1.29)– (1.33) are discretized. The eigenvalue problem is formulated on the same lines as given in section 3.2 and solved using the procedure given by Wilkinson and Reinsch (1971).

4.3 Results and Discussions

This section gives the results of the eigenvalue problems resulting from free vibration and buckling analyses of moderately thick laminated composite sector plates. The effects of orthotropy, number of layers, annularity (μ), thickness ratio (λ), sector angle (Θ), rotary inertia and boundary conditions are studied. The boundary conditions considered are various combinations of simply supported (S), clamped (C) and free (F) edges.

Every layer is assumed to be cylindrically orthotropic. Thus with fibers oriented in radial direction, the required material properties are as follows unless otherwise

specified.

$$E_r/E_\theta = 40, \nu_{r\theta} = 0.25, G_{r\theta} = G_{zr} = 0.6E_\theta, G_{\theta z} = 0.5E_\theta \tag{4.6}$$

The rotation of material axes by 90^oabout the global z-axis gives the material constants for a layer having fibers oriented in circumferential direction. Thus a ten layer $(n = 10)$ cross-ply antisymmetric plate denoted in rectangular domain by $(0^o/90^o)_5$ is represented here by $(R/C)_5$ with 'R' representing radial and 'C' representing circumferential orientation of the fiber.

Table 4.1 Convergence results for non-dimensional natural frequencies $\omega(1-\mu)^2 r_o^2\sqrt{\rho/E_\theta h^2}$ of $SSSS$ plate with respect to number of terms in series expansion, $n = 10$, $(RC)_5$, $\mu = 0.1$, $\lambda = 0.2$, $\Theta = \pi/3$

$(M+1)$	Mode sequence number					
$\times(N+1)$	1	2	3	4	5	6
80	12.36402	15.25554	17.95893	22.99828	25.19537	25.66754
120	12.36342	15.25569	17.90371	22.99736	25.19380	25.66610
168	12.36324	15.25601	17.87369	22.99695	25.19393	25.66603
224	12.36320	15.25606	17.84693	22.99687	25.19384	25.66606
288	12.36319	15.25599	17.82245	22.99685	25.19367	25.66609
324	12.36319	15.25589	17.80329	22.99685	25.19351	25.66610

Table 4.2 Convergence results for non-dimensional natural frequencies $\omega(1-\mu)^2 r_o^2\sqrt{\rho/E_\theta h^2}$ of $FSFS$ plate with respect to number of terms in series expansion, $n = 10$, $(RC)_5$, $\mu = 0.1$, $\lambda = 0.2$, $\Theta = \pi/3$

$(M+1)$	Mode sequence number					
$\times(N+1)$	1	2	3	4	5	6
80	6.760439	15.77599	16.06734	17.17089	18.44083	26.06850
120	6.765566	15.91724	15.93375	17.16948	18.44208	26.60386
168	6.767594	15.87374	15.97915	17.17088	18.44259	26.38041
224	6.768336	16.00553	16.37862	17.17111	18.44282	26.17791
288	6.768574	16.01627	16.10377	17.16955	18.44291	26.11672
324	6.768627	16.02031	16.30925	17.17047	18.44294	26.40108

The convergence study has been carried out and the results are shown in Tables 4.1- 4.3. Two more terms were used in r-dimension than the θ-dimension since

the equilibrium equations were multiplied with r^2 in order to remove r from the denominators of various terms. Tables 4.1 and 4.2 give the convergence of the lowest six frequencies for the vibration problem. Convergence to five significant digits is achieved in the fundamental frequency with ($M = 11$, $N = 9$) in Table 4.1 for $SSSS$ plate and to four significant digits with ($M = 15$, $N = 13$) in Table 4.2 for $FSFS$ plate. Table 4.3 gives the convergence of lowest critical buckling load for the boundary conditions $SSSS$. Convergence to five significant digits is achieved with ($M = 17$, $N = 15$). In the present study total 168 terms ($M = 13, N = 11$) gave satisfactory results for all the combinations of various parameters, and these are thus were taken as default values of M and N.

Table 4.3 Convergence results for non-dimensional critical buckling load $N_{cr}(1-\mu)^2 r_o^2/E_\theta h^3$ of $SSSS$ plate with respect to number of terms in series expansion, $n = 10$, $(RC)_5$, $\mu = 0.1$, $\lambda = 0.2$, $\Theta = \pi/3$

$(M+1)$ $\times(N+1)$	$N_{cr}(1-\mu)^2 r_o^2/E_\theta h^3$
80	7.117115
120	7.117316
168	7.117687
224	7.117802
288	7.117783
324	7.117724

The developed methodology is further validated in Table 4.4 by comparing the results of almost square sector plates with results for free vibration of laminated square plates of Khdeir (1989) using first order shear deformation theory. The results shown are for edge conditions $SSSS$, $SSCS$, $FSFS$ and $FSSS$. The two sets agree well within the range of 1%. The developed methodology was further validated by comparison with available results for isotropic sector plates and the results were given

Table 4.4 Comparison of results for natural frequencies of almost square sector plates, $n = 2$, (RC), $\mu = 0.99$, $\lambda = 0.001$, $\Theta = 0.01$

		$\omega(1-\mu)^2 r_o^2 \sqrt{\rho/E_\theta h^2}$			
n	E_r/E_θ	SSSS	SSCS	FSFS	FSSS
2,(R/C)	2†	6.614	7.761	3.339	4.043
	‡	6.82	7.739	3.309	4.035
	10	7.803	9.375	4.627	5.119
		7.766	9.352	4.584	5.104
	20	8.852	10.683	5.563	5.958
		8.810	10.658	5.511	5.940
	30	9.741	11.742	6.309	6.645
		9.695	11.713	6.251	6.624
	40	10.522	12.640	6.944	7.237
		10.473	12.610	6.881	7.215
10,$(R/C)_5$	2	6.781	7.975	3.482	4.164
		6.749	7.953	3.451	4.156
	10	9.945	11.941	6.366	6.711
		9.899	11.911	6.307	6.691
	20	12.523	14.795	8.438	8.660
		12.466	14.758	8.365	8.634
	30	14.391	16.696	9.882	10.043
		14.327	16.652	9.800	10.014
	40	15.847	18.094	10.987	11.110
		15.779	18.044	10.900	11.079

†: Present ‡: Khdeir (1989)

in Tables 3.3 and 3.5- 3.9.

Tables 4.5 and 4.6 give the effect of number of layers n and moduli ratio E_r/E_θ on lowest six non-dimensional natural frequencies of sector plates with four combinations of clamped and simply supported edges. Tables 4.7 and 4.8 give similar results with one or two edges being free. There is increase in frequencies with the increase in non-homogeneity in terms of n as well as E_r/E_θ. It can be seen there is repetition of certain frequencies over variation of the three parameters - boundary conditions, number of layers n and moduli ratio E_r/E_θ. These repeating modes were found to be those of uncoupled in-plane vibrations. To verify this, all inertia elements in the equations

Table 4.5 Effect of n and E_r/E_θ on non-dimensional natural frequencies $\omega(1-\mu)^2 r_o^2\sqrt{\rho/E_\theta h^2}$ of sector plates with $CCCC$ and $CSCS$ edge conditions, $\mu = 0.1$, $\lambda = 0.2$, $\Theta = \pi/3$

Lamination scheme	E_r/E_θ	Mode sequence number					
		1	2	3	4	5	6
$CCCC$:							
(R/C)	2	13.095	20.964	21.354	25.652	25.789	29.408
	10	14.629	22.846	22.952	31.576	31.684	32.197
	20	15.395	23.819	23.868	32.859	32.896	33.275
	30	15.829	24.350	24.457	33.504	33.679	33.909
	40	16.113	24.720	24.846	33.913	34.216	34.331
$(R/C)_5$	2	13.305	21.274	21.676	25.679	25.990	29.824
	10	15.717	24.181	24.480	33.374	34.068	34.163
	20	16.445	25.147	25.411	34.375	35.065	35.308
	30	16.747	25.579	25.844	34.778	35.485	35.826
	40	16.912	25.827	26.103	34.996	35.719	36.125
$CSCS$:							
(R/C)	2	10.483	12.363	18.795	19.461	21.014	22.997
	10	11.999	12.363	20.658	21.606	22.997	29.957
	20	12.363	12.920	21.829	22.839	22.997	31.355
	30	12.363	13.533	22.592	22.997	23.603	32.171
	40	12.363	13.983	22.997	23.141	24.130	32.722
$(R/C)_5$	2	10.706	12.363	19.425	19.843	20.796	22.997
	10	12.363	13.613	22.927	22.997	23.751	32.489
	20	12.363	14.844	22.997	24.274	25.068	33.719
	30	12.363	15.454	22.997	24.907	25.643	33.719
	40	12.363	15.828	22.997	25.280	25.971	33.719

of motion other than I_0 in the equations (4.1) and (4.2) in r and θ directions were made zero for $SSSS$ plate in Table 4.6 and for $CSFS$ plates in Table 4.8 for the results corresponding to lamination scheme $(R/C)_5$ and $E_r/E_\theta = 40$. The non-dimensional frequencies of the resulting two-dimensional ($u_{,tt}$, $v_{,tt}$) problem are thus shown in bold along with those of the actual five-dimensional problem for comparison. The frequencies of uncoupled in-plane vibrations have been shown italicized. These inplane frequencies remain unchanged since the extensional stiffnesses A_{ij} remain unaffected by the variations in n and E_r/E_θ.

Table 4.6 Effect of n and E_r/E_θ on non-dimensional natural frequencies $\omega(1-\mu)^2 r_o^2\sqrt{\rho/E_\theta h^2}$ of sector plates with $SSSS$ and $CSSS$ edge conditions, $\mu = 0.1$, $\lambda = 0.2$, $\Theta = \pi/3$

Lamination scheme	E_r/E_θ	Mode sequence number					
		1	2	3	4	5	6
$SSSS$:							
(R/C)	2	8.973	11.506	12.363	17.927	18.222	22.286
	10	10.348	12.363	14.691	20.175	20.177	22.997
	20	11.381	12.363	15.876	21.546	21.585	22.997
	30	12.123	12.363	16.519	22.413	22.513	22.997
	40	12.363	12.695	16.962	22.997	23.021	23.176
$(R/C)_5$	2	9.258	11.457	12.363	18.334	18.792	22.149
	10	12.336	12.363	14.983	22.524	22.937	22.997
	20	12.363	13.914	16.487	22.997	24.082	24.529
	30	12.363	14.742	17.314	22.997	24.787	25.251
	40	**12.363**	15.256	**17.874**	**22.997**	25.194	25.666
†	40	**12.363**	**17.868**	**22.997**	**32.605**	**33.719**	**44.512**
$CSSS$:							
(R/C)	2	8.978	11.514	12.363	17.943	18.222	22.286
	10	10.410	12.363	15.532	20.179	20.211	22.997
	20	11.481	12.363	18.290	21.598	21.624	22.997
	30	12.239	12.363	20.399	22.535	22.569	22.997
	40	12.363	12.817	22.042	22.997	23.203	23.359
$(R/C)_5$	2	9.263	11.465	12.363	18.354	18.792	22.149
	10	12.363	12.381	15.731	22.603	22.938	22.997
	20	12.363	13.980	18.789	22.997	24.164	24.532
	30	12.363	14.811	21.255	22.997	24.861	25.256
	40	12.363	15.321	22.997	23.409	25.260	25.672

†: only in-plane inertia acting

The effects of thickness ratio λ and annularity μ on the frequencies are shown in Tables 4.9 and 4.10. Here, when μ is increased from 0.1 to 0.5, the frequencies increase in the absolute sense after removal of the factor $(1-\mu)^2$ from the non-dimensionalization factor $(1-\mu)^2 r_o^2\sqrt{\rho/E_\theta h^2}$. These results also show that the non-dimensional frequencies decrease with increasing thickness parameter λ, but the absolute frequencies actually increase with increasing thickness.

Fig. 4.1 shows the effect of sector angle Θ on the fundamental natural frequency.

Table 4.7 Effect of n and E_r/E_θ on non-dimensional natural frequencies $\omega(1-\mu)^2 r_o^2\sqrt{\rho/E_\theta h^2}$ of sector plates with $FCFC$ and $SFSF$ edge conditions, $\mu = 0.1$, $\lambda = 0.2$, $\Theta = \pi/3$

Lamination scheme	E_r/E_θ	Mode sequence number					
		1	2	3	4	5	6
$FCFC$:							
(R/C)	2	6.289	13.224	13.336	15.174	17.455	21.238
	10	7.537	14.784	15.291	20.457	22.538	23.350
	20	8.214	15.539	16.579	23.759	24.030	24.607
	30	8.629	15.999	17.369	24.869	24.980	26.604
	40	8.918	16.323	17.906	25.352	25.688	27.767
$(R/C)_5$	2	6.416	13.447	13.622	15.101	17.651	21.578
	10	8.371	15.994	16.578	21.082	25.010	25.771
	20	9.154	16.879	17.879	25.862	26.143	27.942
	30	9.555	17.322	18.569	26.649	28.812	29.103
	40	9.814	17.604	19.022	26.967	29.328	29.493
$SFSF$:							
(R/C)	2	3.013	3.158	4.983	6.001	10.589	13.950
	10	4.154	4.487	6.318	7.361	12.902	15.900
	20	4.728	5.316	6.699	8.130	14.117	16.666
	30	5.103	5.857	6.960	8.509	14.875	17.158
	40	5.382	6.265	7.166	8.745	15.409	17.508
$(R/C)_5$	2	3.058	3.239	5.021	6.052	10.900	14.502
	10	4.948	5.009	7.140	7.450	14.949	17.314
	20	5.838	6.139	7.734	8.379	16.384	18.078
	30	6.270	6.906	8.060	8.821	17.026	18.479
	40	6.537	7.475	8.273	9.086	17.392	18.741

It can be seen that the frequency decreases with increasing span in terms of Θ in all plates except for the one having radial edges free - $SFSF$.

The effects of number of layers n and moduli ratio E_r/E_θ on non-dimensional isotropic critical buckling loads of sector plates with four combinations of clamped and simply supported edges are shown in Table 4.11. There is increase in critical buckling load with the increase in non-homogeneity in terms of n as well as E_r/E_θ. Table 4.12 shows the effects of μ, λ and Θ on the critical buckling loads. The non-dimensional critical buckling loads decrease with increasing μ and λ but the absolute

Table 4.8 Effect of n and E_r/E_θ on non-dimensional natural frequencies $\omega(1-\mu)^2 r_o^2\sqrt{\rho/E_\theta h^2}$ of sector plates with $CSFS$ and $SSFS$ edge conditions, $\mu = 0.1$, $\lambda = 0.2$, $\Theta = \pi/3$

Lamination scheme	E_r/E_θ	Mode sequence number					
		1	2	3	4	5	6
$CSFS$:							
(R/C)	2	0.899	3.369	10.708	10.731	12.056	16.725
	10	0.899	4.215	12.183	12.743	16.238	16.725
	20	0.899	4.754	13.411	13.877	16.725	18.854
	30	0.899	5.147	14.317	14.615	16.725	20.804
	40	0.899	5.460	15.022	15.151	16.725	22.375
$(R/C)_5$	2	0.899	3.455	10.977	11.371	11.672	16.725
	10	0.899	5.086	14.632	14.992	15.766	16.725
	20	0.899	6.038	16.071	16.725	16.864	18.620
	30	0.899	6.627	16.725	16.773	17.831	20.958
	40	**0.899**	7.050	**16.725**	17.208	18.432	**23.018**
†	40	**0.899**	**16.725**	**22.960**	**27.770**	**33.875**	**38.691**
$SSFS$:							
(R/C)	2	0.899	3.368	10.708	10.722	12.051	16.725
	10	0.899	4.196	12.002	12.743	15.508	16.725
	20	0.899	4.711	13.039	13.873	16.686	16.725
	30	0.899	5.083	13.798	14.605	16.725	17.286
	40	0.899	5.377	14.388	15.133	16.725	17.681
$(R/C)_5$	2	0.899	3.454	10.977	11.363	11.665	16.725
	10	0.899	5.068	14.632	14.704	15.264	16.725
	20	0.899	5.967	16.067	16.192	16.725	16.960
	30	0.899	6.482	16.725	16.758	16.945	17.887
	40	0.899	6.822	16.725	17.176	17.425	18.477

†: only in-plane inertia acting

critical buckling loads increase with increasing μ and λ. Similar trend was observed for the non-dimensional frequencies. The critical buckling load always decreases with increasing span in terms of Θ. This decrease is largest for the most flexible edge condition $SSSS$ and smallest for the stiffest edge condition $CCCC$.

Table 4.13 gives the effect of ignoring in-plane and rotary inertias on the lowest ten natural frequencies of $SSSS$ and $CCCC$ plates. In $CCCC$ plates the ignoring of in-plane inertia and then additionally rotary inertia raise all the frequencies by less

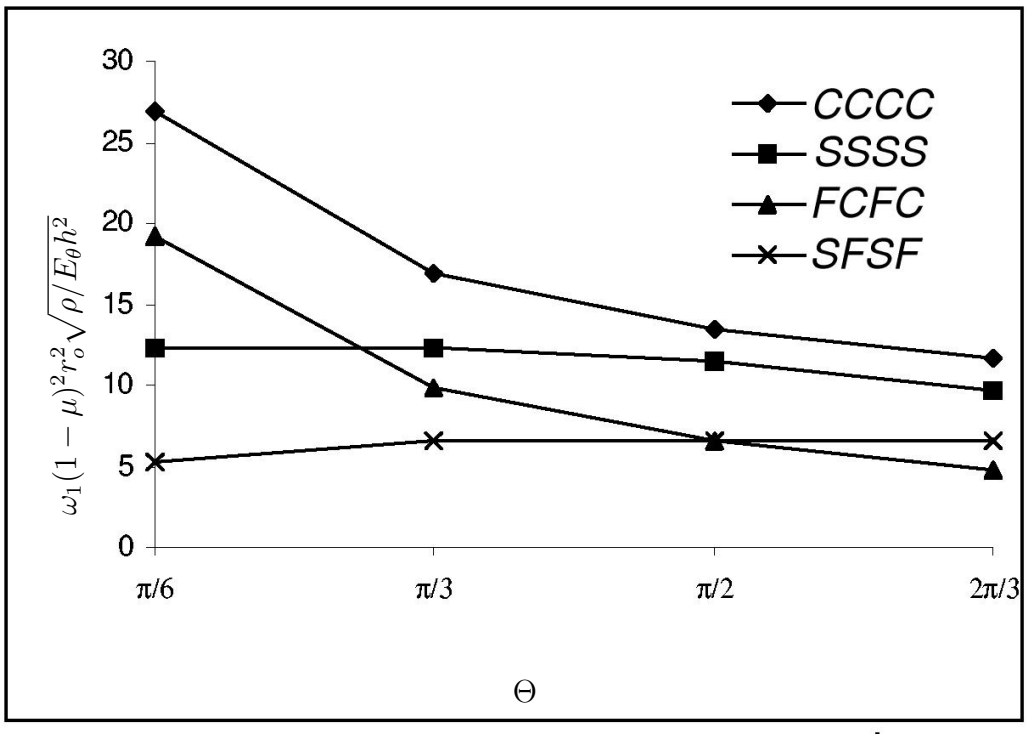

Fig. 4.1 Effect of Θ on non-dimensional fundamental natural frequency $\omega_1(1-\mu)^2 r_o^2\sqrt{\rho/E_\theta h^2}$ of sector plates with combinations of clamped, simply supported and free edges, $n = 10$, $(R/C)_5$, $E_r/E_\theta = 40$, $\lambda = 0.2$, $\mu = 0.1$

than 0.5%. In $SSSS$ plates ignoring of rotary inertia raises all the frequencies by less than 0.5%, but including in-plane inertia introduces certain frequencies of uncoupled in-plane vibrations which are absent from the other two cases considered here.

4.4 Conclusions

Chebyshev series expansions comprising 14 terms in r–dimensions and 12 terms in θ–dimension for each of the five displacement components were found satisfactory for most of the given results. The methodology developed proved to be robust and efficient for all combinations of clamped and simply supported edge conditions and also gives correct free vibration results for two opposite edges being free and the other two either simply supported or clamped. As an unexpected byproduct, accurate results

in terms of critical buckling loads and natural frequencies of laminated composite square plates were also obtained.

Frequencies and buckling loads increase with increasing constraint in terms of boundary conditions and non-homogeneity of the material. The effect of inplane inertia on natural frequencies is dependent on boundary conditions. The effect of rotary inertia is negligible (less than 0.5%).

Table 4.9 Effect of λ and μ on non-dimensional natural frequencies $\omega(1-\mu)^2 r_o^2\sqrt{\rho/E_\theta h^2}$ of sector plates with $CCCC$, $SSSS$, $CSSS$ and $CSCS$ edge conditions, $n = 10$, $(R/C)_5$, $E_r/E_\theta = 40$, $\Theta = \pi/3$

		Mode sequence number					
λ	μ	1	2	3	4	5	6
$CCCC$:							
.2	0.1	16.912	25.827	26.103	34.996	35.719	36.125
	0.5	6.169	8.335	10.952	11.103	12.469	13.916
0.1	0.1	31.063	48.085	48.540	66.492	67.688	67.778
	0.5	11.611	15.621	20.843	21.098	23.686	26.774
0.01	0.1	70.061	131.034	132.817	209.955	213.194	213.588
	0.5	30.413	42.818	66.041	75.149	82.599	95.771
$SSSS$:							
.2	0.1	12.363	15.256	17.874	22.997	25.194	25.666
	0.5	4.526	5.690	6.190	7.847	8.122	10.841
0.1	0.1	23.542	24.726	35.753	43.973	44.807	45.994
	0.5	9.048	9.240	12.380	14.084	15.702	20.102
0.01	0.1	32.950	80.714	81.747	146.511	149.461	152.020
	0.5	14.103	24.953	45.986	50.504	56.406	72.422
$CSSS$:							
.2	0.1	12.363	15.321	22.997	23.409	25.260	25.672
	0.5	5.733	6.190	8.156	10.851	10.974	12.224
0.1	0.1	23.713	24.726	44.256	44.819	45.994	46.880
	0.5	9.734	12.380	14.413	20.275	20.332	23.322
0.01	0.1	32.957	81.140	81.747	149.005	149.461	152.020
	0.5	19.447	27.324	46.263	61.078	65.585	72.422
$CSCS$:							
.2	0.1	12.363	15.828	22.997	25.280	25.971	33.719
	0.5	5.958	6.190	8.297	10.852	11.076	12.224
0.1	0.1	24.726	26.539	45.052	45.994	46.795	64.262
	0.5	10.825	12.380	15.126	20.474	20.804	23.396
0.01	0.1	44.831	96.755	99.805	169.006	171.967	173.459
	0.5	28.395	35.281	54.054	74.190	78.093	81.545

Table 4.10 Effect of λ and μ on non-dimensional natural frequencies $\omega(1-\mu)^2 r_o^2\sqrt{\rho/E_\theta h^2}$ of sector plates with $FCFC$, $SFSF$ and $CFCF$ edge conditions, $n = 10$, $(R/C)_5$, $E_r/E_\theta = 40$, $\Theta = \pi/3$

		Mode sequence number					
λ	μ	1	2	3	4	5	6
$FCFC$:							
.2	0.1	9.814	17.604	19.022	26.967	29.328	29.493
	0.5	2.874	4.675	5.209	7.103	7.515	8.178
0.1	0.1	16.125	31.069	32.864	48.827	52.400	53.757
	0.5	4.705	8.237	9.361	14.204	14.913	15.066
0.01	0.1	26.729	65.853	67.176	126.189	127.602	130.000
	0.5	7.917	18.436	20.707	35.562	38.880	38.945
$SFSF$:							
.2	0.1	6.537	7.475	8.273	9.086	17.392	18.741
	0.5	2.681	4.177	4.784	4.877	6.003	7.566
0.1	0.1	9.784	11.644	14.964	18.173	29.713	31.911
	0.5	5.367	8.037	8.198	8.362	12.007	12.229
0.01	0.1	13.016	14.982	50.913	54.671	57.529	112.487
	0.5	12.818	13.076	18.495	35.188	49.728	50.084
$CFCF$:							
.2	0.1	8.496	9.512	11.746	17.521	19.131	21.665
	0.5	5.197	5.274	6.090	7.853	10.313	10.392
0.1	0.1	14.765	15.855	23.496	31.538	33.618	40.584
	0.5	9.914	9.988	12.181	13.442	19.074	19.856
0.01	0.1	26.826	28.053	70.637	76.370	76.997	134.590
	0.5	27.750	27.891	30.897	43.807	67.655	73.720

Table 4.11 Effect of n and E_r/E_θ on non-dimensional isotropic critical buckling load $N_{cr}(1-\mu)^2 r_o^2/E_\theta h^3$ of sector plates with combinations of clamped and simply supported edges, $\mu = 0.1$, $\lambda = 0.2$, $\Theta = \pi/3$

n, fiber		Boundary conditions			
orientation	E_r/E_θ	$CCCC$	$CSCS$	$SSSS$	$CSSS$
2, (R/C)	2	4.8394	3.8754	2.6736	3.2610
	10	6.1226	5.0890	3.6089	4.2955
	20	6.8289	5.8595	4.2939	4.9863
	30	7.2609	6.3677	4.8057	5.4689
	40	7.5578	6.7347	5.2128	5.8354
2, $(R/C)_5$	2	4.9862	3.9990	2.7787	3.3759
	10	7.1371	6.0918	4.7754	5.3765
	20	7.9346	7.0461	5.9831	6.4221
	30	8.2908	7.5238	6.6706	6.9926
	40	8.4942	7.8166	7.1177	7.3620

Table 4.12 Effect of μ, λ and Θ on non-dimensional isotropic critical buckling load $N_{cr}(1-\mu)^2 r_o^2/E_\theta h^3$ of sector plates with combinations of clamped and simply supported edges, $n = 10$, $(R/C)_5$, $E_r/E_\theta = 40$

			Boundary conditions			
λ	μ	Θ	$CCCC$	$CSCS$	$SSSS$	$CSSS$
0.2	0.1	$\pi/6$	8.905	8.623	8.275	8.348
	0.1	$\pi/3$	8.494	7.817	7.118	7.362
	0.1	$\pi/2$	8.145	7.163	6.298	6.648
	0.1	$2\pi/3$	7.861	6.655	5.785	6.155
	0.5	$\pi/6$	2.768	2.661	2.552	2.577
	0.5	$\pi/3$	2.681	2.481	2.345	2.397
	0.5	$\pi/2$	2.631	2.404	2.312	2.347
	0.5	$2\pi/3$	2.606	2.371	2.321	2.331
0.1	0.1	$\pi/6$	32.209	29.719	25.258	26.974
	0.1	$\pi/3$	27.481	23.027	16.975	19.716
	0.1	$\pi/2$	24.312	18.708	12.915	15.542
	0.1	$2\pi/3$	22.309	15.894	10.984	13.132
	0.5	$\pi/6$	10.103	9.105	7.721	8.245
	0.5	$\pi/3$	9.185	7.283	6.198	6.648
	0.5	$\pi/2$	8.816	6.664	6.179	6.316
	0.5	$2\pi/3$	8.610	6.481	6.198	6.261
0.01	0.1	$\pi/6$	274.543	202.934	82.371	132.804
	0.1	$\pi/3$	114.687	73.694	32.817	50.205
	0.1	$\pi/2$	75.696	44.035	20.281	30.982
	0.1	$2\pi/3$	60.185	32.014	16.052	22.623
	0.5	$\pi/6$	85.671	63.041	24.010	40.371
	0.5	$\pi/3$	51.997	21.095	14.305	16.398
	0.5	$\pi/2$	47.234	16.275	14.930	15.064
	0.5	$2\pi/3$	45.521	15.800	14.305	14.825

Table 4.13 Effect of ignoring in-plane and rotary inertia on non-dimensional natural frequencies $\omega(1-\mu)^2 r_o^2\sqrt{\rho/E_\theta h^2}$ of $CCCC$ and $SSSS$, $\lambda = 0.2$, $\mu = 0.1$, $\Theta = \pi/3$, $n = 10$, $(R/C)_5$, $E_r/E_\theta = 40$

Mode sequence number	$CCCC$			$SSSS$		
	Inertias ignored			Inertias ignored		
	None	In-plane	In-plane and rotary	None	In-plane	In-plane and rotary
1	16.91189	16.91204	16.91984	12.36324	15.26163	15.3217
2	25.82682	25.82768	25.87536	15.25601	25.19409	25.25778
3	26.10315	26.10473	26.18344	17.87369	25.66957	25.73206
4	34.99554	34.9962	35.02473	22.99695	34.49812	34.5652
5	35.71939	35.72054	35.77799	25.19393	35.3995	35.46227
6	36.12453	36.12743	36.21512	25.66603	36.05172	36.10947
7	43.95235	43.95306	43.99203	32.60073	43.61446	43.67999
8	44.99661	44.99819	45.06566	33.71909	44.79206	44.85464
9	45.71234	45.71438	45.78685	34.49660	45.62321	45.68109
10	46.35041	46.35245	46.41758	35.39660	46.29722	46.35353

CHAPTER 5
NON-LINEAR STATIC ANALYSIS OF ISOTROPIC SECTOR PLATES

5.1 Introduction

Non-linear static analysis of moderately thick sector plates under uniformly distributed loading is presented. Using the first order shear deformation theory and von-Kármán type non-linearity, the governing equations of equilibrium are developed and expressed in terms of displacement components. Chebyshev polynomials are used for spatial discretization of the differential equations. An iterative incremental approach based on Newton-Raphson method is used for the solution. Convergence study is carried out. Effects of annularity, thickness ratio, sector angle and boundary conditions are investigated. Results are compared with those available from the literature.

A considerable amount of literature exists on the non-linear analysis of composite rectangular plates and, excellent reviews are given by Chia (1988); Tauchert (1991); Noor and Burton (1992) and Argyris and Tenek (1997), and a monograph by Turvey and Marshall (1995). The governing equations of sector plate undergoing moderately large deflections are more complicated than rectangular plate equations and are not amenable to closed form or exact solutions and, finite element, finite difference etc., are used as a necessity. In spite of being well-established numerical methods, non-linear studies pertaining to sector plates are quite limited in extent. The stud-

ies for large deflection analysis of moderately thick sector plates are due to Turvey and Salehi (1990) and Salehi and Shahidi (1994). They have employed the Dynamic Relaxation (DR) technique for the non-linear static analysis of sector plates. Turvey and Salehi (1998) further analyzed the eccentrically stiffened sector plates using the DR technique. In these studies, the boundary conditions considered were either all edges clamped or all edges simply supported. Very recently, Salehi and Sobhani (2004) have given elastic linear and non-linear analysis of fiber-reinforced symmetrically laminated sector plates with rectilinear orthotropy.

In the present chapter an attempt is made to develop an analytical solution to the problem of static large deflection of moderately thick sector plates using the First Order Shear Deformation Theory. Governing equations of equilibrium are expressed in terms of displacement components and are space-wise discretized using Chebyshev polynomials.

An incremental iterative approach based on Newton-Raphson method is used for the solution of resulting non-linear algebraic equations. In order to have a check on accuracy, the convergence study has been carried out and the results are validated with the results available in literature. The effect of annularity on convergence is studied. Different combinations of immovable clamped and simply supported boundary conditions are analyzed. Influence of annularity, thickness ratio, sector angle and boundary conditions on deformation, moment and stress resultants is investigated.

5.2 Governing Equations and Method of Solution

In the large deflection static analysis of isotropic plates, the in-plane strains, refer equation (1.6), are non-linear functions of derivatives of the transverse deflection w. This leads to bending-stretching coupling. Thus, all five displacement components (u, v, w, ϕ_r, ϕ_θ) are present in the formulation. The non-linear equations of equilibrium of isotropic sector plates are obtained form equations (1.14)– (1.18) after ignoring the piezothermal effects. Making use of equations (1.3)– (1.6) and (1.21)– (1.26), the equilibrium equations for isotropic sector plates become,

$$\begin{aligned}
&\zeta\left[\zeta^{2}\frac{u'_{,rr}}{\zeta'^{2}}+\zeta\frac{u'_{,r}}{\zeta'}-u'+0.5(1-\nu)\frac{u'_{,\theta\theta}}{\Theta^{2}}\right]+\zeta\left[0.5(1+\nu)\zeta\frac{v'_{,r\theta}}{\zeta'\Theta}\right.\\
&\left.-0.5(3-\nu)\frac{v'_{,\theta}}{\Theta}\right]+\zeta\frac{w'_{,r}}{\zeta'}\left[\zeta^{2}\frac{w'_{,rr}}{\zeta'^{2}}+0.5(1-\nu)\left\{\zeta\frac{w'_{,r}}{\zeta'}+\frac{w'_{,\theta\theta}}{\Theta^{2}}\right\}\right]\\
&0.5(1+\nu)\frac{w'_{,\theta}}{\Theta}\left[\zeta\frac{w'_{,r\theta}}{\zeta'\Theta}-\frac{w'_{,\theta}}{\Theta}\right]=0
\end{aligned}\tag{5.1}$$

$$\begin{aligned}
&\zeta\left[0.5(1+\nu)\zeta\frac{u'_{,r\theta}}{\zeta'\Theta}+0.5(3-\nu)\frac{u'_{,\theta}}{\Theta}\right]+\zeta\left[0.5(1-\nu)\left\{\zeta^{2}\frac{v'_{,rr}}{\zeta'^{2}}+\zeta\frac{v'_{,r}}{\zeta'}\right.\right.\\
&\left.\left.-v'\right\}+\frac{v'_{,\theta\theta}}{\Theta^{2}}\right]+\frac{w'_{,\theta}}{\Theta}\left[0.5(1-\nu)\zeta^{2}\frac{w'_{,rr}}{\zeta'^{2}}+\frac{w'_{,\theta\theta}}{\Theta^{2}}\right]\\
&+\zeta\frac{w'_{,r}}{\zeta'}\left[0.5(1+\nu)\zeta\frac{w'_{,r\theta}}{\zeta'\Theta}+0.5(1-\nu)\frac{w'_{,\theta}}{\Theta}\right]=0
\end{aligned}\tag{5.2}$$

$$\begin{aligned}
&\zeta^{2}\left[0.5\,(1-\nu)\left(\frac{k^{2}}{\lambda^{2}}\right)\right]\left[\zeta^{2}\frac{w'_{,rr}}{\zeta'^{2}}+\zeta\frac{w'_{,r}}{\zeta'}+\frac{w'_{,\theta\theta}}{\Theta^{2}}\right]+\zeta^{3}\left[0.5\,(1-\nu)\left(\frac{k^{2}}{\lambda^{3}}\right)\right]\\
&\times\left[\zeta\frac{\phi_{r,r}}{\zeta'}+\phi_r+\frac{\phi_{\theta,\theta}}{\Theta}\right]+\zeta^{3}\left[\zeta\frac{w'_{,rr}}{\zeta'^{2}}+\frac{w'_{,r}}{\zeta'}\right]\left[\frac{u'_{,r}}{\zeta'}+0.5\left(\frac{w'_{,r}}{\zeta'}\right)^{2}\right.\\
&\left.+\frac{\nu}{\zeta}\left\{u'+\frac{v'_{,\theta}}{\Theta}+\frac{0.5}{\zeta}\left(\frac{w'_{,\theta}}{\Theta}\right)^{2}\right\}\right]+\zeta^{2}\frac{w'_{,\theta\theta}}{\Theta^{2}}\left[\nu\left\{\frac{u'_{,r}}{\zeta'}+0.5\left(\frac{w'_{,r}}{\zeta'}\right)^{2}\right\}\right.\\
&\left.+\frac{1}{\zeta}\left\{u'+\frac{v'_{,\theta}}{\Theta}+\frac{0.5}{\zeta}\left(\frac{w'_{,\theta}}{\Theta}\right)^{2}\right\}\right]+0.5(1-\nu)\zeta^{2}\left[\frac{u'_{,\theta}}{\Theta}-v'+\zeta\frac{v'_{,r}}{\zeta'}\right.\\
&\left.+\frac{w'_{,r}}{\zeta'}\frac{w'_{,\theta}}{\Theta}\right]\left[2\frac{w'_{,r\theta}}{\zeta'\Theta}-\frac{1}{\zeta}\frac{w'_{,\theta}}{\Theta}\right]+q'\zeta^{4}=0
\end{aligned}\tag{5.3}$$

$$
\begin{aligned}
&-\left[0.5\left(1-\nu\right)\left(\frac{k^2}{\lambda^2}\right)\right]\zeta^2\frac{w'_{,r}}{\zeta'}+\left(\frac{1}{12\lambda}\right)\left[\zeta^2\frac{\phi_{r,rr}}{\zeta'^2}+\zeta\frac{\phi_{r,r}}{\zeta'}-\phi_r\right]\\
&+\left[\frac{0.5\left(1-\nu\right)}{12\lambda}\right]\frac{\phi_{r,\theta\theta}}{\Theta^2}-\zeta^2\left[0.5\left(1-\nu\right)\left(\frac{k^2}{\lambda^3}\right)\right]\phi_r+\left[\frac{0.5\left(1+\nu\right)}{12\lambda}\right]\zeta\frac{\phi_{\theta,r\theta}}{\zeta'\Theta}\\
&-\left[\frac{0.5\left(3-\nu\right)}{12\lambda}\right]\frac{\phi_{\theta,\theta}}{\Theta}=0
\end{aligned}
\tag{5.4}
$$

$$
\begin{aligned}
&-\left[0.5\left(1-\nu\right)\left(\frac{k^2}{\lambda^2}\right)\right]\zeta\frac{w'_{,\theta}}{\Theta}+\left[\frac{0.5\left(1+\nu\right)}{12\lambda}\right]\zeta\frac{\phi_{r,r\theta}}{\zeta'\Theta}+\left[\frac{0.5\left(3-\nu\right)}{12\lambda}\right]\frac{\phi_{r,\theta}}{\Theta}\\
&+\left[\frac{0.5\left(1-\nu\right)}{12\lambda}\right]\left[\zeta^2\frac{\phi_{\theta,rr}}{\zeta'^2}+\zeta\frac{\phi_{\theta,r}}{\zeta'}-\phi_\theta\right]+\left[\frac{1}{12\lambda}\right]\frac{\phi_{\theta,\theta\theta}}{\Theta^2}\\
&-\zeta^2\left[0.5\left(1-\nu\right)\left(\frac{k^2}{\lambda^3}\right)\right]\phi_\theta=0
\end{aligned}
\tag{5.5}
$$

where,

$$
q'=qr_o^4/Eh^4 \tag{5.6}
$$

Using equation (2.13) for the five displacement components, the equilibrium equations (5.1)– (5.5) are discretized in space domain. Similarly appropriate boundary conditions are also discretized. The redundancy in the application of boundary conditions is removed as given in section 2.3. Further, it was possible to eliminate coefficients in series expansions of ϕ_r and ϕ_θ from the resulting system of equations. The non-linear algebraic equations in terms of the coefficients $(u,v,w)_{ij}$ are solved with Newton-Raphson method.

5.3 Results and Discussions

In this chapter non-linear equations of equilibrium for moderately thick isotropic sector plates subjected to uniformly distributed normal loading are solved analytically

using Chebyshev technique. The effects of annularity (μ), thickness ratio (λ) and sector angle (Θ) on deflections and stress resultants (M_r', M_θ', N_r' and N_θ') are presented. Different combinations of simply supported (S) and clamped (C) edge conditions are considered.

Table 5.1 Convergence results with respect to number of terms in series expansion in terms of w' at $(r = 0.176471, \theta = 0.5)$ with $\lambda = 0.2$, $\mu = 0$, $\Theta = \pi/3$, $q' = 500$

$(M+1)(N+1)$	$CCCC$	$SSSS$
77	1.241322	1.317168
96	1.246089	1.320383
117	1.245560	1.320252
140	1.246497	1.320994
165	1.245975	1.320545

Results for convergence study are given in Tables 5.1 and 5.2. The study revealed that four more terms were needed in r-dimension than the θ-dimension. In the present study a total of 140 terms $(M = 13, N = 9)$ are used for all the combinations of various parameters – λ and μ. Table 5.2 shows the convergence study with respect to μ. A total load q' of 500 was applied in a single step and the deflections are given at the point $(r = 0.176471, \theta = 0.5)$ located close to the singularity at $r = 0$ with $\mu = 0$. The convergence is faster for $\mu \geq 0.05$ as compared to $\mu = 0$. For $SSSS$ edge conditions $\mu = 0$ and the step load of $q' = 500$ gave instability. An incremental load of 100 is thus used in subsequent analysis. The large deflection results are compared with those given by Salehi and Shahidi (1994) using the Dynamic Relaxation technique and the results are shown in Tables 5.3 and 5.4 for clamped ($CCCC$) and simply supported ($SSSS$) boundary conditions respectively. It can be observed that the present results are on the lower side in terms of transverse deflection. A maximum

difference of 2-4% for $SSSS$ plates and 10-13% for $CCCC$ plates was noted. Similar observations may be made for stress resultants. It is observed that for $\lambda = 0.05$, M_r' for $CCCC$ edge conditions is showing oscillatory pattern in the results of Salehi and Shahidi (1994).

The effect of λ on the deflection is depicted in Figs. 5.1 and 5.2. The plot here being with respect to load ($q'\lambda^4$) which itself is independent of λ due to non-dimensionalization of q'. This figure shows a more dominant knee for the thin plates. For $\lambda = 0.05, 0.1$, the deflections ($w' > 2$) are of unrealistically high order. The methodology developed in this study is essentially for large deflection analysis of thick plates and deflections plotted are in realistic range for the thickest plate ($\lambda = 0.2$). For thinner plates, the plotted results demonstrate the robustness of the technique and suggest extensions to formulations involving material non-linearity.

Figs. 5.3 and 5.4 give the variation of displacement w' and M_θ'' respectively over the arc at $r = 0.5294$ for various boundary conditions with $\mu = 0.1$, $\lambda = 0.2$, $\Theta = \pi/3$ and $q' = 500$. It can be noted that the results are asymmetric with respect to $\theta = 0.5$ for the asymmetric edge conditions $CCSS$ and $SCCS$.

The effect of Θ on deflection is shown in Figs. 5.5 and 5.6. These figures give the deflection w' along the arc at $r = 0.5294$ with $\mu = 0$, $\lambda = 0.2$ and $q' = 500$. It is observed that deflections are larger for larger sector angle. Figs. 5.7 and 5.8 show the deflection w' along the radial center-line at $\theta = 0.5$ for different values of the annularity μ. From these results it can be noticed that with $\mu = 0$, there is an erroneous hump near the corner point $r = 0$. This hump has been noticed even for a very small value of μ of 0.0001.

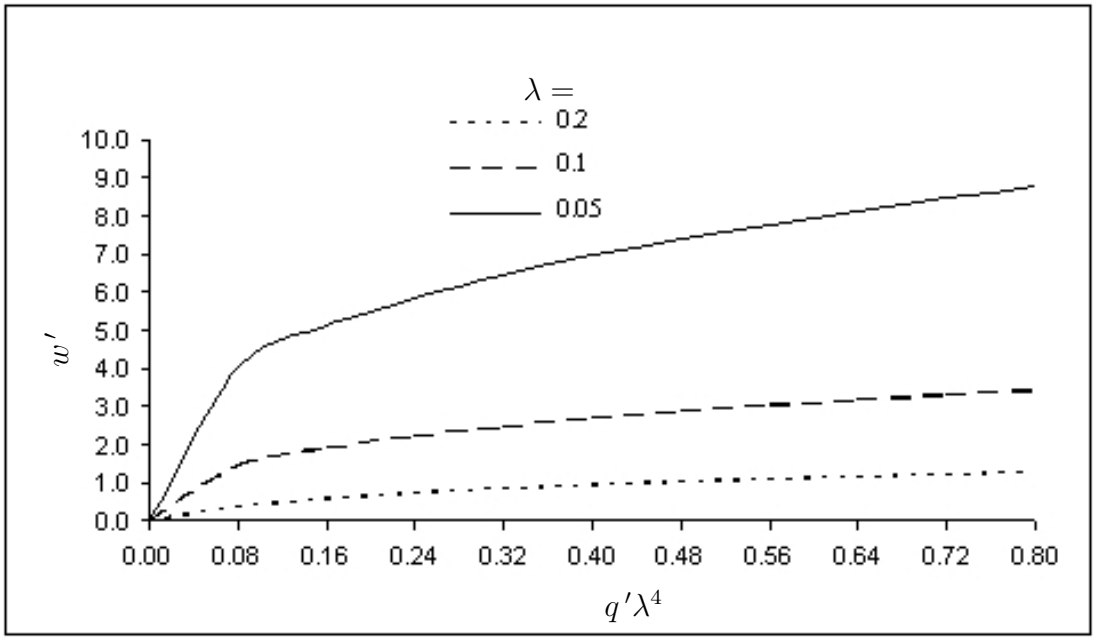

Fig. 5.1 Effect of thickness ratio λ on deflection w' of $CCCC$ plate at $(r = 0.647, \theta = 0.5)$ with $\mu = 0.1$, $\Theta = \pi/3$

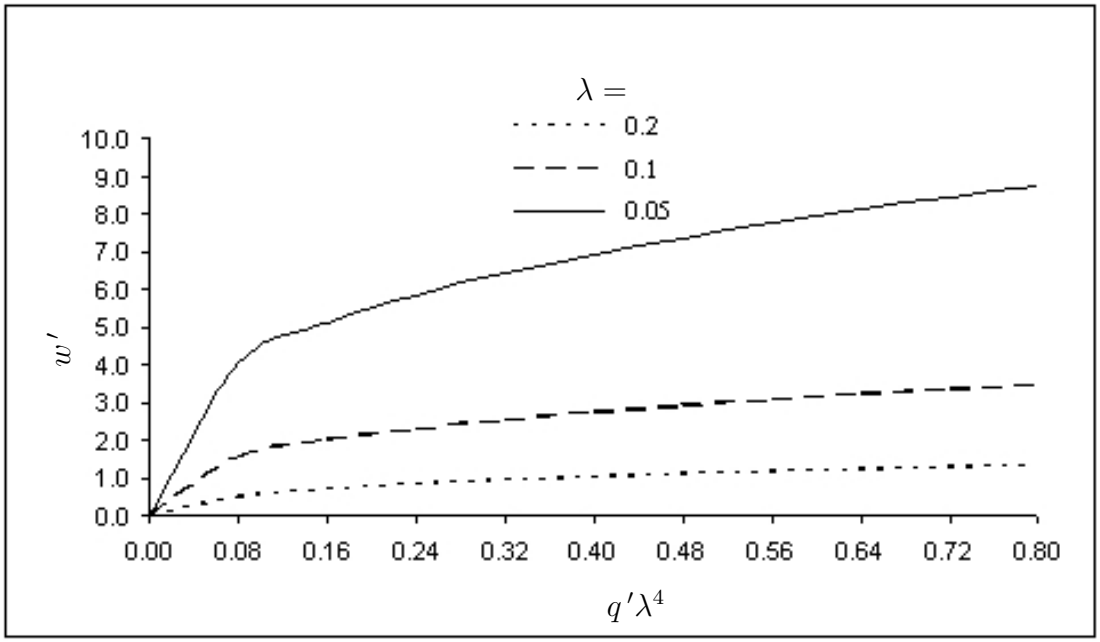

Fig. 5.2 Effect of thickness ratio λ on deflection w' of $SSSS$ plate at $(r = 0.647, \theta = 0.5)$ with $\mu = 0.1$, $\Theta = \pi/3$

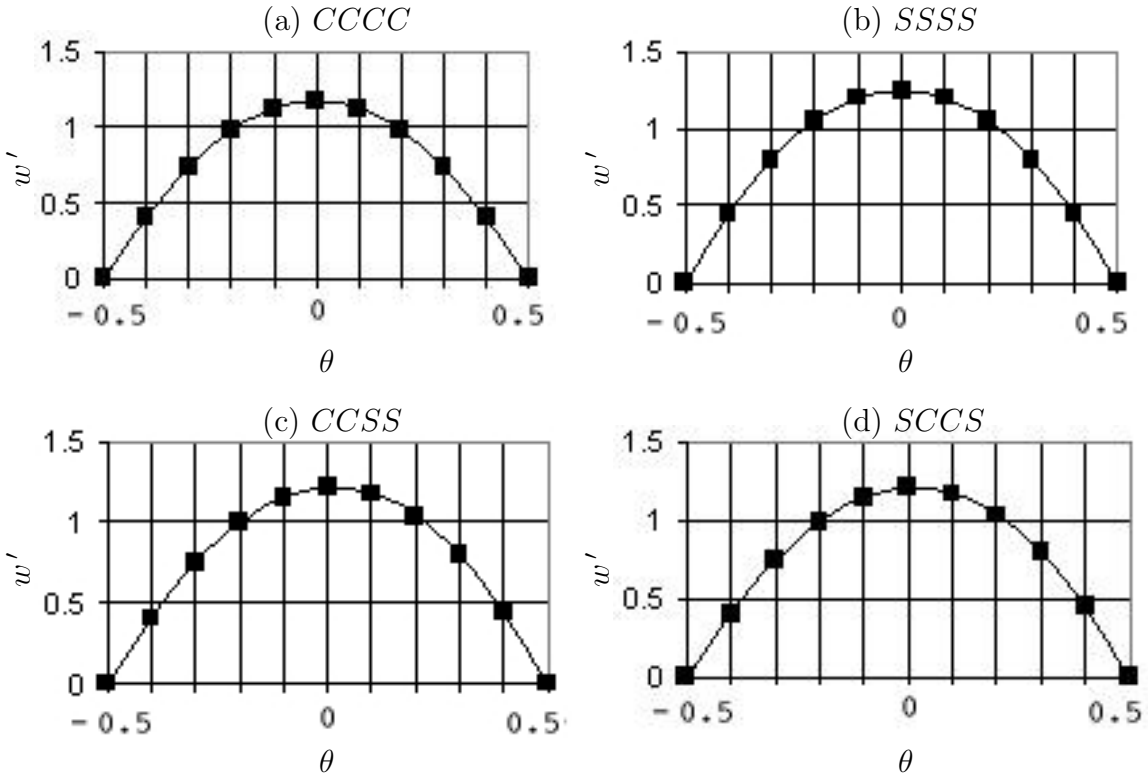

Fig. 5.3 Symmetry in variation of w' with different boundary conditions along the arc at ($r = 0.5294$) with $\lambda = 0.2$, $\mu = 0.1$, $\Theta = \pi/3$, $q' = 500$

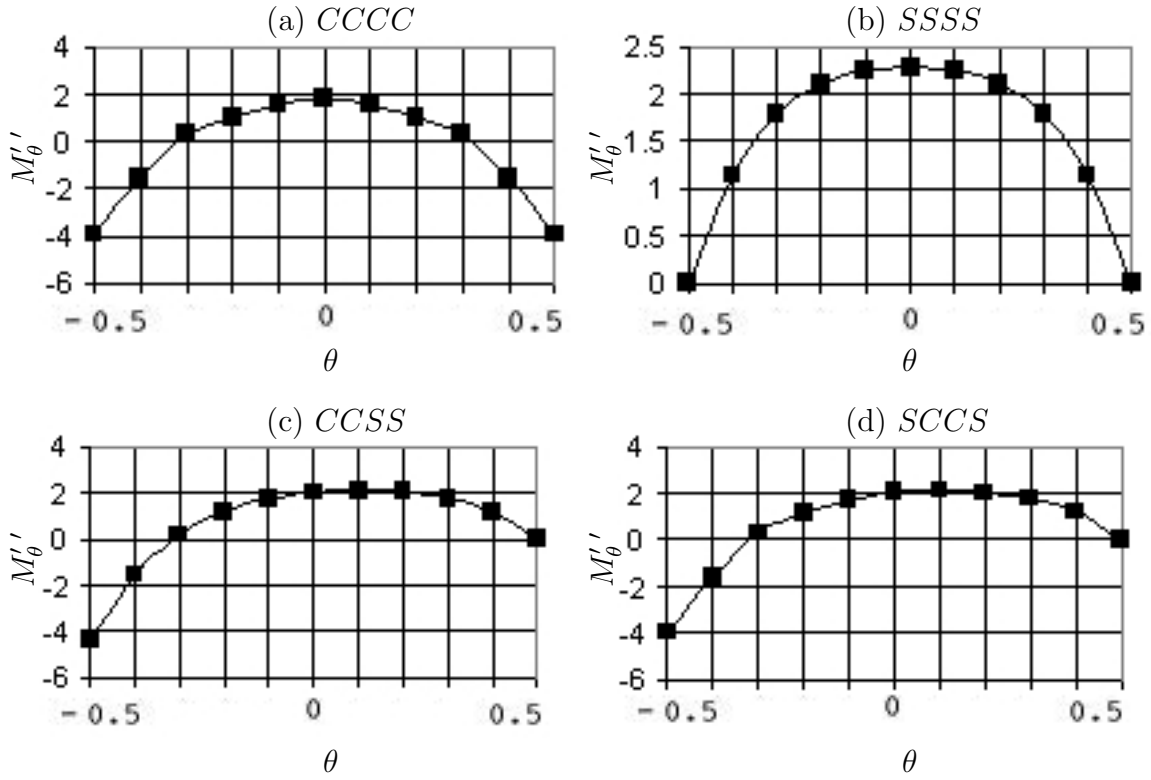

Fig. 5.4 Symmetry in variation of $M_\theta' = M_\theta'/(1-\mu)^2$ with different boundary conditions along the arc at $(r = 0.5294)$ with $\lambda = 0.2$, $\mu = 0.1$, $\Theta = \pi/3$, $q' = 500$

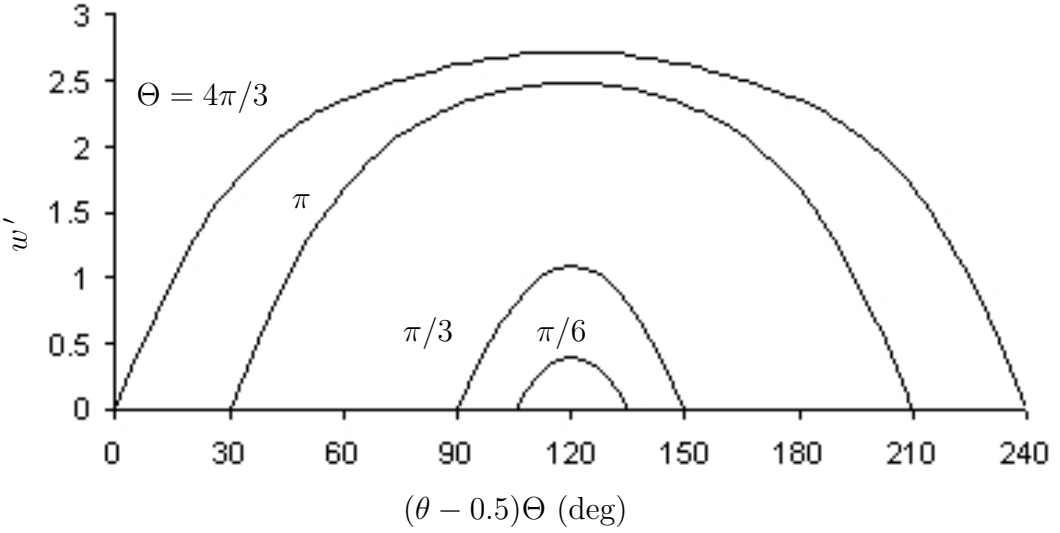

Fig. 5.5 Variation of deflection w' of $CCCC$ plate with Θ along the arc at $(r = 0.5294)$ with $\mu = 0$, $\lambda = 0.2$, $q' = 500$

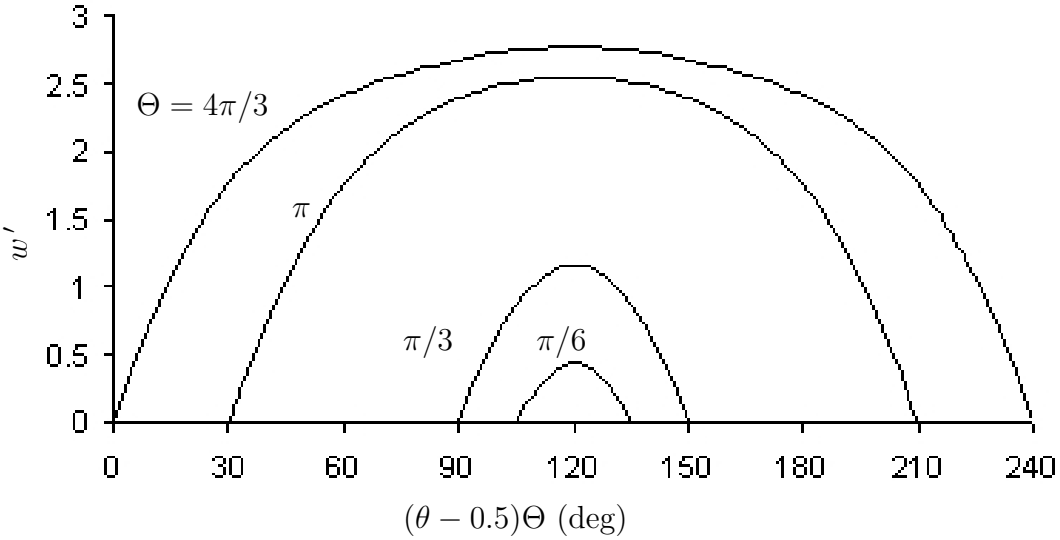

Fig. 5.6 Variation of deflection w' of $SSSS$ plate with Θ along the arc at $(r = 0.5294)$ with $\mu = 0$, $\lambda = 0.2$, $q' = 500$

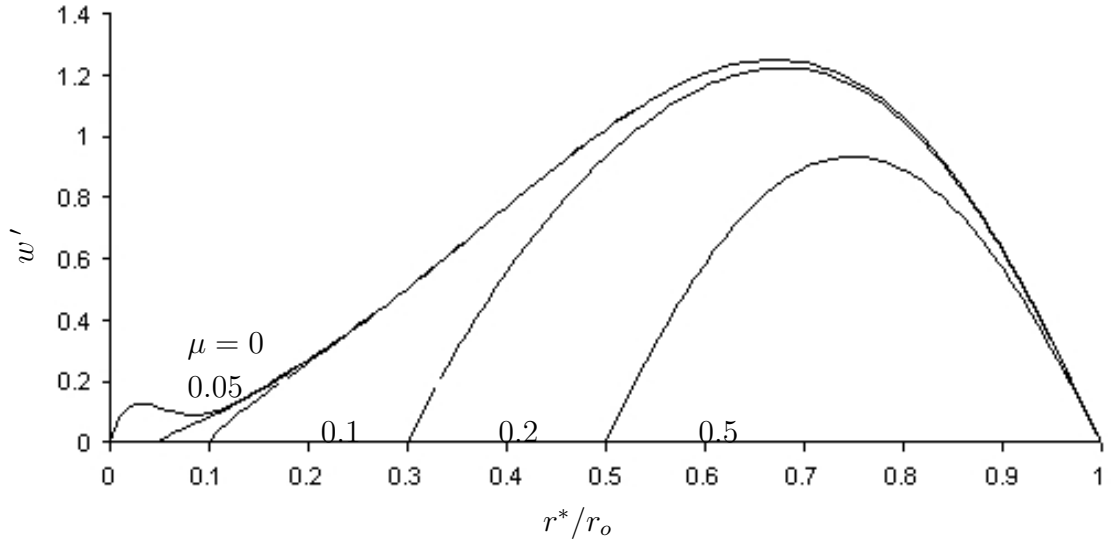

Fig. 5.7 Variation of deflection w' of $CCCC$ plate with μ along radial line at $(\theta = 0.5)$ with $\lambda = 0.2$, $\Theta = \pi/3$, $q' = 500$

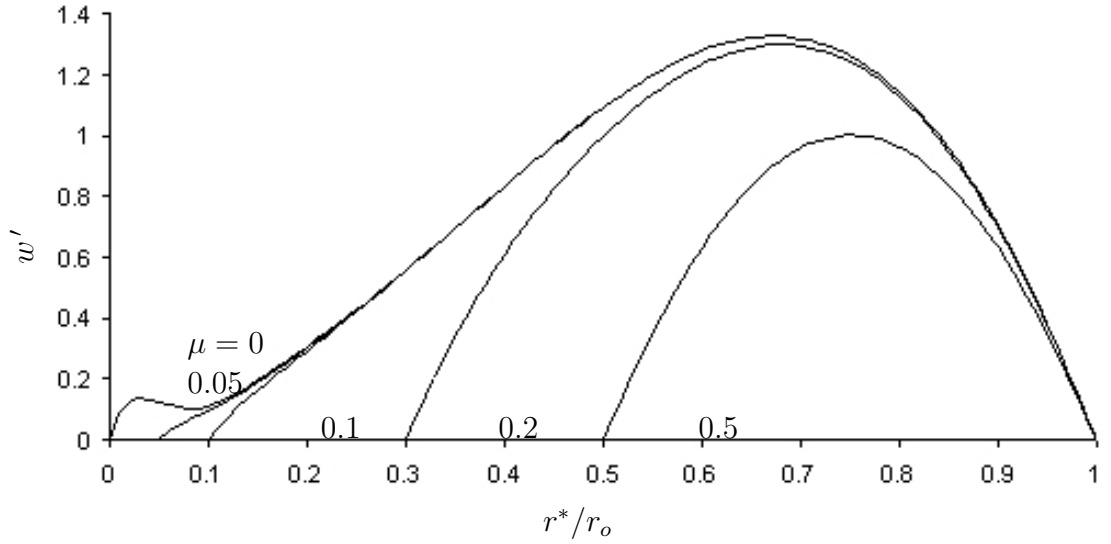

Fig. 5.8 Variation of deflection w' of $SSSS$ plate with μ along radial line at $(\theta = 0.5)$ with $\lambda = 0.2$, $\Theta = \pi/3$, $q' = 500$

5.4 Conclusions

The geometrically non-linear problem of moderately large deflection of thick sector plates has been analyzed analytically using Chebyshev polynomials. An expansion of 14 terms in r-dimensions and 10 terms in θ-dimension was found satisfactory. The methodology developed proved to be robust and efficient, and is expected to be applicable for more complicated problems.

Table 5.2 Convergence speed with respect to annularity in terms of w' at $(r = 0.176471, \theta = 0.5)$ with $\lambda = 0.2$, $\Theta = \pi/3$, $q' = 500$

Iteration	$CCCC$				$SSSS$			
no.	$\mu = 0$	$\mu = 0.05$	$\mu = 0.1$	$\mu = 0.2$	$\mu = 0$	$\mu = 0.05$	$\mu = 0.1$	$\mu = 0.2$
1	0.392601	0.611244	0.875301	1.421576	0.841789	1.331788	1.905128	2.989351
2	0.278974	0.424930	0.601347	0.965988	0.565008	0.892367	1.274674	1.996909
3	0.233575	0.333630	0.455633	0.704118	0.398404	0.610524	0.864945	1.347326
4	0.222891	0.307955	0.405269	0.593778	0.298260	0.444571	0.615727	0.941230
5	0.229828	0.305915	0.398303	0.570660	0.120603	0.367222	0.490119	0.721370
6	0.226531	0.305960	0.398116	0.569318	48.969999	0.345875	0.449682	0.639966
7	0.224144	0.305961	0.398115	0.569311	32.025549	0.343565	0.444376	0.626965
8	0.223345	0.305961	0.398115	0.569311	20.499715	0.343509	0.444239	0.626564
9	0.223330	0.305961	0.398115	0.569311	13.641080	0.343509	0.444239	0.626564
10	0.223330	0.305961	0.398115	0.569311	9.103040	0.343509	0.444239	0.626564
					Unstable			

Table 5.3 Comparison of large deflection results for clamped plates $(CCCC)$ **at** $(r = 0.647,\ \theta = 0.5)$ **with** $\mu = 0,\ \Theta = \pi/3$

		w'		N'_r		N'_θ		M'_r		M'_θ	
λ	q'	(a)	(b)	(a)	(b)	(a)	(b)	(a)	(b)	(a)	(b)
0.01	100.0	0.29953	0.32960	0.60630	0.62970	0.62719	0.61830	0.97754	0.96700	1.03680	1.03000
	200.0	0.54233	0.56410	1.97449	1.91200	2.03881	1.94900	1.71427	1.67200	1.82143	1.77700
	300.0	0.73096	0.74890	3.56181	3.33800	3.66883	3.44400	2.23180	2.18100	2.37577	2.31400
	400.0	0.88231	0.89640	5.15632	4.74200	5.29582	4.93000	2.60840	2.56800	2.78154	2.71900
	500.0	1.00843	1.01900	6.69793	6.08900	6.85666	6.36700	2.89668	2.87800	3.0941	3.04100
0.05	100.0	0.32484	0.36010	0.69078	0.71740	0.71646	0.70000	0.95753	0.94900	1.01757	1.05800
	200.0	0.57860	0.62920	2.17332	2.19700	2.25075	2.12600	1.64170	1.58600	1.74793	1.77200
	300.0	0.77103	0.83100	3.82799	3.83000	3.95698	3.66800	2.10337	2.01200	2.24375	2.25300
	400.0	0.92389	0.99190	5.45819	5.44700	5.63052	5.17100	2.43229	1.95900	2.59922	2.30500
	500.0	1.05078	1.12600	7.02032	7.01100	7.22635	6.60600	2.68104	2.56400	2.86978	2.87700
0.1	100.0	0.39401	0.45760	0.96666	1.03170	1.00727	0.94240	0.91313	0.88100	0.96363	1.06600
	200.0	0.66701	0.75440	2.74887	2.92600	2.86322	2.56200	1.47220	1.38300	1.55517	1.65200
	300.0	0.86158	0.96290	4.56343	4.84900	4.75168	4.17200	1.82196	1.71100	1.92614	2.02700
	400.0	1.01249	1.12460	6.28438	6.66000	6.54178	5.68800	2.06698	1.95900	2.18652	2.30500
	500.0	1.13652	1.25800	7.90757	8.37500	8.22950	7.11100	2.25343	2.16000	2.38495	2.52700
0.2	100.0	0.55999	0.64040	1.91906	2.05990	2.01592	1.65460	0.70894	0.69800	0.73462	0.84000
	200.0	0.82540	0.92600	4.20578	4.47100	4.42254	3.59900	0.99639	1.01700	1.03193	1.18200
	300.0	1.00076	1.11670	6.21770	6.57700	6.54449	5.23200	1.17486	1.22900	1.21671	1.40700
	400.0	1.13540	1.26400	8.03149	8.47600	8.46032	6.88700	1.30849	1.32900	1.35520	1.58100
	500.0	1.24650	1.38600	9.70172	10.22900	10.22711	8.33400	1.41751	1.52700	1.46825	1.72400

(a) Present (b) Salehi and Shahidi (1994)

Table 5.4 Comparison of large deflection results for simply supported plates $(SSSS)$ **at** $(r = 0.647, \theta = 0.5)$ **with** $\mu = 0$, $\Theta = \pi/3$

		w'		N'_r		N'_θ		M'_r		M'_θ	
λ	q'	(a)	(b)	(a)	(b)	(a)	(b)	(a)	(b)	(a)	(b)
0.01	100.0	0.64840	0.66090	2.61887	2.46600	2.75189	2.74000	1.30217	1.26700	1.38008	1.39700
	200.0	0.91164	0.92710	5.20876	4.89400	5.47310	5.42300	1.75074	1.70600	1.85735	1.88800
	300.0	1.08455	1.10300	7.40631	6.95600	7.78214	7.70900	2.02167	1.98000	2.14683	2.19000
	400.0	1.21713	1.23900	9.36242	8.81700	9.83739	9.75200	2.22034	2.18700	2.36001	2.42300
	500.0	1.32642	1.35100	11.15324	10.52000	11.71879	11.63000	2.38005	2.35600	2.53209	2.60000
0.05	100.0	0.65194	0.66470	2.65035	2.50000	2.78644	2.77700	1.28085	1.24500	1.35711	1.37300
	200.0	0.91294	0.92900	5.23093	4.92600	5.50012	5.45700	1.72116	1.67600	1.82552	1.85500
	300.0	1.08449	1.04000	7.41681	6.95600	7.79938	7.70900	1.99049	1.94800	2.11319	2.16000
	400.0	1.21619	1.23900	9.36215	8.84100	9.84602	9.77600	2.18979	2.15400	2.32678	2.38700
	500.0	1.32486	1.35000	11.14319	10.54000	11.72006	11.65000	2.35096	2.32300	2.49996	2.57400
0.1	100.0	0.66182	0.67510	2.74077	2.59200	2.88525	2.87800	1.21659	1.18100	1.28649	1.30300
	200.0	0.91674	0.93430	5.29683	5.01400	5.57764	5.55200	1.63132	1.58800	1.72651	1.57500
	300.0	1.08484	1.07000	7.45303	7.07200	7.84951	7.82300	1.89266	1.85100	2.00468	2.05000
	400.0	1.21436	1.24000	9.37086	8.91600	9.87020	9.85600	2.08997	2.05300	2.21519	2.27300
	500.0	1.32155	1.35000	11.12646	10.61000	11.71927	11.72000	2.25159	2.22000	2.38789	2.45700
0.2	100.0	0.68993	0.70570	3.01176	2.88300	3.17290	3.19900	1.01071	?	1.06044	?
	200.0	0.93017	0.95250	5.50620	5.30500	5.80167	5.87000	1.34355	1.30800	1.41022	1.44400
	300.0	1.09109	1.11900	7.59219	7.35100	8.00489	8.12600	1.56462	1.52100	1.64286	1.69000
	400.0	1.21646	1.24800	9.44313	9.17900	9.96323	10.14200	1.73647	1.69900	1.82381	1.87600
	500.0	1.32099	1.35600	11.13524	10.86000	11.75658	12.00000	1.87969	1.84200	1.97465	2.03300

(a) Present (b) Salehi and Shahidi (1994)

CHAPTER 6
NON-LINEAR STATIC ANALYSIS OF LAMINATED COMPOSITE SECTOR PLATES

6.1 Introduction

This chapter presents the formulation for non-linear static analysis of shear-deformable laminated sector plates made up of cylindrically orthotropic layers. The non-axisymmetric formulation in cylindrical coordinates is discretized in space domain using two-dimensional Chebyshev polynomials and the resulting non-linear algebraic equations are solved through Newton-Raphson method. Convergence study has been carried out and the results are compared with the results of laminated square plates and isotropic sector plates. Effects of boundary conditions, moduli ratio, lamination scheme, sector angle and annularity on deflection and stress resultants are investigated.

Large deformation analysis of plates has also received considerable attention as reviewed by Chia (1988) and Reddy (1997). The non-linear governing equations of plates are discretized using different techniques such as finite elements, Finite difference, boundary element, Fourier series, differential quadrature method and Galerkin method. Recently, Tanriover and Senocak (2004) employed Galerkin method for solving the large deflection problem of thin laminated rectangular plates. Nath and Kumar (1998, 2000) have presented non-linear analyses of laminated axisymmetric shallow spherical shells based on Chebyshev polynomials. Woo et al. (2003) applied p-version FEM for materially and geometrically non-linear analysis of laminated plates.

Non-linear analysis of sector plates has received limited attention. Salehi and Shahidi (1994) have analyzed the large deflection results for thick isotropic sector plates, Turvey and Salehi (1998) gave the large deflection results for stiffened sector plates and Salehi and Sobhani (2004) presented the non-linear analysis of laminated sector plates with rectilinear orthotropy. In all these studies dynamic relaxation with finite difference discretization technique is employed.

Wide applicability and complexity associated with laminated sector configuration demand a rigorous but robust methodology for bench-marking. The present chapter is an effort in this direction. Considering the first order shear deformation theory, analysis of moderately thick laminated sector plates made up of cylindrically orthotropic layers and undergoing moderately large deformation is carried out using Chebyshev technique. An iterative incremental approach based on Newton-Raphson method is used for obtaining the solution.

6.2 Governing Equations

The equations of equilibrium for non-linear large deflection analysis of laminated sector plates are obtained from equations (1.14)- (1.18) after ignoring the inertia and piezothermal effects. The equilibrium equations in terms of displacement components are (refer Chapter 1),

$$
\begin{aligned}
&A_{11}\frac{\zeta^3 r_o}{\zeta'^2}u_{,rr} + 2A_{16}\frac{\zeta^2 r_o}{\zeta'\Theta}u_{,r\theta} + A_{66}\frac{\zeta r_o}{\Theta^2}u_{,\theta\theta} + A_{11}\frac{\zeta^2 r_o}{\zeta'}u_{,r} - A_{22}\zeta r_o u \\
&+A_{16}\frac{\zeta^3 r_o}{\zeta'^2}v_{,rr} + (A_{12}+A_{66})\frac{\zeta^2 r_o}{\zeta'\Theta}v_{,r\theta} + A_{26}\frac{\zeta r_o}{\Theta^2}v_{,\theta\theta} - A_{26}\frac{\zeta^2 r_o}{\zeta'}v_{,r} \\
&-(A_{22}+A_{66})\frac{\zeta r_o}{\Theta}v_{,\theta} - A_{26}\zeta r_o v + B_{11}\frac{\zeta^3 r_o}{\zeta'^2}\phi_{r,rr} + 2B_{16}\frac{\zeta^2 r_o}{\zeta'\Theta}\phi_{r,r\theta} \\
&+B_{66}\frac{\zeta r_o}{\Theta^2}\phi_{r,\theta\theta} + B_{11}\frac{\zeta^2 r_o}{\zeta'}\phi_{r,r} - B_{22}\zeta r_o\phi_r + B_{16}\frac{\zeta^3 r_o}{\zeta'^2}\phi_{\theta,rr}
\end{aligned}
$$

$$
\begin{aligned}
&+ (B_{12}+B_{66})\frac{\zeta^2 r_o}{\zeta'\Theta}\phi_{\theta,r\theta} + B_{26}\frac{\zeta r_o}{\Theta^2}\phi_{\theta,\theta\theta} - B_{26}\frac{\zeta^2 r_o}{\zeta'}\phi_{\theta,r} \\
&- (B_{22}+B_{66})\frac{\zeta r_o}{\Theta}\phi_{\theta,\theta} - B_{26}\zeta r_o\phi_\theta + (A_{11}-A_{12})\zeta^2\left(\frac{w_{,r}}{\zeta'}\right)^2 \\
&+ (A_{12}-A_{22})\left(\frac{w_{,\theta}}{\Theta}\right)^2 + (A_{16}-A_{26})\zeta\left(\frac{w_{,r}}{\zeta'}\right)\left(\frac{w_{,\theta}}{\Theta}\right) \\
&+ A_{11}\zeta^3\left(\frac{w_{,r}}{\zeta'}\right)\left(\frac{w_{,rr}}{\zeta'^2}\right) + A_{12}\left\{\zeta\left(\frac{w_{,\theta}}{\Theta}\right)\left(\frac{w_{,r\theta}}{\zeta'\Theta}\right) - \left(\frac{w_{,\theta}}{\Theta}\right)^2\right\} \\
&+ A_{16}\zeta\left\{\zeta\left(\frac{w_{,\theta}}{\Theta}\right)\left(\frac{w_{,rr}}{\zeta'^2}\right) + \zeta\left(\frac{w_{,r}}{\zeta'}\right)\left(\frac{w_{,r\theta}}{\zeta'\Theta}\right) - \left(\frac{w_{,r}}{\zeta'}\right)\left(\frac{w_{,\theta}}{\Theta}\right)\right\} \\
&+ A_{16}\zeta^2\left(\frac{w_{,r}}{\zeta'}\right)\left(\frac{w_{,r\theta}}{\zeta'\Theta}\right) + A_{26}\left(\frac{w_{,\theta}}{\Theta}\right)\left(\frac{w_{,\theta\theta}}{\Theta^2}\right) \\
&+ A_{66}\zeta\left\{\left(\frac{w_{,\theta}}{\Theta}\right)\left(\frac{w_{,r\theta}}{\zeta'\Theta}\right) + \left(\frac{w_{,r}}{\zeta'}\right)\left(\frac{w_{,\theta\theta}}{\Theta^2}\right)\right\} = 0
\end{aligned} \tag{6.1}
$$

$$
\begin{aligned}
&A_{16}\frac{\zeta^3 r_o}{\zeta'^2}u_{,rr} + (A_{12}+A_{66})\frac{\zeta^2 r_o}{\zeta'\Theta}u_{,r\theta} + A_{26}\frac{\zeta r_o}{\Theta^2}u_{,\theta\theta} + (2A_{16}+A_{26})\frac{\zeta^2 r_o}{\zeta'}u_{,r} \\
&+ (A_{22}+A_{66})\frac{\zeta r_o}{\Theta}u_{,\theta} - A_{26}\zeta r_o u + A_{66}\frac{\zeta^3 r_o}{\zeta'^2}v_{,rr} + 2A_{26}\frac{\zeta^2 r_o}{\zeta'\Theta}v_{,r\theta} + A_{22}\frac{\zeta r_o}{\Theta^2}v_{,\theta\theta} \\
&- A_{66}\frac{\zeta^2 r_o}{\zeta'}v_{,r} - A_{66}\zeta r_o v + B_{16}\frac{\zeta^3 r_o}{\zeta'^2}\phi_{r,rr} + (B_{12}+B_{66})\frac{\zeta^2 r_o}{\zeta'\Theta}\phi_{r,r\theta} + B_{26}\frac{\zeta r_o}{\Theta^2}\phi_{r,\theta\theta} \\
&+ (2B_{16}+B_{26})\frac{\zeta^2 r_o}{\zeta'}\phi_{r,r} + (B_{22}+B_{66})\frac{\zeta r_o}{\Theta}\phi_{r,\theta} - B_{26}\zeta r_o\phi_r + B_{66}\frac{\zeta^3 r_o}{\zeta'^2}\phi_{\theta,rr} \\
&+ 2B_{26}\frac{\zeta^2 r_o}{\zeta'\Theta}\phi_{\theta,r\theta} + B_{22}\frac{\zeta r_o}{\Theta^2}\phi_{\theta,\theta\theta} - B_{66}\frac{\zeta^2 r_o}{\zeta'}\phi_{\theta,r} - B_{66}\zeta r_o\phi_\theta \\
&+ 2\left\{A_{16}\zeta^2\left(\frac{w_{,r}}{\zeta'}\right)^2 + A_{26}\left(\frac{w_{,\theta}}{\Theta}\right)^2 + A_{66}\zeta\left(\frac{w_{,r}}{\zeta'}\right)\left(\frac{w_{,\theta}}{\Theta}\right)\right\} \\
&+ A_{16}\zeta^3\left(\frac{w_{,r}}{\zeta'}\right)\left(\frac{w_{,rr}}{\zeta'^2}\right) + A_{26}\left\{\zeta\left(\frac{w_{,\theta}}{\Theta}\right)\left(\frac{w_{,r\theta}}{\zeta'\Theta}\right) - \left(\frac{w_{,\theta}}{\Theta}\right)^2\right\} \\
&+ A_{66}\zeta\left\{\zeta\left(\frac{w_{,\theta}}{\Theta}\right)\left(\frac{w_{,rr}}{\zeta'^2}\right) + \zeta\left(\frac{w_{,r}}{\zeta'}\right)\left(\frac{w_{,r\theta}}{\zeta'\Theta}\right) - \left(\frac{w_{,r}}{\zeta'}\right)\left(\frac{w_{,\theta}}{\Theta}\right)\right\} \\
&+ A_{12}\zeta^2\left(\frac{w_{,r}}{\zeta'}\right)\left(\frac{w_{,r\theta}}{\zeta'\Theta}\right) + A_{22}\left(\frac{w_{,\theta}}{\Theta}\right)\left(\frac{w_{,\theta\theta}}{\Theta^2}\right) \\
&+ A_{26}\zeta\left\{\left(\frac{w_{,\theta}}{\Theta}\right)\left(\frac{w_{,r\theta}}{\zeta'\Theta}\right) + \left(\frac{w_{,r}}{\zeta'}\right)\left(\frac{w_{,\theta\theta}}{\Theta^2}\right)\right\} = 0
\end{aligned} \tag{6.2}
$$

$$
\begin{aligned}
&k^2 A_{55}\frac{\zeta^4 r_o^2}{\zeta'^2}w_{,rr} + 2k^2 A_{45}\zeta^3 r_o^2\frac{w_{,r\theta}}{\zeta'\Theta} + k^2 A_{44}\zeta^2 r_o^2\frac{w_{,\theta\theta}}{\Theta^2} + k^2 A_{55}\frac{\zeta^3 r_o^2}{\zeta'}w_{,r} \\
&+k^2 A_{55}\frac{\zeta^4 r_o^3}{\zeta'}\phi_{r,r} + k^2 A_{45}\frac{\zeta^3 r_o^3}{\Theta}\phi_{r,\theta} + k^2 A_{55}\zeta^3 r_o^3\phi_r \\
&+k^2 A_{45}\frac{\zeta^4 r_o^3}{\zeta'}\phi_{\theta,r} + k^2 A_{45}\frac{\zeta^3 r_o^3}{\Theta}\phi_{\theta,\theta} + k^2 A_{44}\zeta^3 r_o^3\phi_\theta
\end{aligned}
$$

$$+\zeta\left(\zeta\frac{w_{,rr}}{\zeta'^2}+\frac{w_{,r}}{\zeta'}\right)\left\{0.5A_{11}\zeta^2\left(\frac{w_{,r}}{\zeta'}\right)^2+0.5A_{12}\left(\frac{w_{,\theta}}{\Theta}\right)^2+A_{16}\zeta\left(\frac{w_{,r}}{\zeta'}\right)\left(\frac{w_{,\theta}}{\Theta}\right)\right\}$$
$$+\frac{w_{,\theta\theta}}{\Theta^2}\left\{0.5A_{12}\zeta^2\left(\frac{w_{,r}}{\zeta'}\right)^2+0.5A_{22}\left(\frac{w_{,\theta}}{\Theta}\right)^2+A_{26}\zeta\left(\frac{w_{,r}}{\zeta'}\right)\left(\frac{w_{,\theta}}{\Theta}\right)\right\}$$
$$+\left(2\zeta\frac{w_{,r\theta}}{\zeta'\Theta}-\frac{w_{,\theta}}{\Theta}\right)\left\{0.5A_{16}\zeta^2\left(\frac{w_{,r}}{\zeta'}\right)^2+0.5A_{26}\left(\frac{w_{,\theta}}{\Theta}\right)^2+A_{66}\zeta\left(\frac{w_{,r}}{\zeta'}\right)\left(\frac{w_{,\theta}}{\Theta}\right)\right\}$$
$$+\zeta^4 r_o^4 q=0 \tag{6.3}$$

$$\begin{aligned}
&B_{11}\frac{\zeta^3 r_o}{\zeta'^2}u_{,rr}+2B_{16}\frac{\zeta^2 r_o}{\zeta'\Theta}u_{,r\theta}+B_{66}\frac{\zeta r_o}{\Theta^2}u_{,\theta\theta}+B_{11}\frac{\zeta^2 r_o}{\zeta'}u_{,r}-B_{22}\zeta r_o u\\
&+B_{16}\frac{\zeta^3 r_o}{\zeta'^2}v_{,rr}+(B_{12}+B_{66})\frac{\zeta^2 r_o}{\zeta'\Theta}v_{,r\theta}+B_{26}\frac{\zeta r_o}{\Theta^2}v_{,\theta\theta}-B_{26}\frac{\zeta^2 r_o}{\zeta'}v_{,r}\\
&-(B_{22}+B_{66})\frac{\zeta r_o}{\Theta}v_{,\theta}-B_{26}\zeta r_o v-k^2A_{55}\frac{\zeta^3 r_o^2}{\zeta'}w_{,r}-k^2A_{45}\frac{\zeta^2 r_o^2}{\Theta}w_{,\theta}\\
&+D_{11}\frac{\zeta^3 r_o}{\zeta'^2}\phi_{r,rr}+2D_{16}\frac{\zeta^2 r_o}{\zeta'\Theta}\phi_{r,r\theta}+D_{66}\frac{\zeta r_o}{\Theta^2}\phi_{r,\theta\theta}+D_{11}\frac{\zeta^2 r_o}{\zeta'}\phi_{r,r}-D_{22}\zeta r_o\phi_r\\
&-k^2A_{55}\zeta^3 r_o^3\phi_r+D_{16}\frac{\zeta^3 r_o}{\zeta'^2}\phi_{\theta,rr}+(D_{12}+D_{66})\frac{\zeta^2 r_o}{\zeta'\Theta}\phi_{\theta,r\theta}\\
&+D_{26}\frac{\zeta r_o}{\Theta^2}\phi_{\theta,\theta\theta}-D_{26}\frac{\zeta^2 r_o}{\zeta'}\phi_{\theta,r}-(D_{22}+D_{66})\frac{\zeta r_o}{\Theta}\phi_{\theta,\theta}-D_{26}\zeta r_o\phi_\theta\\
&-k^2A_{45}\zeta^3 r_o^3\phi_\theta+(B_{11}-B_{12})\zeta^2\left(\frac{w_{,r}}{\zeta'}\right)^2\\
&+(B_{12}-B_{22})\left(\frac{w_{,\theta}}{\Theta}\right)^2+(B_{16}-B_{26})\zeta\left(\frac{w_{,r}}{\zeta'}\right)\left(\frac{w_{,\theta}}{\Theta}\right)\\
&+B_{11}\zeta^3\left(\frac{w_{,r}}{\zeta'}\right)\left(\frac{w_{,rr}}{\zeta'^2}\right)+B_{12}\left\{\zeta\left(\frac{w_{,\theta}}{\Theta}\right)\left(\frac{w_{,r\theta}}{\zeta'\Theta}\right)-\left(\frac{w_{,\theta}}{\Theta}\right)^2\right\}\\
&+B_{16}\zeta\left\{\zeta\left(\frac{w_{,\theta}}{\Theta}\right)\left(\frac{w_{,rr}}{\zeta'^2}\right)+\zeta\left(\frac{w_{,r}}{\zeta'}\right)\left(\frac{w_{,r\theta}}{\zeta'\Theta}\right)-\left(\frac{w_{,r}}{\zeta'}\right)\left(\frac{w_{,\theta}}{\Theta}\right)\right\}\\
&+B_{16}\zeta^2\left(\frac{w_{,r}}{\zeta'}\right)\left(\frac{w_{,r\theta}}{\zeta'\Theta}\right)+B_{26}\left(\frac{w_{,\theta}}{\Theta}\right)\left(\frac{w_{,\theta\theta}}{\Theta^2}\right)\\
&+B_{66}\zeta\left\{\left(\frac{w_{,\theta}}{\Theta}\right)\left(\frac{w_{,r\theta}}{\zeta'\Theta}\right)+\left(\frac{w_{,r}}{\zeta'}\right)\left(\frac{w_{,\theta\theta}}{\Theta^2}\right)\right\}=0
\end{aligned} \tag{6.4}$$

$$\begin{aligned}
&B_{16}\frac{\zeta^3 r_o}{\zeta'^2}u_{,rr}+(B_{12}+B_{66})\frac{\zeta^2 r_o}{\zeta'\Theta}u_{,r\theta}+B_{26}\frac{\zeta r_o}{\Theta^2}u_{,\theta\theta}+(2B_{16}+B_{26})\frac{\zeta^2 r_o}{\zeta'}u_{,r}\\
&+(B_{22}+B_{66})\frac{\zeta r_o}{\Theta}u_{,\theta}-B_{26}\zeta r_o u+b_{66}\frac{\zeta^3 r_o}{\zeta'^2}v_{,rr}+2B_{26}\frac{\zeta^2 r_o}{\zeta'\Theta}v_{,r\theta}+B_{22}\frac{\zeta r_o}{\Theta^2}v_{,\theta\theta}\\
&-B_{66}\frac{\zeta^2 r_o}{\zeta'}v_{,r}-B_{66}\zeta r_o v-k^2A_{45}\frac{\zeta^3 r_o^2}{\zeta'}w_{,r}-k^2A_{55}\frac{\zeta^2 r_o^2}{\Theta}w_{,\theta}+D_{16}\frac{\zeta^3 r_o}{\zeta'^2}\phi_{r,rr}
\end{aligned}$$

$$
\begin{aligned}
&+ (D_{12} + D_{66}) \frac{\zeta^2 r_o}{\zeta' \Theta} \phi_{r,r\theta} + D_{26} \frac{\zeta r_o}{\Theta^2} \phi_{r,\theta\theta} + (2D_{16} + D_{26}) \frac{\zeta^2 r_o}{\zeta'} \phi_{r,r} \\
&+ (D_{22} + D_{66}) \frac{\zeta r_o}{\Theta} \phi_{r,\theta} - D_{26} \zeta r_o \phi_r - k^2 A_{45} \zeta^3 r_o^3 \phi_r + D_{66} \frac{\zeta^3 r_o}{\zeta'^2} \phi_{\theta,rr} \\
&+ 2D_{26} \frac{\zeta^2 r_o}{\zeta' \Theta} \phi_{\theta,r\theta} + D_{22} \frac{\zeta r_o}{\Theta^2} \phi_{\theta,\theta\theta} - D_{66} \frac{\zeta^2 r_o}{\zeta'} \phi_{\theta,r} - D_{66} \zeta r_o \phi_\theta - k^2 A_{44} \zeta^3 r_o^3 \phi_\theta \\
&+ 2 \left\{ B_{16} \zeta^2 \left(\frac{w_{,r}}{\zeta'} \right)^2 + B_{26} \left(\frac{w_{,\theta}}{\Theta} \right)^2 + B_{66} \zeta \left(\frac{w_{,r}}{\zeta'} \right) \left(\frac{w_{,\theta}}{\Theta} \right) \right\} \\
&+ B_{16} \zeta^3 \left(\frac{w_{,r}}{\zeta'} \right) \left(\frac{w_{,rr}}{\zeta'^2} \right) + B_{26} \left\{ \zeta \left(\frac{w_{,\theta}}{\Theta} \right) \left(\frac{w_{,r\theta}}{\zeta' \Theta} \right) - \left(\frac{w_{,\theta}}{\Theta} \right)^2 \right\} \\
&+ B_{66} \zeta \left\{ \zeta \left(\frac{w_{,\theta}}{\Theta} \right) \left(\frac{w_{,rr}}{\zeta'^2} \right) + \zeta \left(\frac{w_{,r}}{\zeta'} \right) \left(\frac{w_{,r\theta}}{\zeta' \Theta} \right) - \left(\frac{w_{,r}}{\zeta'} \right) \left(\frac{w_{,\theta}}{\Theta} \right) \right\} \\
&+ B_{12} \zeta^2 \left(\frac{w_{,r}}{\zeta'} \right) \left(\frac{w_{,r\theta}}{\zeta' \Theta} \right) + B_{22} \left(\frac{w_{,\theta}}{\Theta} \right) \left(\frac{w_{,\theta\theta}}{\Theta^2} \right) \\
&+ B_{26} \zeta \left\{ \left(\frac{w_{,\theta}}{\Theta} \right) \left(\frac{w_{,r\theta}}{\zeta' \Theta} \right) + \left(\frac{w_{,r}}{\zeta'} \right) \left(\frac{w_{,\theta\theta}}{\Theta^2} \right) \right\} = 0
\end{aligned} \tag{6.5}
$$

The $5(M+1)(N+1)$ number of non-linear algebraic equations in terms of the $5(M+1)(N+1)$ number of unknown coefficients are thus generated. An iterative incremental approach based on Newton-Raphson technique is used for the solution of the non-linear algebraic equations.

6.3 Results and Discussions

The present study deals with the large deflection analysis of moderately thick laminated sector plates, made up of cylindrically orthotropic layers subjected to uniformly distributed lateral loading. The boundary conditions considered here are various combinations of simply supported (S), clamped (C) and free (F) edges.

Each layer is assumed to be cylindrically orthotropic and of uniform thickness. With fibers oriented in radial direction, the required material properties are as follows unless otherwise specified: $E_r/E_\theta = 25$, $\nu_{r\theta} = 0.25$. $G_{r\theta} = G_{zr} = 0.5E_\theta$, $G_{\theta z} = 0.2E_\theta$. The material properties shown in figures and tables are also for fibers oriented in

Table 6.1 Convergence of results in terms of M and N with $n = 2$, (RC), $\mu = 0.05$, $\lambda = 0.1$, $\Theta = \pi/3$, $Q = 100$

	w' at $r = 0.65$, $\theta = 0.5$ for various edge conditions		
$M \times N$	CCCC	CCSS	SSFS
10×6	0.230259	0.311417	0.455019
11×7	0.230102	0.311468	0.420662
12×8	0.229749	0.310977	0.421844
13×9	0.229864	0.311112	0.420876
14×10	0.229872	0.311102	0.422071
15×11	0.229870	0.311111	0.421318
16×12	0.229886	0.311135	0.421973

radial direction. The properties of orthotropic layers with circumferential orientation of fibers are obtained by rotation of the material axes by 90^o. The results given are for ($r = 0.65$, $\theta = 0.5$, $\mu = 0.2$, $\lambda = 0.1$ and $\Theta = \pi/3$ (unless otherwise specified). Results for convergence study are given in Table 6.1. The results are validated with the available results for isotropic sector plates and are given in Tables 5.3 and 5.4. Comparisons of central deflection ($r = 0.5$, $\theta = 0.5$) for almost square

Table 6.2 Comparison of large deflection results at ($r = 0.5$, $\theta = 0.5$) of laminated (RC) almost square plates. (a) Shukla and Nath (2000), $E_r/E_\theta = 25$, $\nu_{r\theta} = 0.25$, $G_{r\theta} = G_{rz} = 0.5E_\theta$, $G_{\theta z} = 0.2E_\theta$, $r_o/h = 10^5$, $r_i/h = (10^5 - 10)$, $\lambda = 0.1$ and $\Theta = 10^{-4}$ rad (b) Tanriover and Senocak (2004), $E_r/E_\theta = 27.273$, $\nu_{r\theta} = 0.3$, $G_{r\theta} = G_{rz} = G_{\theta z} = 0.6363E_\theta$, $r_o/h = 10^6$, $r_i/h = (10^5 - 100)$, $\lambda = 0.01$ and $\Theta = 10^{-4}$ rad.

Q	Boundary Condition	side to thickness ratio	w' Present	w' Reference
200	CCCC	10	0.6435	0.643 (a)
40	CSCS	10	0.2471	0.257 (a)
40	CSSS	10	0.3020	0.288 (a)
40	CCCF	10	0.2883	0.287 (a)
1000	CCCC	100	1.2374	1.209 (b)
1000	SSSS	100	1.4046	1.38 (b)

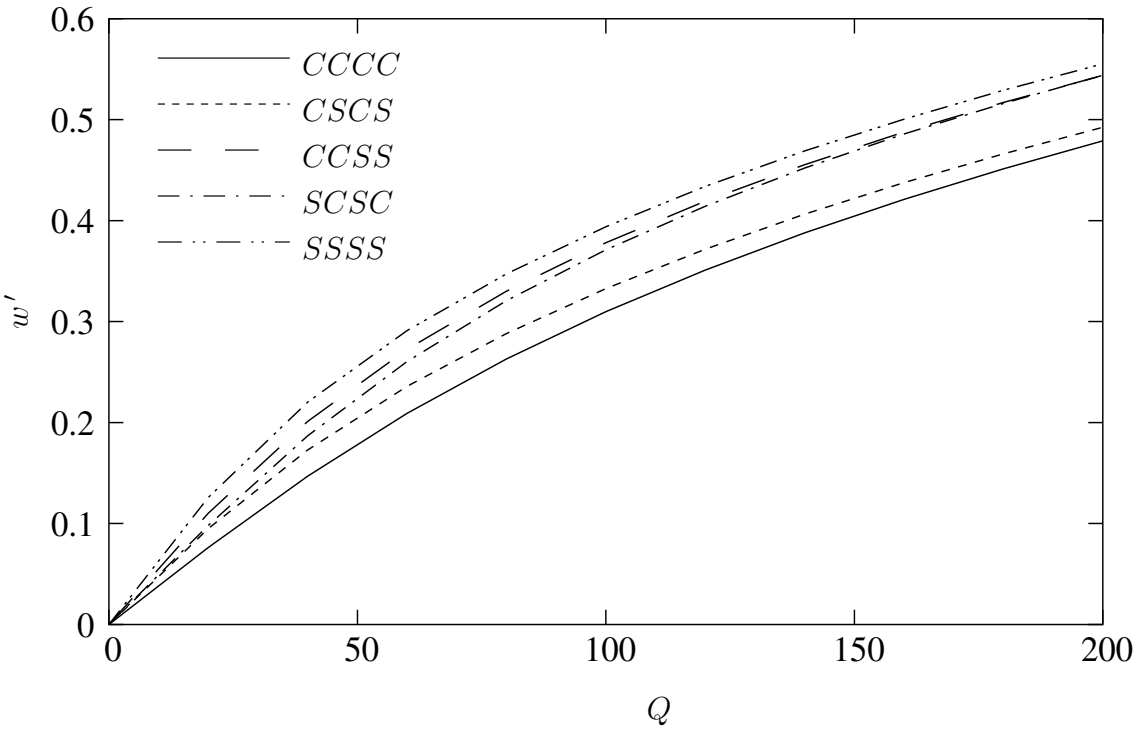

Fig. 6.1 Effect of combinations of simply supported and clamped edge conditions on deflection w' of laminated $(n = 4,\ RCRC)$ sector plates.

laminated plates (RC) simulated by taking appropriate values of λ, μ and Θ are given in Table 6.2. It can be seen that the present results are in good agreement with the available solutions (Shukla and Nath, 2000; Tanriover and Senocak, 2004)).

Effects of combinations of clamped and simply supported edge conditions on the deflection w' and moments (M_r' and M_θ') are given in Figs. 6.1- 6.3 for $RCRC$ laminated plates. In Figs. 6.1 and 6.2, the response is similar for the edge conditions $CCCC$ and $CSCS$, and for $CCSS$ and $SCSC$. Figs. 6.4- 6.6 give these results for plates having one free edge or two opposite edges free. In these figures, the similarity is observed between the behavior for the edge conditions $CCFC$ and $FCFC$, and between $CSFC$ and $FSFS$. Effects of boundary conditions are more noticeable on the moments. Considering three values of moduli ratio (E_r/E_θ), the effects of orthotropy are plotted in Figs. 6.7- 6.9 for for $SFSF$ plates. The results for isotropic

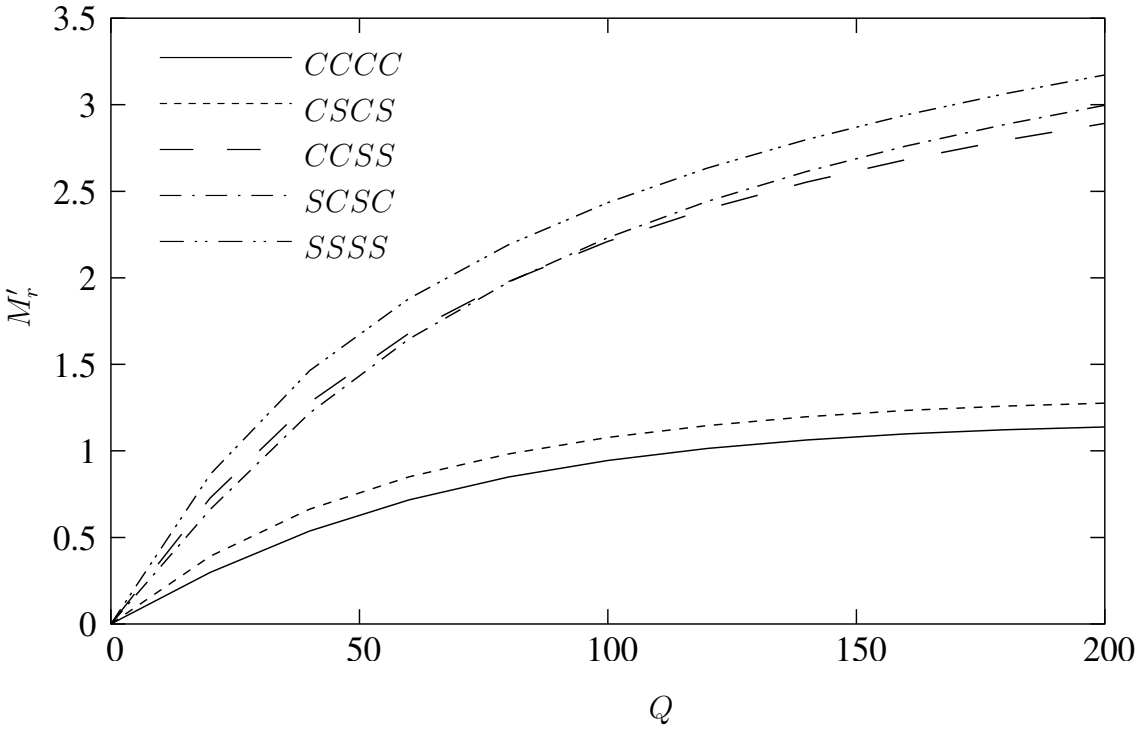

Fig. 6.2 Effect of combinations of simply supported and clamped edge conditions on moment M_r' of laminated $(n = 4,\ RCRC)$ sector plates.

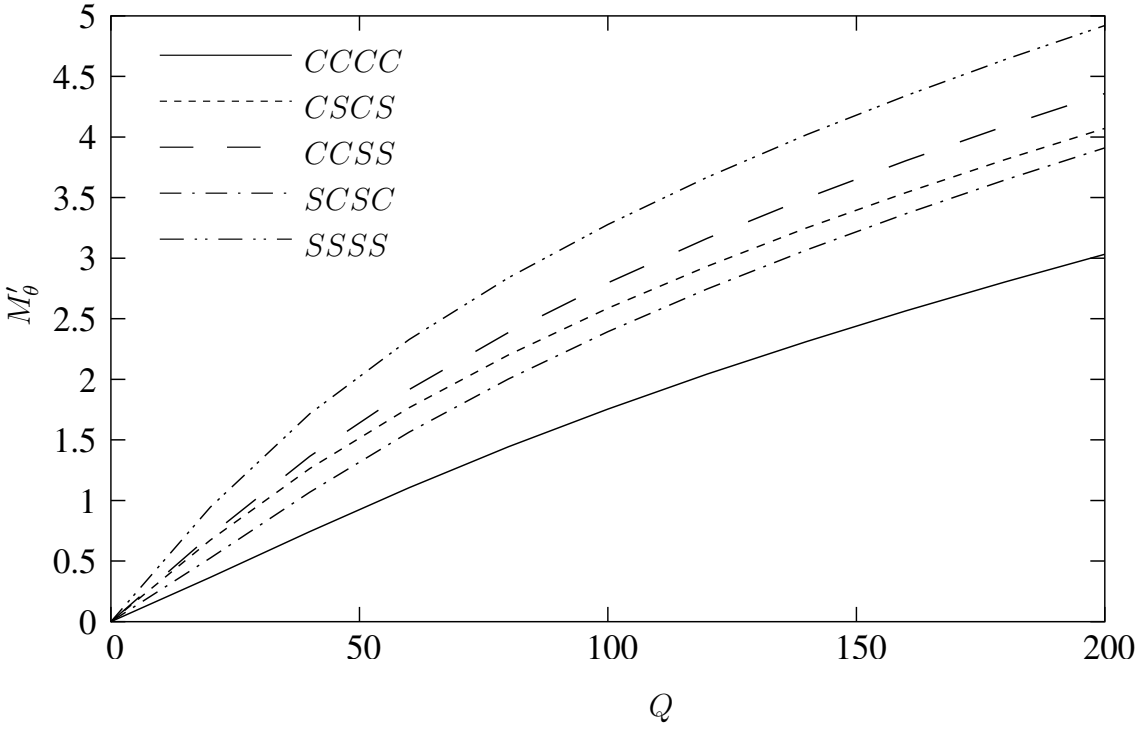

Fig. 6.3 Effect of combinations of simply supported and clamped edge conditions on moment M_θ' of laminated $(n = 4,\ RCRC)$ sector plates.

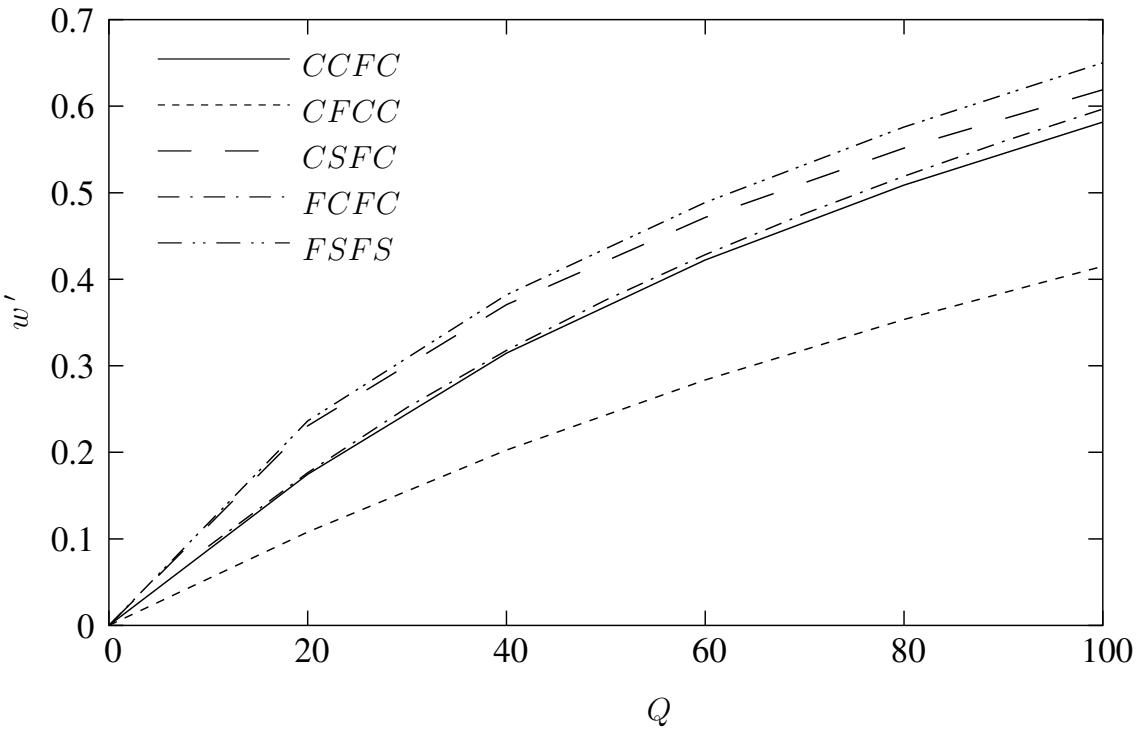

Fig. 6.4 Effect of combinations of free, simply supported and clamped edge conditions on deflection w' of laminated $(n = 4,\ RCRC)$ sector plates.

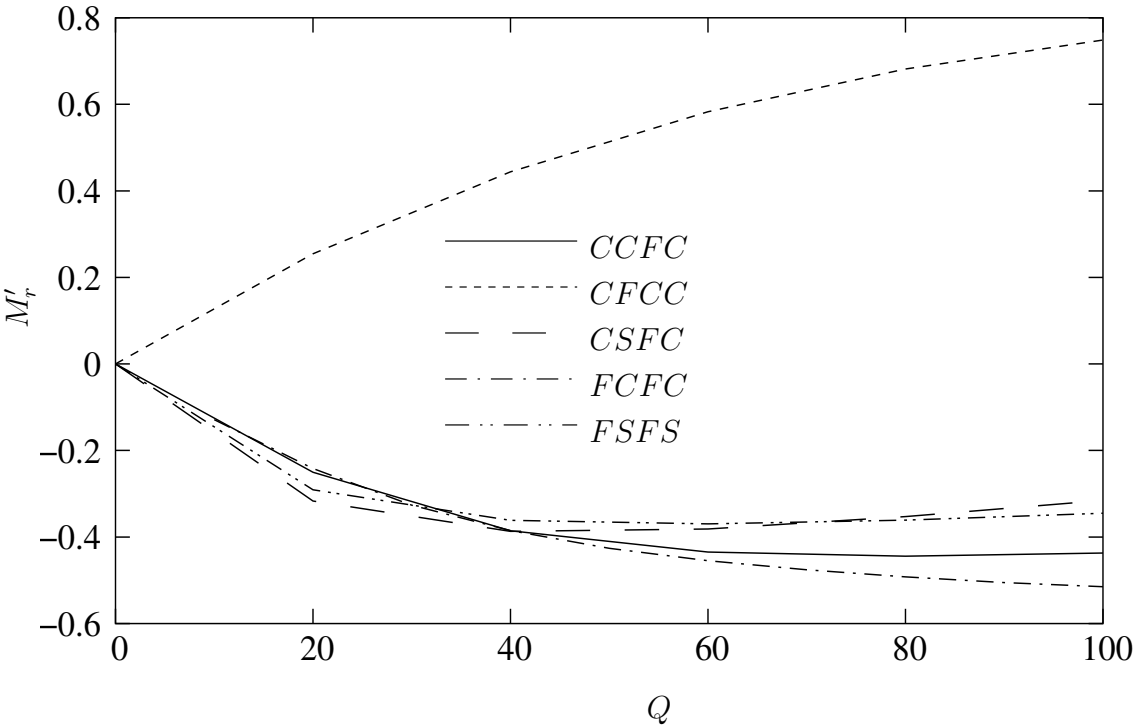

Fig. 6.5 Effect of combinations of free, simply supported and clamped edge conditions on moment M_r' of laminated $(n = 4,\ RCRC)$ sector plates.

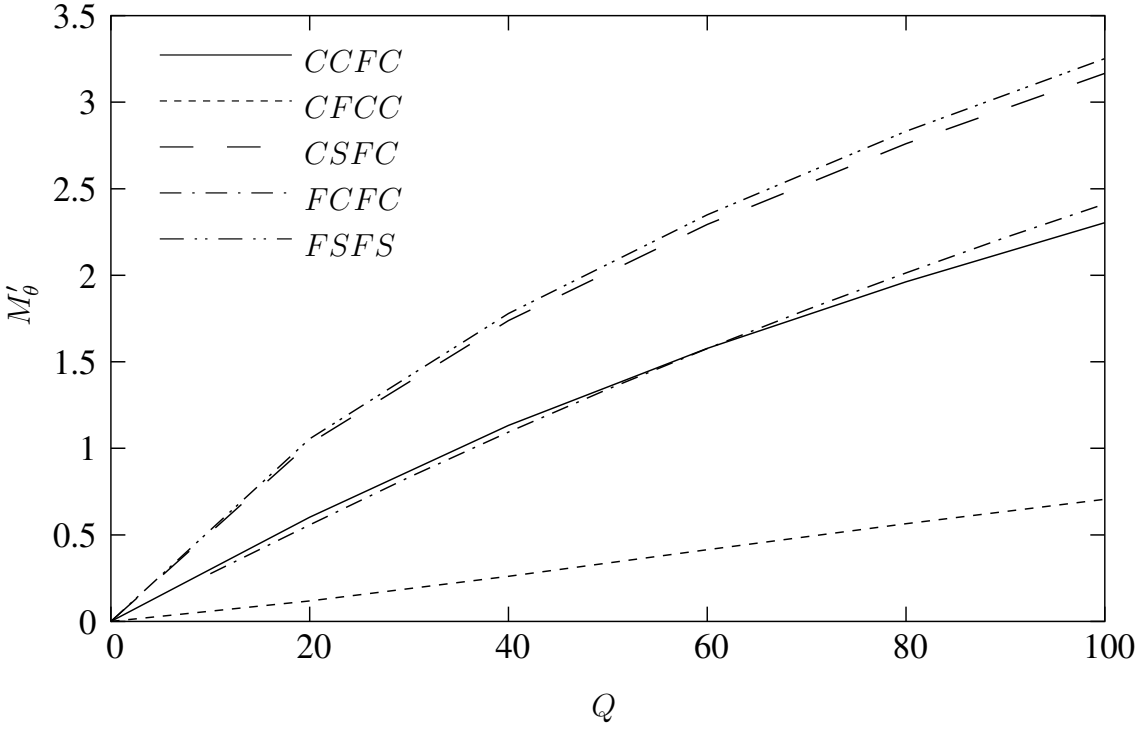

Fig. 6.6 Effect of combinations of free, simply supported and clamped edge conditions on moment M'_θ of laminated $(n = 4,\ RCRC)$ sector plates.

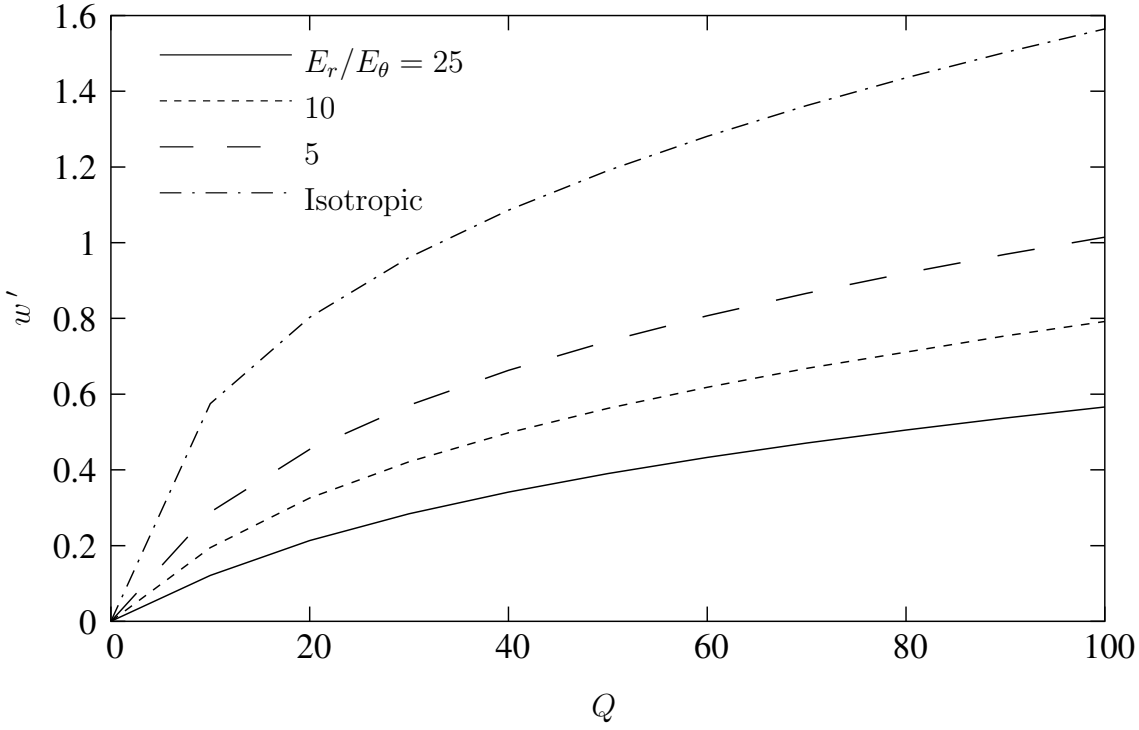

Fig. 6.7 Effect of orthotropy on deflection w' of laminated $(n = 4,\ RCCR)$ sector plates having $SFSF$ edge condition.

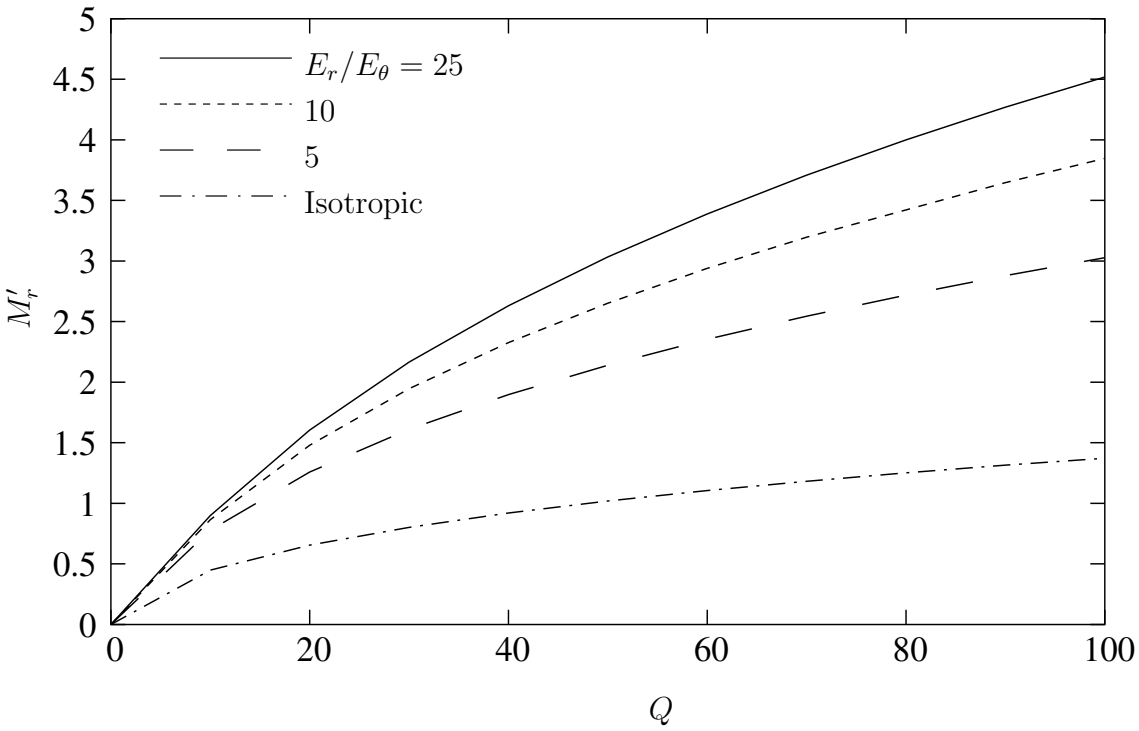

Fig. 6.8 Effect of orthotropy on moment M_r' of laminated ($n = 4$, $RCCR$) sector plates having $SFSF$ edge condition.

case are also depicted. As the moduli ratio increases, there is monotonous decrease in w', increase in M_r' and decrease in M_θ'.

Figs. 6.10- 6.12 give the effect of lamination scheme on $CCSS$ plates. Four lamination schemes are considered – $RCCR$, $CRRC$, $RCRC$ and RC. The two-layer RC plate is having maximum deflection. It can be seen that the effect is much larger on the moments than on the deflection. Fig. 6.13 gives the deflection w' along the arc at ($r = 0.65$) from one radial edge to the other for plates having various sector angles Θ . Fig. 6.14 shows the deflection w' along the radial line of symmetry at ($\theta = 0.5$) for plates having different values of the annularity μ. In Fig. 6.14 the load is specified as ($Q/(1-\mu)^4 = 100$) so that the plates of different annularity are subjected to equal transverse loads. From these figures it can be noticed that, as expected, the deflection increases with increasing span.

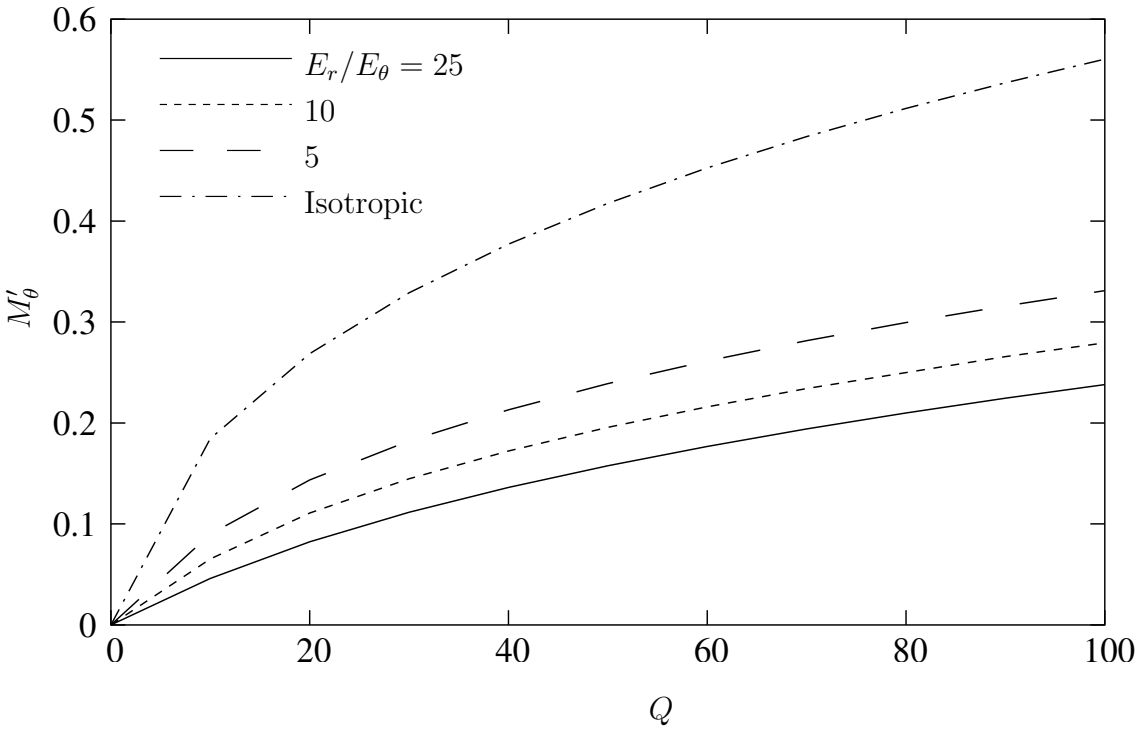

Fig. 6.9 Effect of orthotropy on moment M'_θ of laminated ($n = 4$, $RCCR$) sector plates having $SFSF$ edge condition.

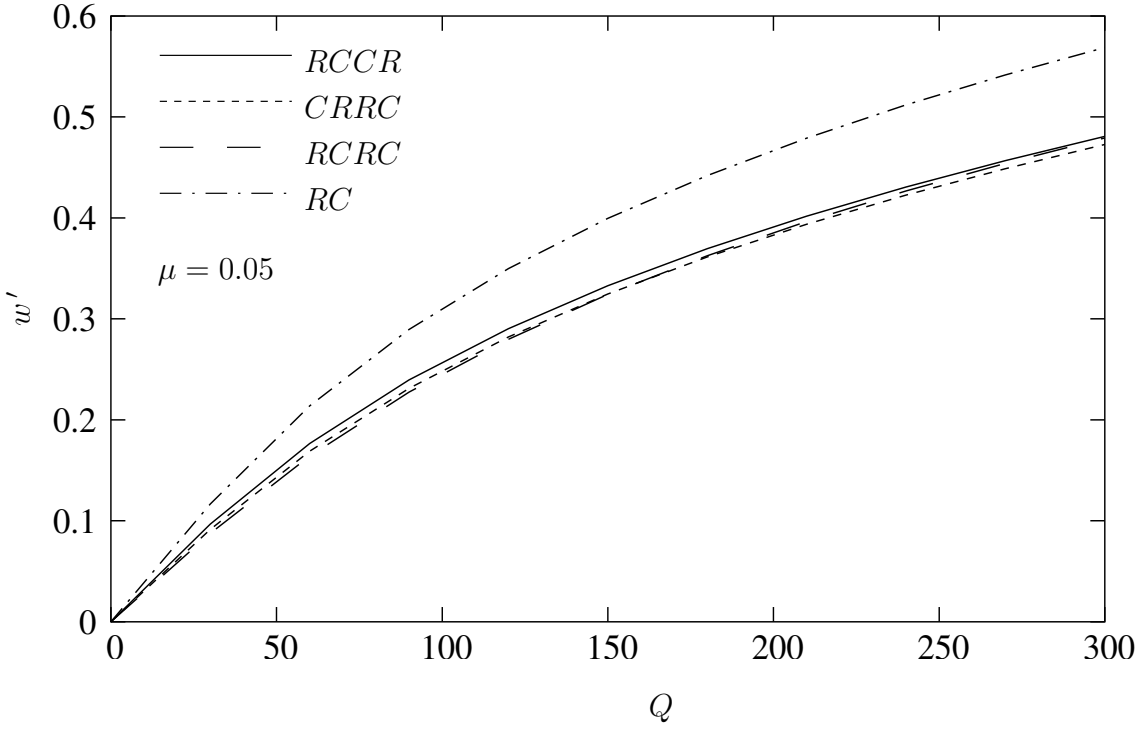

Fig. 6.10 Effect of lamination scheme on deflection w' of laminated sector plates having $CCSS$ edge condition.

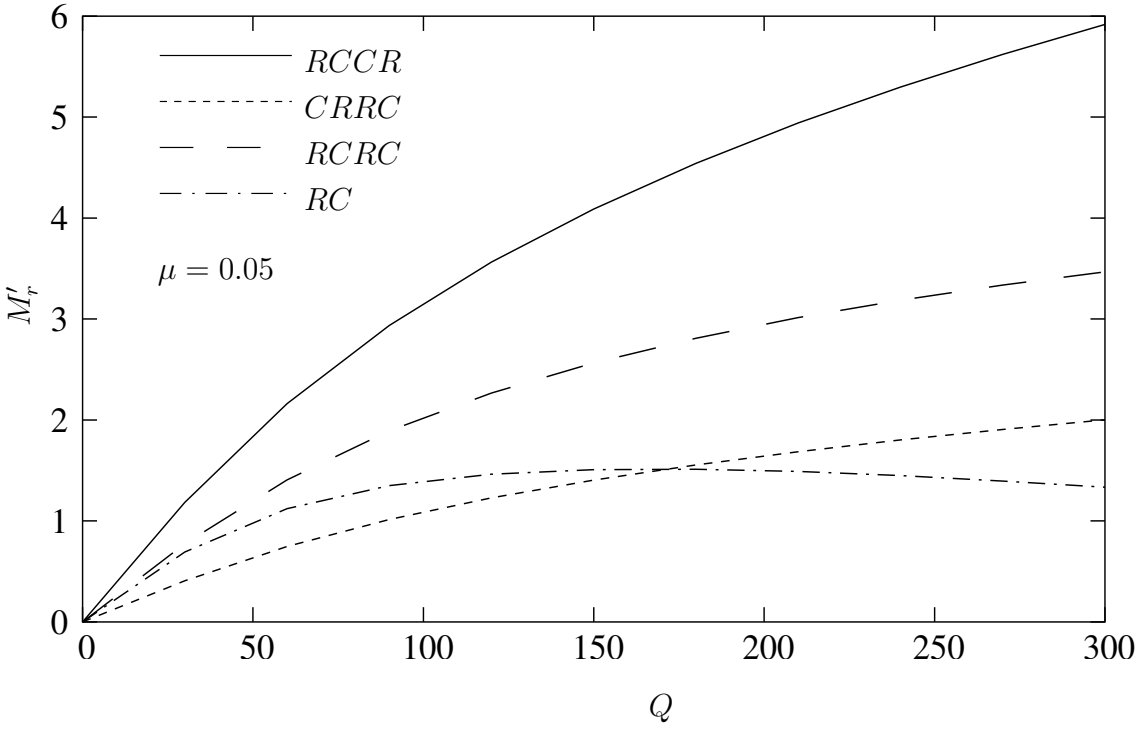

Fig. 6.11 Effect of lamination scheme on moment M_r' of laminated sector plates having $CCSS$ edge condition.

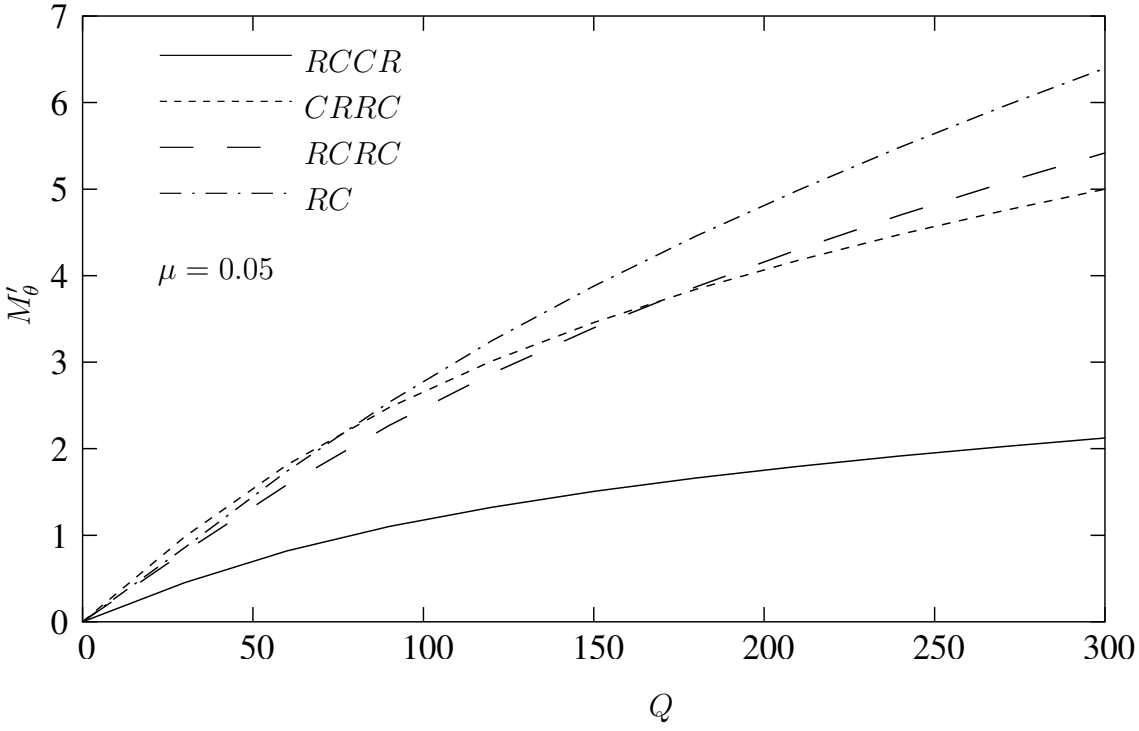

Fig. 6.12 Effect of lamination scheme on moment M_θ' of laminated sector plates having $CCSS$ edge condition.

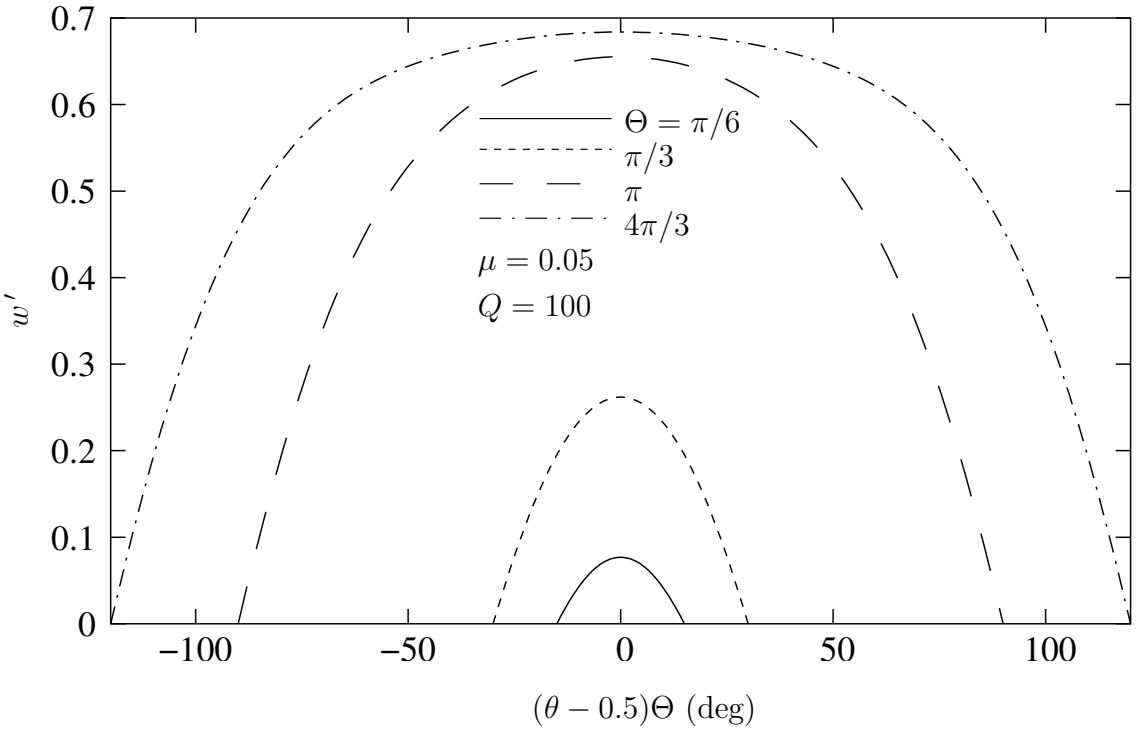

Fig. 6.13 Effect of total sector angle Θ on deflection w' along the arc at $(r = 0.65)$ of laminated $(n = 4, RCRC)$ sector plates having $SSSS$ edge condition.

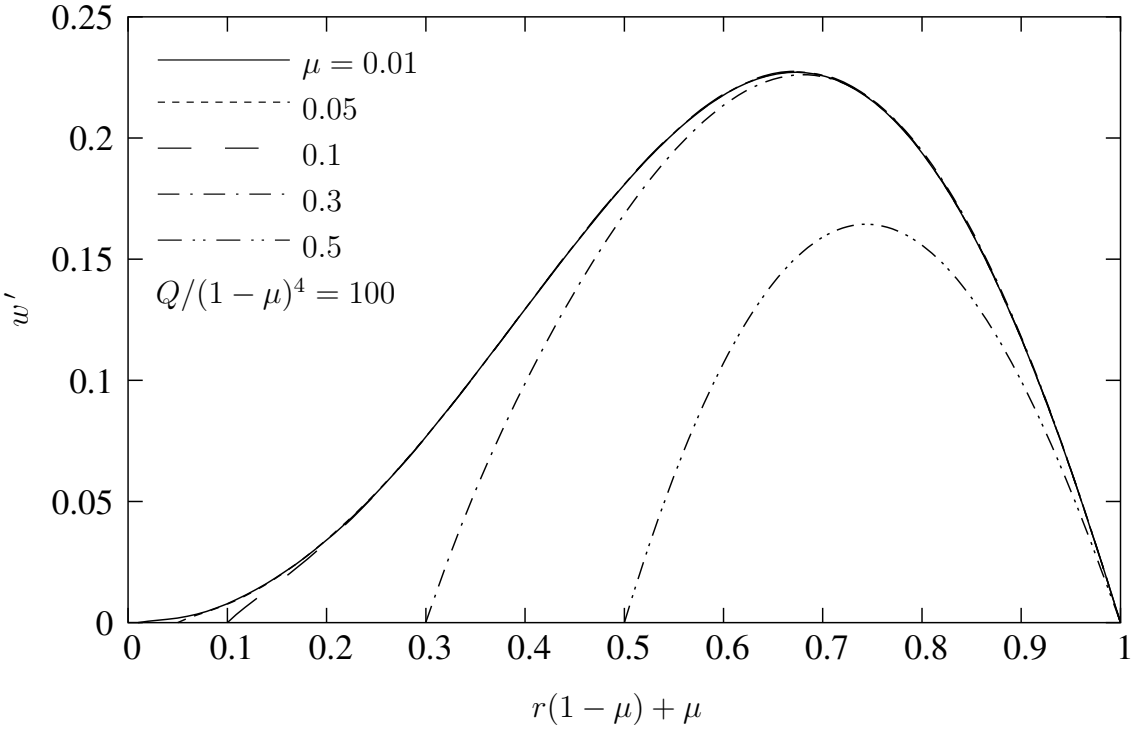

Fig. 6.14 Effect of annularity μ on deflection w' along the radial line at $(\theta = 0.5)$ of laminated $(n = 4, RCRC)$ sector plates having $SSSS$ edge condition.

6.4 Conclusions

The large deflection problem of moderately thick laminated sector plates has been solved using Chebyshev polynomials. The formulation facilitates a simple and efficient solution in the sense that an expansion of 14 terms in r-dimensions and 10 terms in θ-dimension for each of the five displacement components was found satisfactory for all cases dealt in herein. The methodology developed proved robust and efficient for all combinations of clamped and simply supported edge conditions. The method also gives correct results for two opposite edges being free and the other two having any combination simply supported and clamped edge conditions. Effects of boundary conditions are significant, but, response is closer for certain combinations of edge conditions. The deflections reduce with increasing non-homogeneity in terms of moduli ratio and lamination scheme.

CHAPTER 7
NON-LINEAR DYNAMIC ANALYSIS OF LAMINATED COMPOSITE SECTOR PLATES

7.1 Introduction

The structural elements are often subjected to dynamic loading environments and experience deflection of the order of plate thickness. It is important to study the non-linear dynamic behavior for the adequate design estimates. incorporating the large deflection effects. However, to the author's knowledge, there are no studies available on the non-linear dynamic response of laminated sector plates. Study presented in this chapter is an effort in this direction.

The non-linear dynamic analysis of shear-deformable laminated sector plates made up of cylindrically orthotropic layers is presented. Houbolt time marching is used for temporal discretization. Quadratic extrapolation is used for linearization along with fixed-point iteration for obtaining the results. Several combinations of simply supported, clamped and free edge conditions are analyzed. Convergence study has been carried out and the results are compared with the results of square plates. Effects of boundary conditions, moduli ratio, lamination scheme, sector angle and annularity on the transient deflection response are plotted graphically. Step, saw-tooth and sinusoidal loadings are considered.

Sathyamoorthy (1987) gave a comprehensive survey of non-linear vibration analysis of plates using approximate analytical and Finite-element methods. Yamada and

Irie (1987) and Reddy (1997) reviewed the studies on vibration of plates. The large amplitude-free vibration analysis of composite simply supported plate, using a multi-mode time-domain modal formulation based on the FEM was carried out by Shi et al. (1997). Kadiri et al. (1999) applied spectral analysis to obtain the second non-linear mode of a fully clamped rectangular plate. Qatu (2002) reviewed the advances in dynamic analysis of laminated composite shells.

Recently Kirby and Yosibash (2004) and Yosibash et al. (2004) applied Chebyshev polynomials along with Newmark-β time marching scheme for the study of transient response of thin rectangular isotropic plates. Nath and Shukla (2001b) studied the moderately large transient response of laminated square plates using Chebyshev Polynomials. Nath et al. (2005) further presented the linear free vibration response of laminated sector plates with the help of Chebyshev Polynomials.

7.2 Equations of motion and method of solution

The equations of motion for studying non-linear transient response of laminated sector plates are obtained from equations (1.14)- (1.18) after ignoring the piezothermal effects. The equations of motion in terms of displacement components are (refer Chapter 1),

$$
\begin{aligned}
&A_{11}\frac{\zeta^3 r_o}{\zeta'^2}u_{,rr} + 2A_{16}\frac{\zeta^2 r_o}{\zeta'\Theta}u_{,r\theta} + A_{66}\frac{\zeta r_o}{\Theta^2}u_{,\theta\theta} + A_{11}\frac{\zeta^2 r_o}{\zeta'}u_{,r} - A_{22}\zeta r_o u \\
&+A_{16}\frac{\zeta^3 r_o}{\zeta'^2}v_{,rr} + (A_{12}+A_{66})\frac{\zeta^2 r_o}{\zeta'\Theta}v_{,r\theta} + A_{26}\frac{\zeta r_o}{\Theta^2}v_{,\theta\theta} - A_{26}\frac{\zeta^2 r_o}{\zeta'}v_{,r} \\
&-(A_{22}+A_{66})\frac{\zeta r_o}{\Theta}v_{,\theta} - A_{26}\zeta r_o v + B_{11}\frac{\zeta^3 r_o}{\zeta'^2}\phi_{r,rr} + 2B_{16}\frac{\zeta^2 r_o}{\zeta'\Theta}\phi_{r,r\theta} \\
&+B_{66}\frac{\zeta r_o}{\Theta^2}\phi_{r,\theta\theta} + B_{11}\frac{\zeta^2 r_o}{\zeta'}\phi_{r,r} - B_{22}\zeta r_o\phi_r + B_{16}\frac{\zeta^3 r_o}{\zeta'^2}\phi_{\theta,rr} \\
&+(B_{12}+B_{66})\frac{\zeta^2 r_o}{\zeta'\Theta}\phi_{\theta,r\theta} + B_{26}\frac{\zeta r_o}{\Theta^2}\phi_{\theta,\theta\theta} - B_{26}\frac{\zeta^2 r_o}{\zeta'}\phi_{\theta,r}
\end{aligned}
$$

$$
\begin{aligned}
&-\left(B_{22}+B_{66}\right)\frac{\zeta r_o}{\Theta}\phi_{\theta,\theta}-B_{26}\zeta r_o\phi_\theta+\left(A_{11}-A_{12}\right)\zeta^2\left(\frac{w_{,r}}{\zeta'}\right)^2\\
&+\left(A_{12}-A_{22}\right)\left(\frac{w_{,\theta}}{\Theta}\right)^2+\left(A_{16}-A_{26}\right)\zeta\left(\frac{w_{,r}}{\zeta'}\right)\left(\frac{w_{,\theta}}{\Theta}\right)\\
&+A_{11}\zeta^3\left(\frac{w_{,r}}{\zeta'}\right)\left(\frac{w_{,rr}}{\zeta'^2}\right)+A_{12}\left\{\zeta\left(\frac{w_{,\theta}}{\Theta}\right)\left(\frac{w_{,r\theta}}{\zeta'\Theta}\right)-\left(\frac{w_{,\theta}}{\Theta}\right)^2\right\}\\
&+A_{16}\zeta\left\{\zeta\left(\frac{w_{,\theta}}{\Theta}\right)\left(\frac{w_{,rr}}{\zeta'^2}\right)+\zeta\left(\frac{w_{,r}}{\zeta'}\right)\left(\frac{w_{,r\theta}}{\zeta'\Theta}\right)-\left(\frac{w_{,r}}{\zeta'}\right)\left(\frac{w_{,\theta}}{\Theta}\right)\right\}\\
&+A_{16}\zeta^2\left(\frac{w_{,r}}{\zeta'}\right)\left(\frac{w_{,r\theta}}{\zeta'\Theta}\right)+A_{26}\left(\frac{w_{,\theta}}{\Theta}\right)\left(\frac{w_{,\theta\theta}}{\Theta^2}\right)\\
&+A_{66}\zeta\left\{\left(\frac{w_{,\theta}}{\Theta}\right)\left(\frac{w_{,r\theta}}{\zeta'\Theta}\right)+\left(\frac{w_{,r}}{\zeta'}\right)\left(\frac{w_{,\theta\theta}}{\Theta^2}\right)\right\}=\zeta^3 r_o^3\left(I_0u_{,tt}+I_1\phi_{r,tt}\right)
\end{aligned}
\tag{7.1}
$$

$$
\begin{aligned}
&A_{16}\frac{\zeta^3 r_o}{\zeta'^2}u_{,rr}+\left(A_{12}+A_{66}\right)\frac{\zeta^2 r_o}{\zeta'\Theta}u_{,r\theta}+A_{26}\frac{\zeta r_o}{\Theta^2}u_{,\theta\theta}+\left(2A_{16}+A_{26}\right)\frac{\zeta^2 r_o}{\zeta'}u_{,r}\\
&+\left(A_{22}+A_{66}\right)\frac{\zeta r_o}{\Theta}u_{,\theta}-A_{26}\zeta r_o u+A_{66}\frac{\zeta^3 r_o}{\zeta'^2}v_{,rr}+2A_{26}\frac{\zeta^2 r_o}{\zeta'\Theta}v_{,r\theta}+A_{22}\frac{\zeta r_o}{\Theta^2}v_{,\theta\theta}\\
&-A_{66}\frac{\zeta^2 r_o}{\zeta'}v_{,r}-A_{66}\zeta r_o v+B_{16}\frac{\zeta^3 r_o}{\zeta'^2}\phi_{r,rr}+\left(B_{12}+B_{66}\right)\frac{\zeta^2 r_o}{\zeta'\Theta}\phi_{r,r\theta}+B_{26}\frac{\zeta r_o}{\Theta^2}\phi_{r,\theta\theta}\\
&+\left(2B_{16}+B_{26}\right)\frac{\zeta^2 r_o}{\zeta'}\phi_{r,r}+\left(B_{22}+B_{66}\right)\frac{\zeta r_o}{\Theta}\phi_{r,\theta}-B_{26}\zeta r_o\phi_r+B_{66}\frac{\zeta^3 r_o}{\zeta'^2}\phi_{\theta,rr}\\
&+2B_{26}\frac{\zeta^2 r_o}{\zeta'\Theta}\phi_{\theta,r\theta}+B_{22}\frac{\zeta r_o}{\Theta^2}\phi_{\theta,\theta\theta}-B_{66}\frac{\zeta^2 r_o}{\zeta'}\phi_{\theta,r}-B_{66}\zeta r_o\phi_\theta\\
&+2\left\{A_{16}\zeta^2\left(\frac{w_{,r}}{\zeta'}\right)^2+A_{26}\left(\frac{w_{,\theta}}{\Theta}\right)^2+A_{66}\zeta\left(\frac{w_{,r}}{\zeta'}\right)\left(\frac{w_{,\theta}}{\Theta}\right)\right\}\\
&+A_{16}\zeta^3\left(\frac{w_{,r}}{\zeta'}\right)\left(\frac{w_{,rr}}{\zeta'^2}\right)+A_{26}\left\{\zeta\left(\frac{w_{,\theta}}{\Theta}\right)\left(\frac{w_{,r\theta}}{\zeta'\Theta}\right)-\left(\frac{w_{,\theta}}{\Theta}\right)^2\right\}\\
&+A_{66}\zeta\left\{\zeta\left(\frac{w_{,\theta}}{\Theta}\right)\left(\frac{w_{,rr}}{\zeta'^2}\right)+\zeta\left(\frac{w_{,r}}{\zeta'}\right)\left(\frac{w_{,r\theta}}{\zeta'\Theta}\right)-\left(\frac{w_{,r}}{\zeta'}\right)\left(\frac{w_{,\theta}}{\Theta}\right)\right\}\\
&+A_{12}\zeta^2\left(\frac{w_{,r}}{\zeta'}\right)\left(\frac{w_{,r\theta}}{\zeta'\Theta}\right)+A_{22}\left(\frac{w_{,\theta}}{\Theta}\right)\left(\frac{w_{,\theta\theta}}{\Theta^2}\right)\\
&+A_{26}\zeta\left\{\left(\frac{w_{,\theta}}{\Theta}\right)\left(\frac{w_{,r\theta}}{\zeta'\Theta}\right)+\left(\frac{w_{,r}}{\zeta'}\right)\left(\frac{w_{,\theta\theta}}{\Theta^2}\right)\right\}=\zeta^3 r_o^3\left(I_0v_{,tt}+I_1\phi_{\theta,tt}\right)
\end{aligned}
\tag{7.2}
$$

$$
\begin{aligned}
&k^2A_{55}\frac{\zeta^4 r_o^2}{\zeta'^2}w_{,rr}+2k^2A_{45}\zeta^3 r_o^2\frac{w_{,r\theta}}{\zeta'\Theta}+k^2A_{44}\zeta^2 r_o^2\frac{w_{,\theta\theta}}{\Theta^2}+k^2A_{55}\frac{\zeta^3 r_o^2}{\zeta'}w_{,r}\\
&+k^2A_{55}\frac{\zeta^4 r_o^3}{\zeta'}\phi_{r,r}+k^2A_{45}\frac{\zeta^3 r_o^3}{\Theta}\phi_{r,\theta}+k^2A_{55}\zeta^3 r_o^3\phi_r
\end{aligned}
$$

$$
\begin{aligned}
&+k^2A_{45}\frac{\zeta^4r_o^3}{\zeta'}\phi_{\theta,r}+k^2A_{45}\frac{\zeta^3r_o^3}{\Theta}\phi_{\theta,\theta}+k^2A_{44}\zeta^3r_o^3\phi_\theta\\
&+\zeta\left(\zeta\frac{w_{,rr}}{\zeta'^2}+\frac{w_{,r}}{\zeta'}\right)\left\{0.5A_{11}\zeta^2\left(\frac{w_{,r}}{\zeta'}\right)^2+0.5A_{12}\left(\frac{w_{,\theta}}{\Theta}\right)^2\right.\\
&\left.+A_{16}\zeta\left(\frac{w_{,r}}{\zeta'}\right)\left(\frac{w_{,\theta}}{\Theta}\right)\right\}+\frac{w_{,\theta\theta}}{\Theta^2}\left\{0.5A_{12}\zeta^2\left(\frac{w_{,r}}{\zeta'}\right)^2+0.5A_{22}\left(\frac{w_{,\theta}}{\Theta}\right)^2\right.\\
&\left.+A_{26}\zeta\left(\frac{w_{,r}}{\zeta'}\right)\left(\frac{w_{,\theta}}{\Theta}\right)\right\}+\left(2\zeta\frac{w_{,r\theta}}{\zeta'\Theta}-\frac{w_{,\theta}}{\Theta}\right)\left\{0.5A_{16}\zeta^2\left(\frac{w_{,r}}{\zeta'}\right)^2\right.\\
&\left.+0.5A_{26}\left(\frac{w_{,\theta}}{\Theta}\right)^2+A_{66}\zeta\left(\frac{w_{,r}}{\zeta'}\right)\left(\frac{w_{,\theta}}{\Theta}\right)\right\}+\zeta^4r_o^4q=\zeta^4r_o^4I_0w_{,tt}
\end{aligned}
\tag{7.3}
$$

$$
\begin{aligned}
&B_{11}\frac{\zeta^3r_o}{\zeta'^2}u_{,rr}+2B_{16}\frac{\zeta^2r_o}{\zeta'\Theta}u_{,r\theta}+B_{66}\frac{\zeta r_o}{\Theta^2}u_{,\theta\theta}+B_{11}\frac{\zeta^2r_o}{\zeta'}u_{,r}-B_{22}\zeta r_ou\\
&+B_{16}\frac{\zeta^3r_o}{\zeta'^2}v_{,rr}+\left(B_{12}+B_{66}\right)\frac{\zeta^2r_o}{\zeta'\Theta}v_{,r\theta}+B_{26}\frac{\zeta r_o}{\Theta^2}v_{,\theta\theta}-B_{26}\frac{\zeta^2r_o}{\zeta'}v_{,r}\\
&-\left(B_{22}+B_{66}\right)\frac{\zeta r_o}{\Theta}v_{,\theta}-B_{26}\zeta r_ov-k^2A_{55}\frac{\zeta^3r_o^2}{\zeta'}w_{,r}-k^2A_{45}\frac{\zeta^2r_o^2}{\Theta}w_{,\theta}\\
&+D_{11}\frac{\zeta^3r_o}{\zeta'^2}\phi_{r,rr}+2D_{16}\frac{\zeta^2r_o}{\zeta'\Theta}\phi_{r,r\theta}+D_{66}\frac{\zeta r_o}{\Theta^2}\phi_{r,\theta\theta}+D_{11}\frac{\zeta^2r_o}{\zeta'}\phi_{r,r}-D_{22}\zeta r_o\phi_r\\
&-k^2A_{55}\zeta^3r_o^3\phi_r+D_{16}\frac{\zeta^3r_o}{\zeta'^2}\phi_{\theta,rr}+\left(D_{12}+D_{66}\right)\frac{\zeta^2r_o}{\zeta'\Theta}\phi_{\theta,r\theta}\\
&+D_{26}\frac{\zeta r_o}{\Theta^2}\phi_{\theta,\theta\theta}-D_{26}\frac{\zeta^2r_o}{\zeta'}\phi_{\theta,r}-\left(D_{22}+D_{66}\right)\frac{\zeta r_o}{\Theta}\phi_{\theta,\theta}-D_{26}\zeta r_o\phi_\theta\\
&-k^2A_{45}\zeta^3r_o^3\phi_\theta+(B_{11}-B_{12})\zeta^2\left(\frac{w_{,r}}{\zeta'}\right)^2\\
&+\left(B_{12}-B_{22}\right)\left(\frac{w_{,\theta}}{\Theta}\right)^2+(B_{16}-B_{26})\zeta\left(\frac{w_{,r}}{\zeta'}\right)\left(\frac{w_{,\theta}}{\Theta}\right)\\
&+B_{11}\zeta^3\left(\frac{w_{,r}}{\zeta'}\right)\left(\frac{w_{,rr}}{\zeta'^2}\right)+B_{12}\left\{\zeta\left(\frac{w_{,\theta}}{\Theta}\right)\left(\frac{w_{,r\theta}}{\zeta'\Theta}\right)-\left(\frac{w_{,\theta}}{\Theta}\right)^2\right\}\\
&+B_{16}\zeta\left\{\zeta\left(\frac{w_{,\theta}}{\Theta}\right)\left(\frac{w_{,rr}}{\zeta'^2}\right)+\zeta\left(\frac{w_{,r}}{\zeta'}\right)\left(\frac{w_{,r\theta}}{\zeta'\Theta}\right)-\left(\frac{w_{,r}}{\zeta'}\right)\left(\frac{w_{,\theta}}{\Theta}\right)\right\}\\
&+B_{16}\zeta^2\left(\frac{w_{,r}}{\zeta'}\right)\left(\frac{w_{,r\theta}}{\zeta'\Theta}\right)+B_{26}\left(\frac{w_{,\theta}}{\Theta}\right)\left(\frac{w_{,\theta\theta}}{\Theta^2}\right)\\
&+B_{66}\zeta\left\{\left(\frac{w_{,\theta}}{\Theta}\right)\left(\frac{w_{,r\theta}}{\zeta'\Theta}\right)+\left(\frac{w_{,r}}{\zeta'}\right)\left(\frac{w_{,\theta\theta}}{\Theta^2}\right)\right\}=\zeta^3r_o^3\left(I_1u_{,tt}+I_2\phi_{r,tt}\right)
\end{aligned}
\tag{7.4}
$$

$$
B_{16}\frac{\zeta^3r_o}{\zeta'^2}u_{,rr}+\left(B_{12}+B_{66}\right)\frac{\zeta^2r_o}{\zeta'\Theta}u_{,r\theta}+B_{26}\frac{\zeta r_o}{\Theta^2}u_{,\theta\theta}+\left(2B_{16}+B_{26}\right)\frac{\zeta^2r_o}{\zeta'}u_{,r}
$$

$$
\begin{aligned}
&+ (B_{22} + B_{66}) \frac{\zeta r_o}{\Theta} u_{,\theta} - B_{26}\zeta r_o u + b_{66}\frac{\zeta^3 r_o}{\zeta'^2} v_{,rr} + 2B_{26}\frac{\zeta^2 r_o}{\zeta'\Theta} v_{,r\theta} + B_{22}\frac{\zeta r_o}{\Theta^2} v_{,\theta\theta} \\
&- B_{66}\frac{\zeta^2 r_o}{\zeta'} v_{,r} - B_{66}\zeta r_o v - k^2 A_{45}\frac{\zeta^3 r_o^2}{\zeta'} w_{,r} - k^2 A_{55}\frac{\zeta^2 r_o^2}{\Theta} w_{,\theta} + D_{16}\frac{\zeta^3 r_o}{\zeta'^2}\phi_{r,rr} \\
&+ (D_{12} + D_{66})\frac{\zeta^2 r_o}{\zeta'\Theta}\phi_{r,r\theta} + D_{26}\frac{\zeta r_o}{\Theta^2}\phi_{r,\theta\theta} + (2D_{16} + D_{26})\frac{\zeta^2 r_o}{\zeta'}\phi_{r,r} \\
&+ (D_{22} + D_{66})\frac{\zeta r_o}{\Theta}\phi_{r,\theta} - D_{26}\zeta r_o\phi_r - k^2 A_{45}\zeta^3 r_o^3\phi_r + D_{66}\frac{\zeta^3 r_o}{\zeta'^2}\phi_{\theta,rr} \\
&+ 2D_{26}\frac{\zeta^2 r_o}{\zeta'\Theta}\phi_{\theta,r\theta} + D_{22}\frac{\zeta r_o}{\Theta^2}\phi_{\theta,\theta\theta} - D_{66}\frac{\zeta^2 r_o}{\zeta'}\phi_{\theta,r} - D_{66}\zeta r_o\phi_\theta - k^2 A_{44}\zeta^3 r_o^3\phi_\theta \\
&+ 2\left\{ B_{16}\zeta^2\left(\frac{w_{,r}}{\zeta'}\right)^2 + B_{26}\left(\frac{w_{,\theta}}{\Theta}\right)^2 + B_{66}\zeta\left(\frac{w_{,r}}{\zeta'}\right)\left(\frac{w_{,\theta}}{\Theta}\right)\right\} \\
&+ B_{16}\zeta^3\left(\frac{w_{,r}}{\zeta'}\right)\left(\frac{w_{,rr}}{\zeta'^2}\right) + B_{26}\left\{\zeta\left(\frac{w_{,\theta}}{\Theta}\right)\left(\frac{w_{,r\theta}}{\zeta'\Theta}\right) - \left(\frac{w_{,\theta}}{\Theta}\right)^2\right\} \\
&+ B_{66}\zeta\left\{\zeta\left(\frac{w_{,\theta}}{\Theta}\right)\left(\frac{w_{,rr}}{\zeta'^2}\right) + \zeta\left(\frac{w_{,r}}{\zeta'}\right)\left(\frac{w_{,r\theta}}{\zeta'\Theta}\right) - \left(\frac{w_{,r}}{\zeta'}\right)\left(\frac{w_{,\theta}}{\Theta}\right)\right\} \\
&+ B_{12}\zeta^2\left(\frac{w_{,r}}{\zeta'}\right)\left(\frac{w_{,r\theta}}{\zeta'\Theta}\right) + B_{22}\left(\frac{w_{,\theta}}{\Theta}\right)\left(\frac{w_{,\theta\theta}}{\Theta^2}\right) \\
&+ B_{26}\zeta\left\{\left(\frac{w_{,\theta}}{\Theta}\right)\left(\frac{w_{,r\theta}}{\zeta'\Theta}\right) + \left(\frac{w_{,r}}{\zeta'}\right)\left(\frac{w_{,\theta\theta}}{\Theta^2}\right)\right\} = \zeta^3 r_o^3\left(I_0 v_{,tt} + I_1\phi_{\theta,tt}\right)
\end{aligned}
\tag{7.5}
$$

The ramp load is specified as follows.

$$
Q(t) = 10\left[1 - \widehat{\left(\frac{\tau}{T}\right)}\right] \tag{7.6}
$$

For evaluating the quotient in $\widehat{\left(\frac{\tau}{T}\right)}$, τ is reset to zero at the end of every non-dimensional time period T. The sinusoidal load is,

$$
Q(t) = 10\cos(2\pi\tau/T) \tag{7.7}
$$

The non-linear quantities at the Jth step of the marching variable are calculated by approximating the displacement components at that step with quadratic extrapolation scheme. Thus if $(\hat{u}, \hat{v}, \hat{w}, \hat{\phi_r}, \hat{\phi_\theta})_{ij,J}$ denotes the approximated coefficients at the Jth step, then,

$$
(\hat{u}, \hat{v}, \hat{w}, \hat{\phi_r}, \hat{\phi_\theta})_{ij,J} \;=\; A(u, v, w, \phi_r, \phi_\theta)_{ij,J-1} + B(u, v, w, \phi_r, \phi_\theta)_{ij,J-2}
$$

$$+C(u, v, w, \phi_r, \phi_\theta)_{ij,J-3} \tag{7.8}$$

The coefficients A,B and C of quadratic extrapolation scheme are $(1, 0, 0)$ at $(J = 1)$, $(2, -1, 0)$ at $(J = 2)$ and $(3, -3, 1)$ at $(J \geq 3)$. Implicit Houbolt time-marching method (Houbolt, 1950) is used to evaluate the acceleration terms in the governing equations (7.1)- (7.5). At time-step J, the acceleration $(u_{,tt})_J$ for example, is evaluated as follows.

$$(u_{,tt})_J = \frac{1}{\Delta t^2}\left(\beta_1 u_J + \beta_2 u_{J-1} + \beta_3 u_{J-2} + \beta_4 u_{J-3} + \beta_5\right) \tag{7.9}$$

Houbolt coefficients β_i for $(i = 1, 5)$ are as given in Appendix 9.2.

From these equations, a system of $5(M + 1)(N + 1)$ number of non-linear algebraic equations in terms of the $5(M + 1)(N + 1)$ number of unknown coefficients are generated. This system of equations is solved using fixed-point iteration scheme at each time step.

7.3 Results and Discussions

The present chapter gives the dynamic large deflection results of moderately thick laminated sector plates made up of cylindrically orthotropic layers subjected to uniformly distributed step, sinusoidal and ramp loadings. The boundary conditions considered are various combinations of simply supported , clamped and free edges. The effects of boundary conditions, moduli ratio, lamination scheme, sector angle, annularity and, the type and the period of the dynamic uniformly distributed loadings are studied.

Every layer is assumed to be cylindrically orthotropic. With fiber orientation in radial direction, the required material properties are as follows unless otherwise

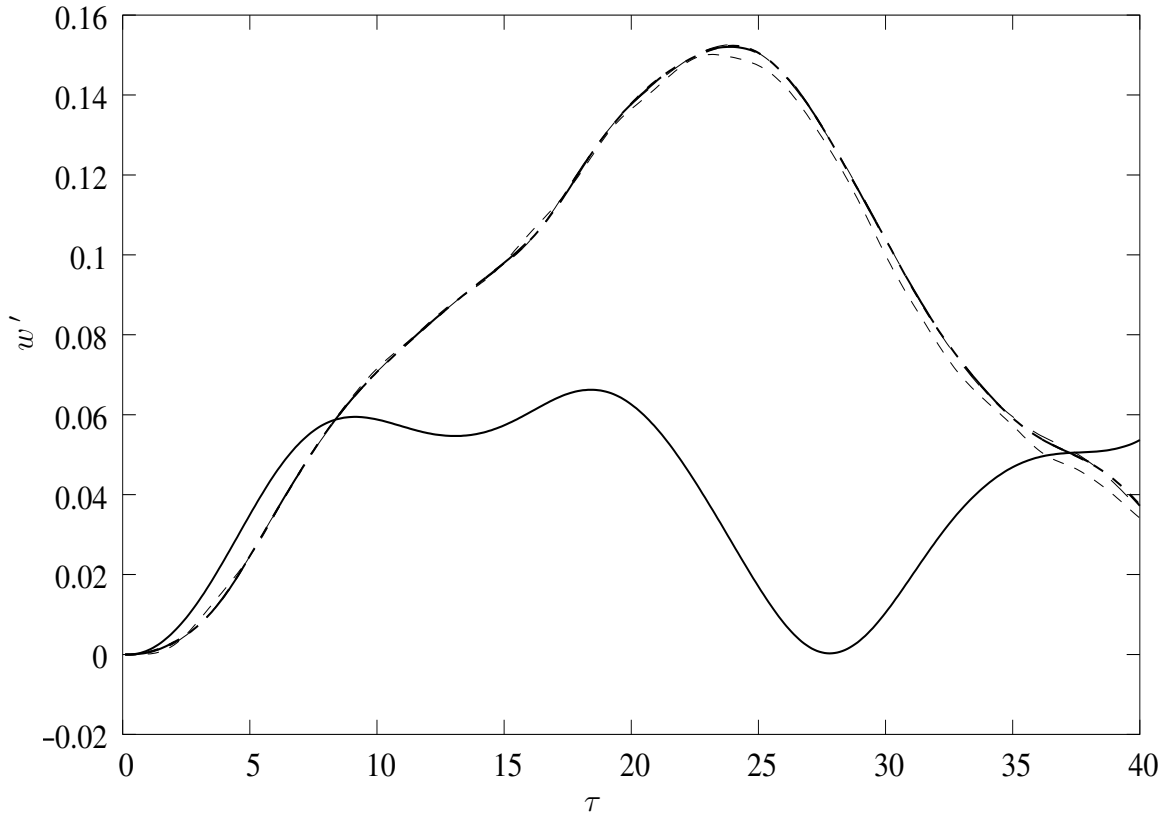

Fig. 7.1 Convergence with respect to the degrees of the polynomials ($M \times N$)**. The parameters are:** ($n = 4$, $RCRC$)**, boundary condition is** $SSFS$**,** $\mu = 0.01$**,** $\Theta = \pi/3$**,** $\lambda = 0.1$**,** ($r = 0.65, \theta = 0.5$)**, step load of** $Q = 10$**,** $\Delta\tau = 0.1$**.** ——— **:** 7×3 - - - - - - - - - **:** 9×5 — — **:** 11×7 — · — · — · **:** 13×9 — ·· — ·· — **:** 15×11

specified.

$$E_r/E_\theta = 25, \quad \nu_{r\theta} = 0.25, \quad G_{r\theta} = G_{rz} = 0.5E_\theta, \quad G_{\theta z} = 0.2E_\theta \tag{7.10}$$

Spatial convergence is given in Figure 7.1 in terms of transient response w' for ($Q = 10$, $r = 0.65$, $\theta = 0.5$). It can be seen that satisfactory results are obtained with as small degrees as (9×5), and, no appreciable change is noticed beyond the size of (13×9). In the subsequent analysis ($M = 13$) $\times$ ($N = 9$). Based on the convergence study for choosing time step ($\Delta\tau$), as highlighted in Figure 7.2, the time step of ($\Delta\tau = 0.1$) is taken for the detailed parametric studies.

The linear and non-linear responses for $CSSS$ and $CCFC$ sector plates for ($n =$

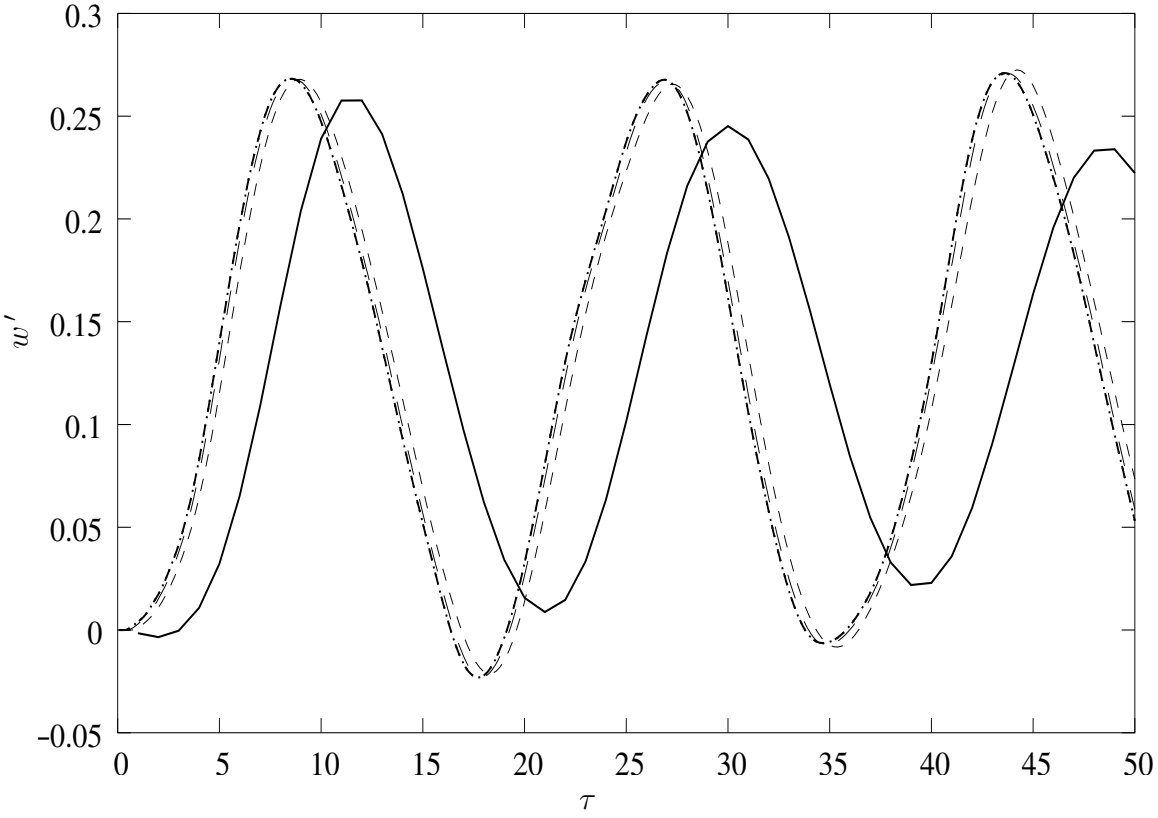

Fig. 7.2 Convergence with respect to the size of the time-step $\Delta\tau$. The parameters are: $(n = 4, RCRC)$, boundary condition is $SSSS$, $\mu = 0.01$, $\Theta = \pi/3$, $\lambda = 0.1$, $(r = 0.65, \theta = 0.5)$, step load of $Q = 50$. ———— **: $\Delta\tau = 1$,** - - - - - - - - - - **: 0.2,** — — **: 0.1 and** — · — · — **: 0.05 .**

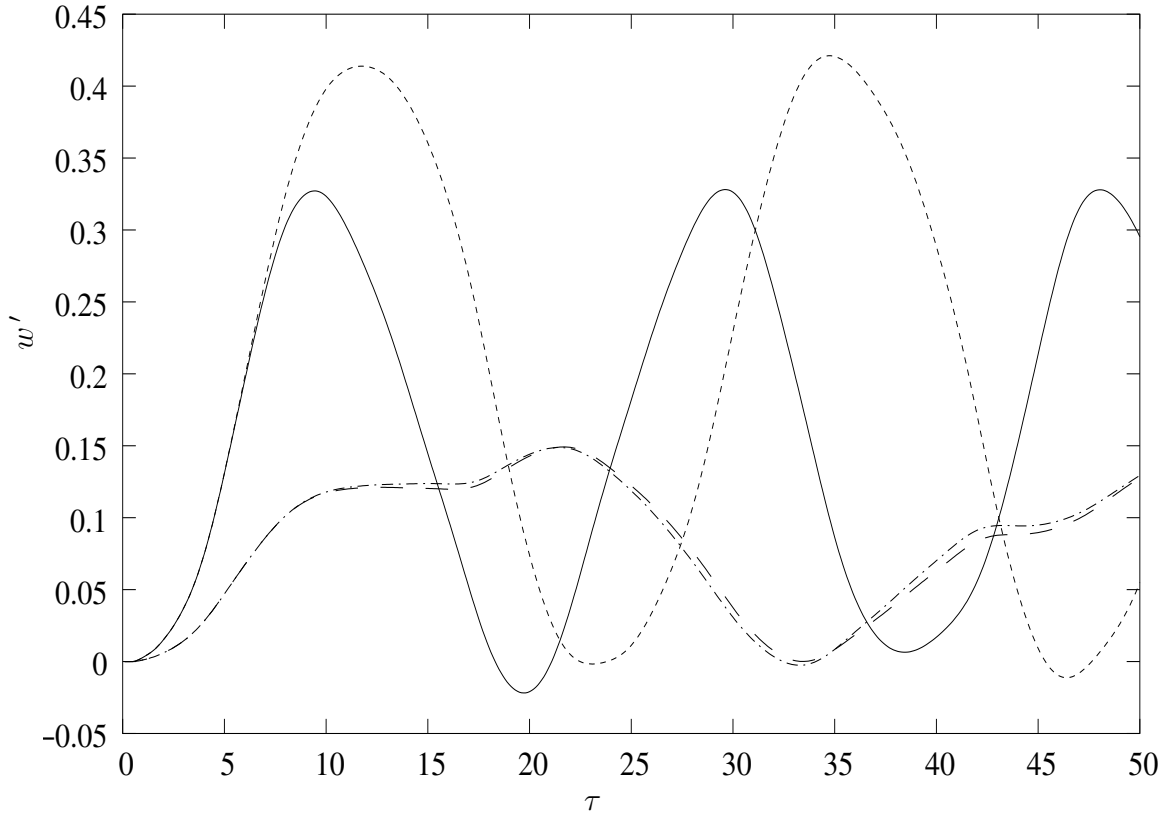

Fig. 7.3 Effect of non-linear analysis. The parameters are: $(n = 2, RC)$, $\mu = 0.01$, $\Theta = \pi/3$, $\lambda = 0.1$, $(r = 0.65, \theta = 0.5)$. (a) With $CSSS$ as boundary condition and $Q = 50$: ———— : non-linear analysis, and , - - - - - - - - - : linear analysis. (b) With $CCFC$ as boundary condition and $Q = 20$: — — : non-linear analysis, and , — · — · — : linear analysis.

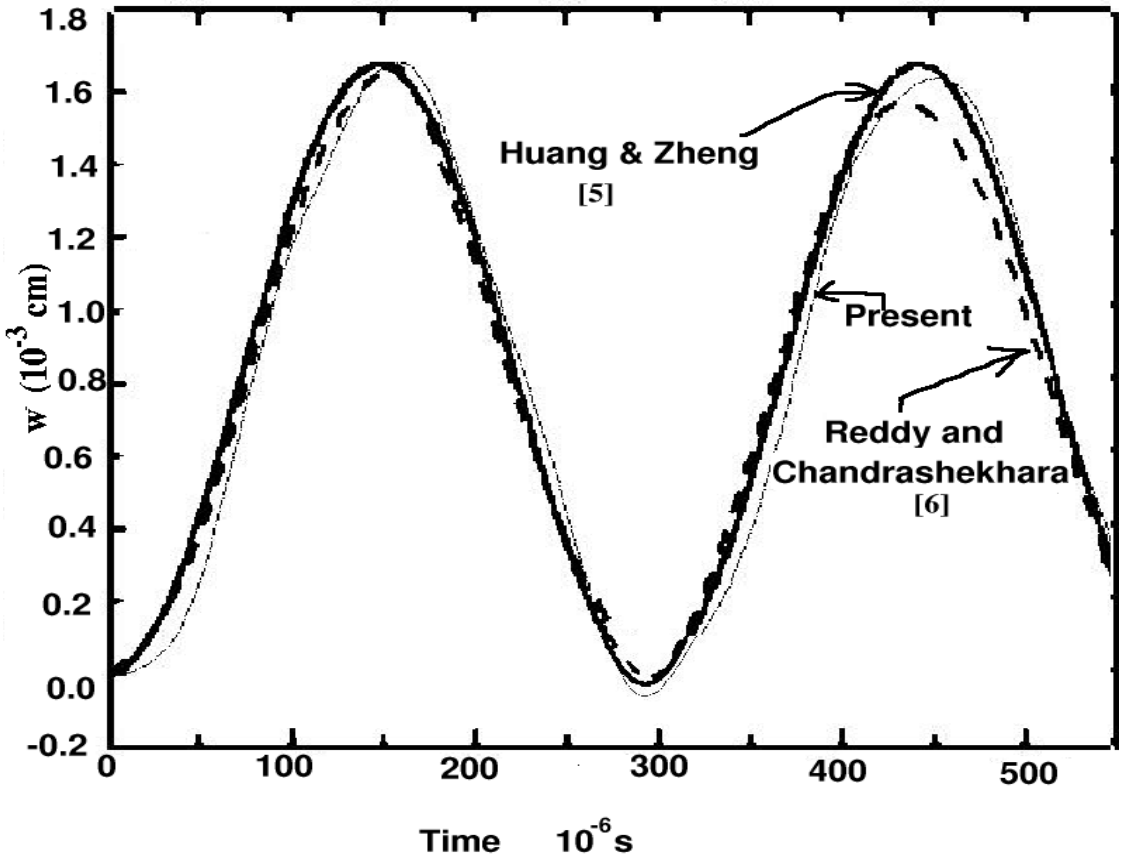

Fig. 7.4 Comparison of results of almost square isotropic plate subjected to a step load of $q = 10$ N/cm^2 with the results of Huang and Zheng (2003) and Reddy and Chandrashekhara (1985) The parameters are: boundary condition is $SSSS$, $\Delta\tau = 0.1$, $\mu = 0.999995$, $\Theta = 5 \times 10^{-6}$, $\lambda = 10^{-6}$, $(r = 0.5, \theta = 0.5)$, $\mathbf{E} = 2.1 \times 10^6$ N/cm^2, $\nu = 0.25$ and $\rho = 8 \times 10^{-6}$ N-s^2 /cm^4 .

2, RC) lamination scheme are given in Figure 7.3. The difference between non-linear analysis and linear analysis is significant for the $CSSS$ plate subjected to a larger load of $Q = 50$ in comparison to the $CCCF$ plate subjected to $Q = 20$. The effect of non-linearity is significant when the resulting transverse displacement is comparable to the plate thickness.

Comparison of almost square isotropic plate results with Huang and Zheng (2003) and Reddy and Chandrashekhara (1985) are given in Figure 7.4 in terms of deflection w' at $(r = 0.5, \theta = 0.5)$. Figure 7.5 shows the transient response to step load of

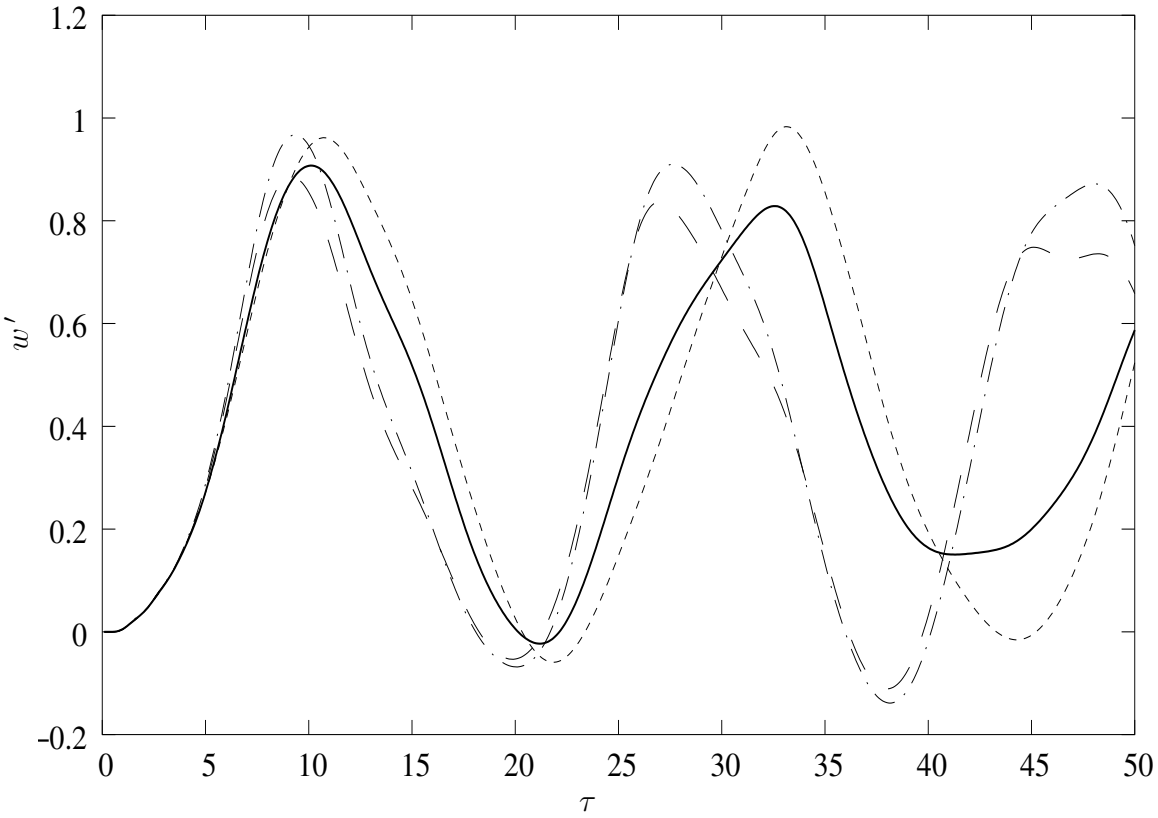

Fig. 7.5 Square plate results for comparison with the results of Nath and Shukla (2001b). The parameters are: $(n = 2, RC)$**, boundary condition is** $SSSS$**,** $\mu = 0.999990$**,** $\lambda = 10^{-6}$**,** $\Theta = 10^{-5}$**, step load of** $Q = 125$**,** $\Delta\tau = 0.1$ **and** $(r = 0.5, \theta = 0.5)$**.** ———— **:** $CCCF$**,** - - - - - - - - - - **:** $CFCF$ — — **:** $CCSS$ **and** — · — · — · **:** $SSSS$**.**

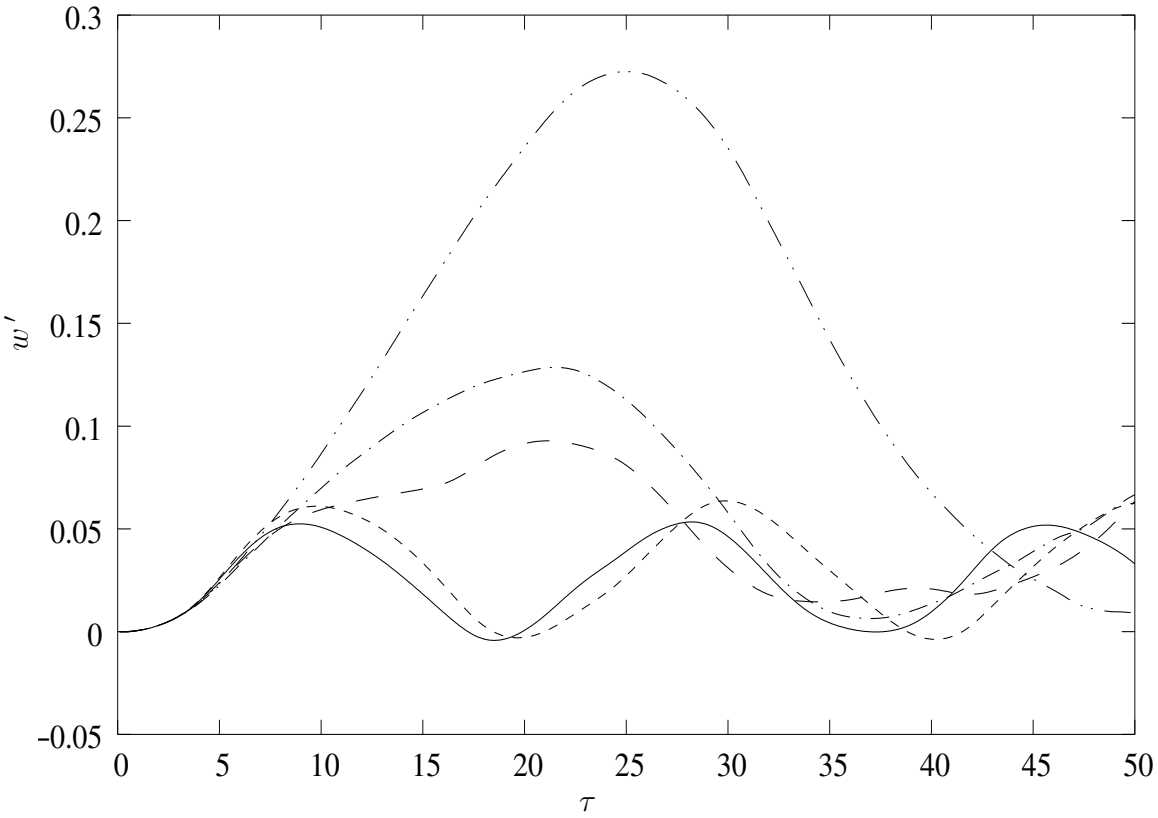

Fig. 7.6 Effect of boundary condition. The parameters are: $(n = 4,\ RCRC)$**,** $\mu = 0.01$**,** $\Theta = \pi/3$**,** $\lambda = 0.1$**,** $(r = 0.65, \theta = 0.5)$ **and step load of** $Q = 10$**.** ———— **:** $CCSS$**,** - - - - - - - - - - **:** $SSSS$**,** — — **:** $CCFS$**,** — · — · — · **:** $CFCF$ **and** — ·· — ·· — **:** $CFSF$**.**

almost square laminated ($n = 2$, RC) plates for four kinds of boundary conditions. These results compare very well with the results given by Nath and Shukla (2001b) in their Figure (8).

Effect of combinations of clamped, simply supported and free edge conditions is shown in Figure 7.6. The methodology gives satisfactory and stable results with these wide variety of edge-conditions ($CCSS$, $CCFS$ and $CFSF$). Figure 7.7 shows the effect of moduli-ratio (E_r/E_θ) on laminated (RC) sector plates having $FSCF$ edge-condition. Here, the number of peaks decreases with increasing (E_r/E_θ). This observation is contrary to the trend observed by Khdeir (1989) and Sharma et al. (2005) of increasing frequency with increasing moduli ratio in the linear vibration

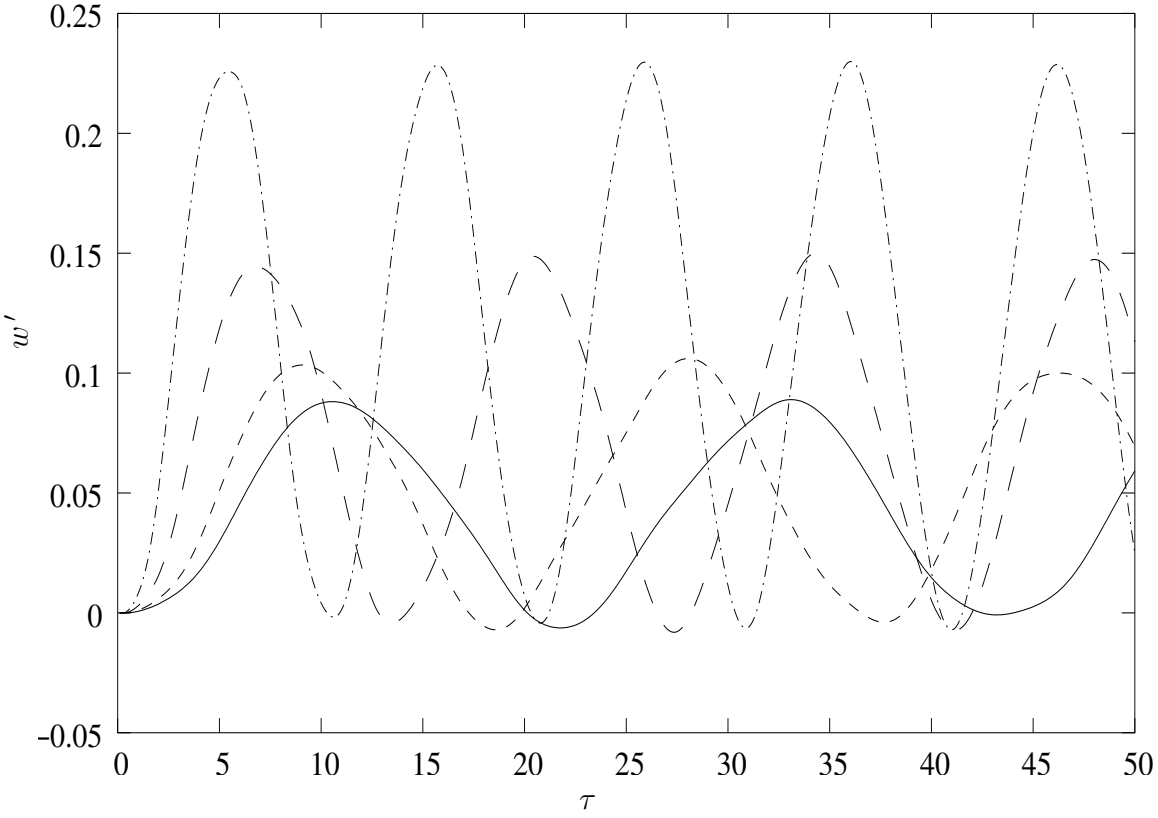

Fig. 7.7 Effect of moduli ratio E_r/E_θ. The parameters are: $(n = 2, RC)$, boundary condition is $FSCS$, $\mu = 0.1$, $\Theta = \pi/3$, $\lambda = 0.1$, $(r = 0.65, \theta = 0.5)$ and step load of $Q = 10$. ———— : $E_r/E_\theta = 25$ ---------- : 15, — — : 5 and — · — · — : isotropic.

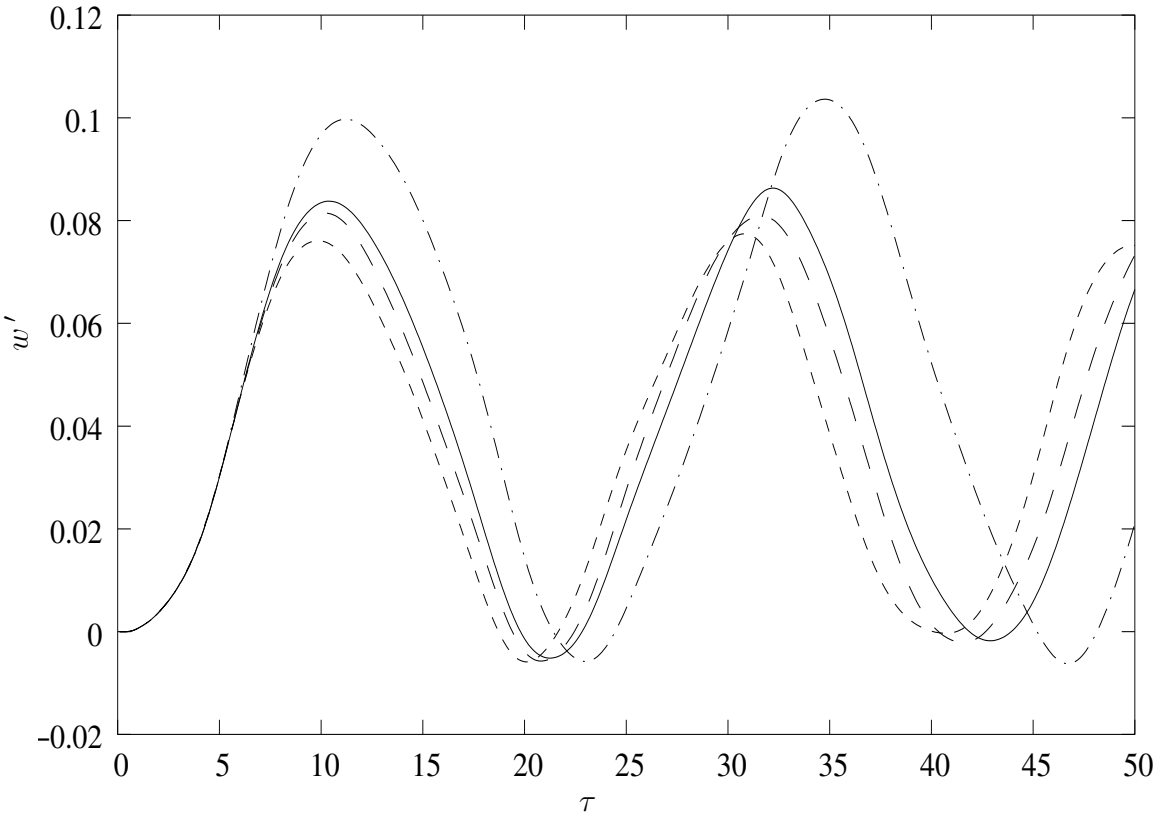

Fig. 7.8 Effect of lamination scheme. The parameters are: boundary condition is $CSSC$**,** $\mu = 0.1$**,** $\Theta = \pi/3$**,** $\lambda = 0.1$**,** $(r = 0.65, \theta = 0.5)$ **and step load of** $Q = 10$**.** ———— **:** $n = 4$, $RCCR$**,** - - - - - - - - - - **:** $n = 4$, $RCRC$**,** — — **:** $n = 4$, $CRRC$ **and** — . — . — . **:** $n = 2$, RC**.**

analysis of laminated plates. But, if the non-dimensionalization of time t to τ is taken in to account, it is found that (A_{22}) taking the values of $(13.0, 8.03, 3.03$ and $1.07)$ for $(E_r/E_\theta = 25, 15, 5)$ and the isotropic case respectively decreases the size of the time-range in terms of t for the stiffer plates. Thus, it is observed that the number of peaks over the same time increases with moduli ratio.

Effect of lamination scheme is shown in Figure 7.8 for $RCCR$, $RCRC$, $CRRC$ and RC plates. Very little difference is noticed in terms of amplitude and frequency of peaks. The effect of lamination scheme is more pronounced on RC plate than the $RCRC$ plate. Figure 7.9 shows the effect of total sector angle (Θ) for $RCRC$ laminated plates having $SSSC$ edge-conditions. The sector angle (Θ) significantly

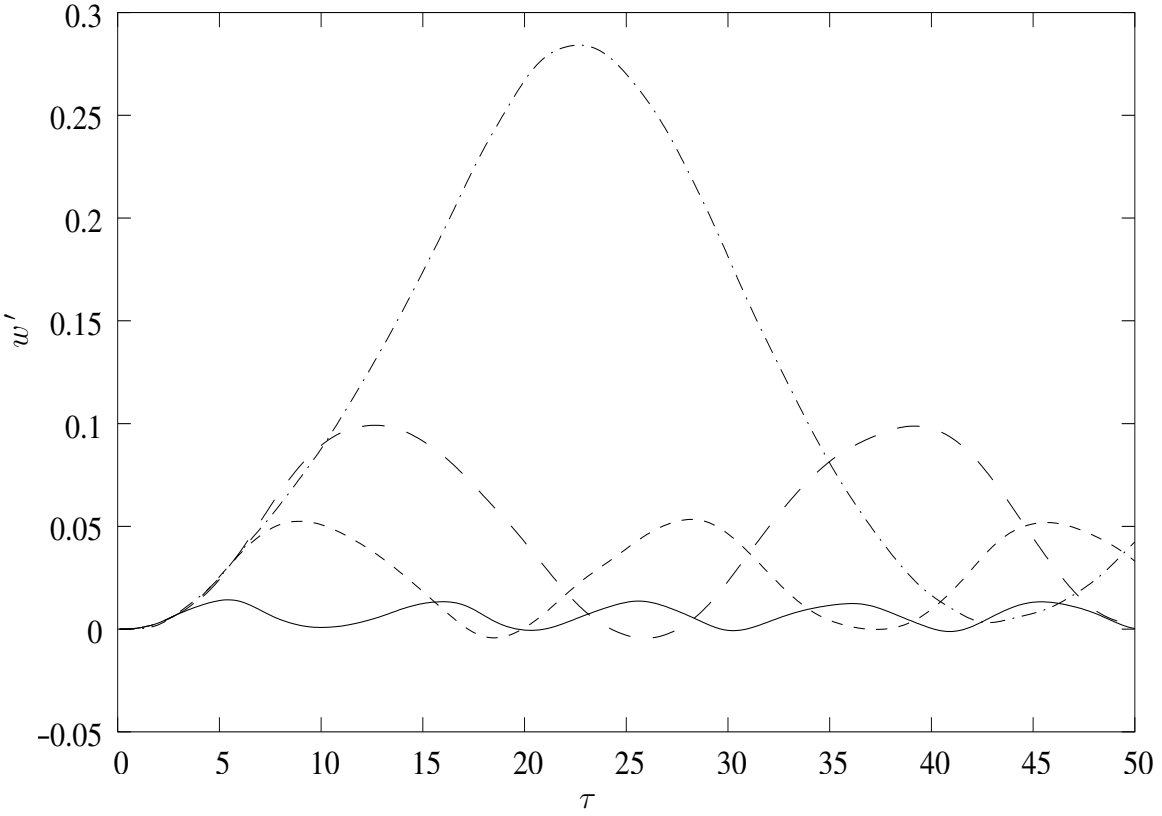

Fig. 7.9 Effect of sector angle Θ. The parameters are: ($n = 4$, $RCRC$), boundary condition is $SSSC$, $\mu = 0.01$, $\lambda = 0.1$, ($r = 0.65, \theta = 0.5$) and step load of $Q = 10$. ———— **:** $\Theta = \pi/6$, ---------- **:** $\pi/3$, — — **:** $\pi/2$ **and** — · — · — · **:** $4\pi/3$.

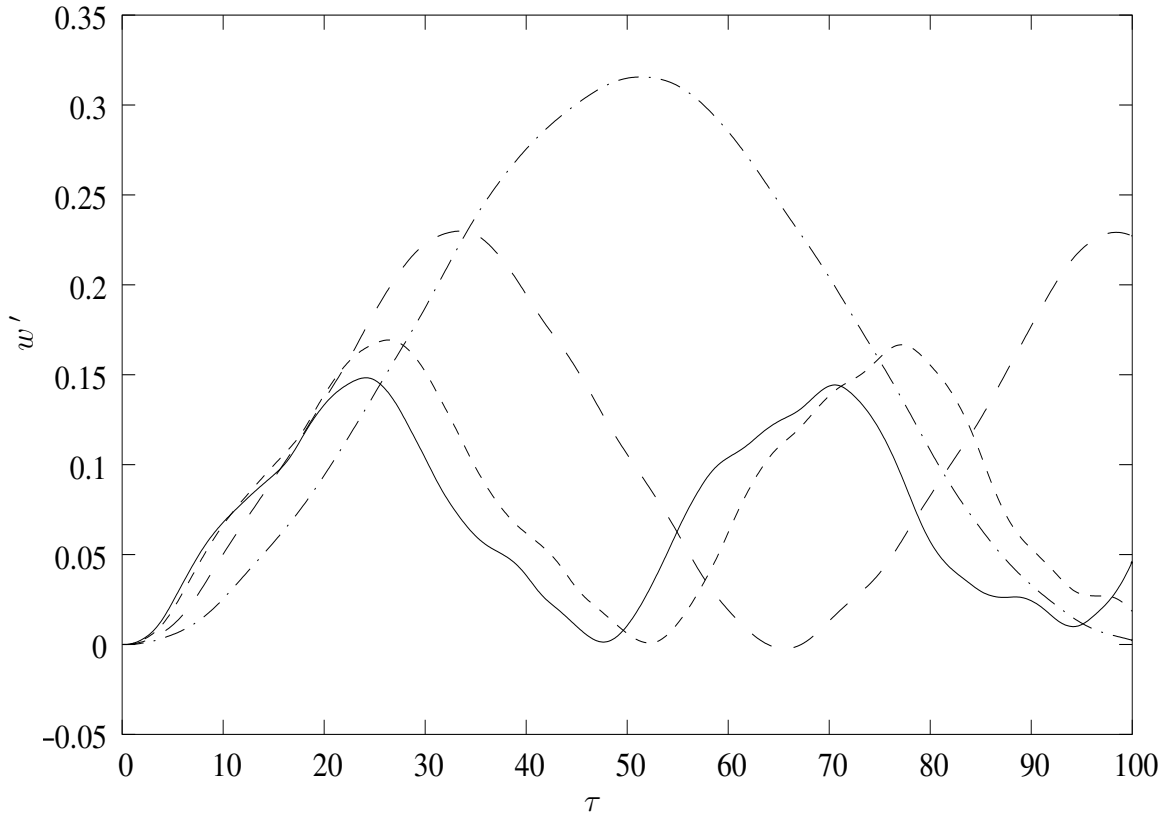

Fig. 7.10 Effect of annularity μ. The parameters are: $(n = 4, RCRC)$, boundary condition is $SSFS$, $\Theta = \pi/3$, $\lambda = 0.1$, $(r = 0.65, \theta = 0.5)$ and step load of $(Q/(1-\mu)^4 = 10)$. ———— : $\mu = 0.01$, - - - - - - - - - - : $\mu = 0.1$, — — : $\mu = 0.3$ and — . — . — . : $\mu = 0.5$.

increases both the amplitude as well as the time-gap between the peaks.

The effect of annularity (μ) is shown in Figure 7.10. In order to make the non-dimensionalized load independent of μ, the magnitude of the step load for all the cases in this figure is specified as $(Q/(1-\mu)^4 = 10)$. It can be seen that the amplitude increases and the frequency of peaks reduces with increasing μ.

The transient response to ramp and sinusoidal loadings of two periods each is given in Figure 7.11. step load response is also shown for comparison. Maximum dynamic defection is obtained with step load.

7.4 Conclusions

The dynamic large deflection problem of moderately thick laminated sector plates has been solved using Chebyshev polynomials, Houbolt time-marching and fixed-point iteration. The formulation facilitates for the first time a simple and efficient solution in the sense that an expansion of 14 terms in r-dimensions and 10 terms in θ-dimension for each of the five displacement components was found satisfactory for all cases dealt herein. Rectangular plate results given by earlier researchers were also matched with the methodology developed essentially for sectoral domain. Boundary conditions have significant effect on the non-linear transient response. The dynamic response is more affected by moduli ratio than the lamination scheme. The deflections increased with increasing span in terms of Θ and μ. The type of dynamic load affects both the wave-shape as well as the magnitude of the dynamic response.

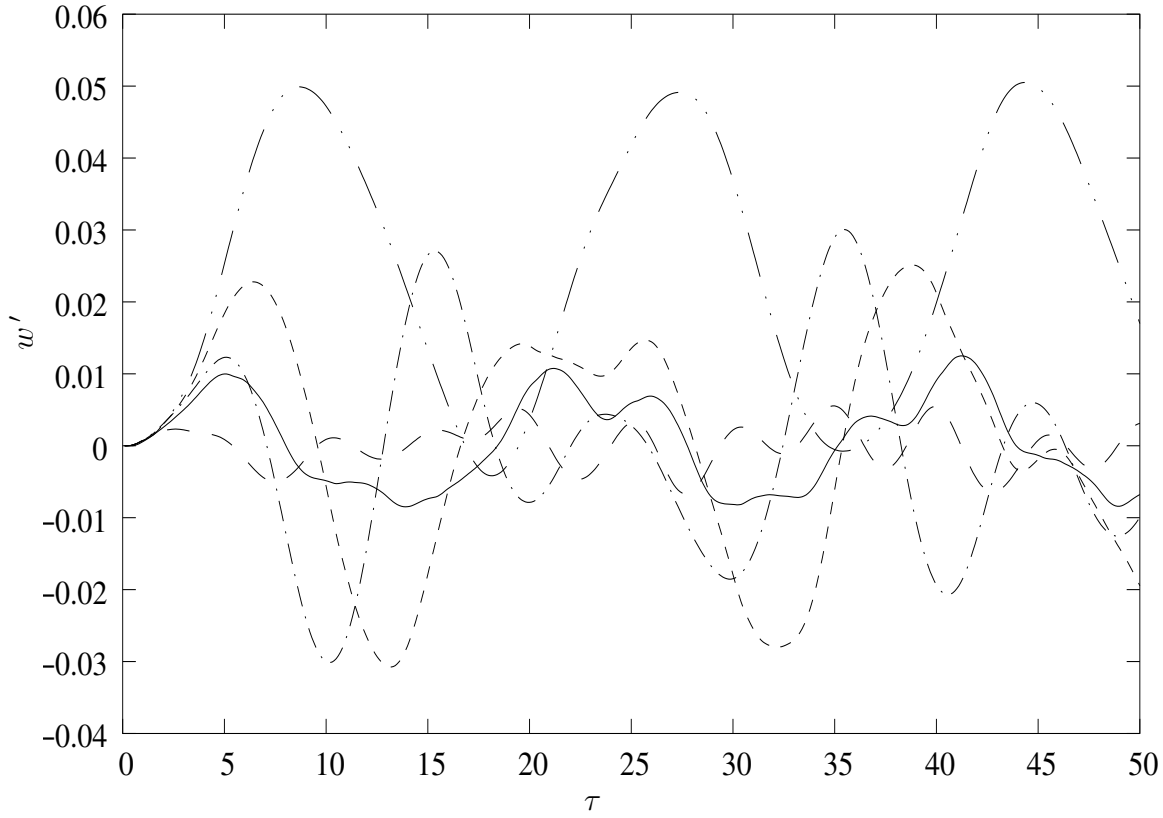

Fig. 7.11 Effect of type and period of load. The parameters are: ($n = 4$, $RCRC$)**, boundary condition is** $SSCS$, $\mu = 0.01$, $\Theta = \pi/3$, $\lambda = 0.1$ **and** ($r = 0.65, \theta = 0.5$)**.** ———— **, ramp load,** $T = 5$; - - - - - - - - - - **, ramp load,** $T = 10$; — — **, sinusoidal load,**$T = 5$; — · — · **, sinusoidal load,** $T = 10$ **and** — ·· — ·· **: step loading,** $Q = 10$**.**

CHAPTER 8
PIEZOTHERMOELASTIC RESPONSE OF LAMINATED SECTOR PLATES

8.1 Introduction

This Chapter deals with the non-linear static response of shear-deformable laminated sector plates having surface bonded piezoelectric layers. The non-axisymmetric formulation based on von-Kármán type kinematics and first order shear deformation theory in cylindrical coordinates is discretized in space domain using two-dimensional Chebyshev polynomials. An incremental iterative approach based on Newton-Raphson technique is used for solving the non-linear algebraic equations. Convergence study has been carried out and the results are compared with the results of square plates. Several combinations of simply supported, clamped and free edge conditions are considered. Thermal effects arising out of prescribed surface temperatures are also studied assuming uniform temperature in a plane parallel to the surfaces. Effects of temperature rise and electric fields on the non-linear static response are analyzed and shown graphically.

The bending, buckling and vibration of piezoelectric laminated plates have been the subject of many investigations. Benjeddou (2000) and Mackerle (2001) have given excellent bibliographies of the research conducted in the area of smart structures. Librescu and Marzocca (2005) studied advances in linear and non-linear control of structures.

Jonnalagadda et al. (1994) presented a Navier type solution for simply supported piezolaminated plates. They further employed nine-noded Lagrangian elements for the analysis of plates with various edge conditions. Kapuria et al. (1997) gave Levy-type solutions for piezolaminated plates based on First order shear deformation theory (FSDT). Oh et al. (2000) gave non-linear finite element formulation for postbuckling and vibration analysis of piezolaminated plates subjected to piezothermomechanical loads. Bisegna et al. (2001) presented a variational formulation and a locking-free finite element formulation based on a layer-wise model of three-layer piezoelectric sandwich plates for the study of vibration suppression of a thick cantilever steel plate having piezoelectric actuators bonded on the surfaces. Loja et al. (2001) applied higher order B-spline finite strip models to the static and free vibration analysis of laminated plates, with arbitrary shape and lay-ups, loading and boundary conditions. Sekouri et al. (2004) presented an analytical approach for the modeling of circular plates with piezoelectric actuators based on Kirchhoff plate theory. Shen (2004) presented the non-linear bending analysis of unsymmetric cross-ply laminated rectangular plates with piezoelectric actuators in thermal environments. The study is based on stress-function approach and non-linear analysis of simply supported rectangular plates is carried out. Yang et al. (2004) applied Galerkin procedure for geometrically non-linear analysis of laminated plates having piezoelectric actuator layers bonded on the surfaces of a functionally graded sub-grade.

Most of these studies have been carried out in either rectangular or circular domains employing linear mathematical models. Common methods employed are finite element methods and boundary element methods for arbitrary boundary conditions

and Levy type analytical methods for certain combinations of edge conditions.

8.2 Governing Equations

The equations of equilibrium for analyzing the piezothermomechanical large deflection static response of piezolaminated sector plates are derived from equations (1.14)-(1.18) by dropping the inertia terms. As mentioned in Chapter 1, assuming uniform temperature over any plane parallel to the plate's mid-plane, the temperature is a piecewise linear function of z-coordinate. The temperature at each interface can easily be determined using the heat continuity equations. Thus, thermal actuation is prescribed in terms of temperatures at the top (T_0) and bottom (T_n) surfaces. Electrical actuation is prescribed in terms of potential gradient $E_z^{(k)}$ across piezoelectric layers. The equilibrium equations in terms of displacement components, transverse pressure q and piezothermal loads (N_r^P, N_θ^p, M_r^P, M_θ^P, N_r^T, N_θ^T, M_r^T and M_θ^T) are,

$$
\begin{aligned}
&A_{11}\frac{\zeta^3 r_o}{\zeta'^2}u_{,rr} + 2A_{16}\frac{\zeta^2 r_o}{\zeta'\Theta}u_{,r\theta} + A_{66}\frac{\zeta r_o}{\Theta^2}u_{,\theta\theta} + A_{11}\frac{\zeta^2 r_o}{\zeta'}u_{,r} - A_{22}\zeta r_o u \\
&+A_{16}\frac{\zeta^3 r_o}{\zeta'^2}v_{,rr} + (A_{12}+A_{66})\frac{\zeta^2 r_o}{\zeta'\Theta}v_{,r\theta} + A_{26}\frac{\zeta r_o}{\Theta^2}v_{,\theta\theta} - A_{26}\frac{\zeta^2 r_o}{\zeta'}v_{,r} \\
&-(A_{22}+A_{66})\frac{\zeta r_o}{\Theta}v_{,\theta} - A_{26}\zeta r_o v + B_{11}\frac{\zeta^3 r_o}{\zeta'^2}\phi_{r,rr} + 2B_{16}\frac{\zeta^2 r_o}{\zeta'\Theta}\phi_{r,r\theta} \\
&+B_{66}\frac{\zeta r_o}{\Theta^2}\phi_{r,\theta\theta} + B_{11}\frac{\zeta^2 r_o}{\zeta'}\phi_{r,r} - B_{22}\zeta r_o\phi_r + B_{16}\frac{\zeta^3 r_o}{\zeta'^2}\phi_{\theta,rr} \\
&+(B_{12}+B_{66})\frac{\zeta^2 r_o}{\zeta'\Theta}\phi_{\theta,r\theta} + B_{26}\frac{\zeta r_o}{\Theta^2}\phi_{\theta,\theta\theta} - B_{26}\frac{\zeta^2 r_o}{\zeta'}\phi_{\theta,r} \\
&-(B_{22}+B_{66})\frac{\zeta r_o}{\Theta}\phi_{\theta,\theta} - B_{26}\zeta r_o\phi_\theta + 0.5(A_{11}-A_{12})\zeta^2\left(\frac{w_{,r}}{\zeta'}\right)^2 \\
&+0.5(A_{12}-A_{22})\left(\frac{w_{,\theta}}{\Theta}\right)^2 + (A_{16}-A_{26})\zeta\left(\frac{w_{,r}}{\zeta'}\right)\left(\frac{w_{,\theta}}{\Theta}\right) \\
&+A_{11}\zeta^3\left(\frac{w_{,r}}{\zeta'}\right)\left(\frac{w_{,rr}}{\zeta'^2}\right) + A_{12}\left\{\zeta\left(\frac{w_{,\theta}}{\Theta}\right)\left(\frac{w_{,r\theta}}{\zeta'\Theta}\right) - \left(\frac{w_{,\theta}}{\Theta}\right)^2\right\} \\
&+A_{16}\zeta\left\{\zeta\left(\frac{w_{,\theta}}{\Theta}\right)\left(\frac{w_{,rr}}{\zeta'^2}\right) + \zeta\left(\frac{w_{,r}}{\zeta'}\right)\left(\frac{w_{,r\theta}}{\zeta'\Theta}\right) - \left(\frac{w_{,r}}{\zeta'}\right)\left(\frac{w_{,\theta}}{\Theta}\right)\right\}
\end{aligned}
$$

$$
\begin{aligned}
&+ A_{16}\zeta^2\left(\frac{w_{,r}}{\zeta'}\right)\left(\frac{w_{,r\theta}}{\zeta'\Theta}\right) + A_{26}\left(\frac{w_{,\theta}}{\Theta}\right)\left(\frac{w_{,\theta\theta}}{\Theta^2}\right)\\
&+ A_{66}\zeta\left\{\left(\frac{w_{,\theta}}{\Theta}\right)\left(\frac{w_{,r\theta}}{\zeta'\Theta}\right) + \left(\frac{w_{,r}}{\zeta'}\right)\left(\frac{w_{,\theta\theta}}{\Theta^2}\right)\right\}\\
&+ \zeta^2 r_o^2\left(N_r^T + N_r^P - N_\theta^T - N_\theta^P\right) = 0
\end{aligned} \tag{8.1}
$$

$$
\begin{aligned}
&A_{16}\frac{\zeta^3 r_o}{\zeta'^2}u_{,rr} + \left(A_{12}+A_{66}\right)\frac{\zeta^2 r_o}{\zeta'\Theta}u_{,r\theta} + A_{26}\frac{\zeta r_o}{\Theta^2}u_{,\theta\theta} + \left(2A_{16}+A_{26}\right)\frac{\zeta^2 r_o}{\zeta'}u_{,r}\\
&+ \left(A_{22}+A_{66}\right)\frac{\zeta r_o}{\Theta}u_{,\theta} - A_{26}\zeta r_o u + A_{66}\frac{\zeta^3 r_o}{\zeta'^2}v_{,rr} + 2A_{26}\frac{\zeta^2 r_o}{\zeta'\Theta}v_{,r\theta} + A_{22}\frac{\zeta r_o}{\Theta^2}v_{,\theta\theta}\\
&- A_{66}\frac{\zeta^2 r_o}{\zeta'}v_{,r} - A_{66}\zeta r_o v + B_{16}\frac{\zeta^3 r_o}{\zeta'^2}\phi_{r,rr} + \left(B_{12}+B_{66}\right)\frac{\zeta^2 r_o}{\zeta'\Theta}\phi_{r,r\theta} + B_{26}\frac{\zeta r_o}{\Theta^2}\phi_{r,\theta\theta}\\
&+ \left(2B_{16}+B_{26}\right)\frac{\zeta^2 r_o}{\zeta'}\phi_{r,r} + \left(B_{22}+B_{66}\right)\frac{\zeta r_o}{\Theta}\phi_{r,\theta} - B_{26}\zeta r_o\phi_r + B_{66}\frac{\zeta^3 r_o}{\zeta'^2}\phi_{\theta,rr}\\
&+ 2B_{26}\frac{\zeta^2 r_o}{\zeta'\Theta}\phi_{\theta,r\theta} + B_{22}\frac{\zeta r_o}{\Theta^2}\phi_{\theta,\theta\theta} - B_{66}\frac{\zeta^2 r_o}{\zeta'}\phi_{\theta,r} - B_{66}\zeta r_o\phi_\theta\\
&+ 2\left\{0.5A_{16}\zeta^2\left(\frac{w_{,r}}{\zeta'}\right)^2 + 0.5A_{26}\left(\frac{w_{,\theta}}{\Theta}\right)^2 + A_{66}\zeta\left(\frac{w_{,r}}{\zeta'}\right)\left(\frac{w_{,\theta}}{\Theta}\right)\right\}\\
&+ A_{16}\zeta^3\left(\frac{w_{,r}}{\zeta'}\right)\left(\frac{w_{,rr}}{\zeta'^2}\right) + A_{26}\left\{\zeta\left(\frac{w_{,\theta}}{\Theta}\right)\left(\frac{w_{,r\theta}}{\zeta'\Theta}\right) - \left(\frac{w_{,\theta}}{\Theta}\right)^2\right\}\\
&+ A_{66}\zeta\left\{\zeta\left(\frac{w_{,\theta}}{\Theta}\right)\left(\frac{w_{,rr}}{\zeta'^2}\right) + \zeta\left(\frac{w_{,r}}{\zeta'}\right)\left(\frac{w_{,r\theta}}{\zeta'\Theta}\right) - \left(\frac{w_{,r}}{\zeta'}\right)\left(\frac{w_{,\theta}}{\Theta}\right)\right\}\\
&+ A_{12}\zeta^2\left(\frac{w_{,r}}{\zeta'}\right)\left(\frac{w_{,r\theta}}{\zeta'\Theta}\right) + A_{22}\left(\frac{w_{,\theta}}{\Theta}\right)\left(\frac{w_{,\theta\theta}}{\Theta^2}\right)\\
&+ A_{26}\zeta\left\{\left(\frac{w_{,\theta}}{\Theta}\right)\left(\frac{w_{,r\theta}}{\zeta'\Theta}\right) + \left(\frac{w_{,r}}{\zeta'}\right)\left(\frac{w_{,\theta\theta}}{\Theta^2}\right)\right\} = 0
\end{aligned} \tag{8.2}
$$

$$
\begin{aligned}
&k^2 A_{55}\frac{\zeta^4 r_o^2}{\zeta'^2}w_{,rr} + 2k^2 A_{45}\zeta^3 r_o^2\frac{w_{,r\theta}}{\zeta'\Theta} + k^2 A_{44}\zeta^2 r_o^2\frac{w_{,\theta\theta}}{\Theta^2} + k^2 A_{55}\frac{\zeta^3 r_o^2}{\zeta'}w_{,r}\\
&+k^2 A_{55}\frac{\zeta^4 r_o^3}{\zeta'}\phi_{r,r} + k^2 A_{45}\frac{\zeta^3 r_o^3}{\Theta}\phi_{r,\theta} + k^2 A_{55}\zeta^3 r_o^3\phi_r\\
&+k^2 A_{45}\frac{\zeta^4 r_o^3}{\zeta'}\phi_{\theta,r} + k^2 A_{45}\frac{\zeta^3 r_o^3}{\Theta}\phi_{\theta,\theta} + k^2 A_{44}\zeta^3 r_o^3\phi_\theta + \zeta\left(\zeta\frac{w_{,rr}}{\zeta'^2} + \frac{w_{,r}}{\zeta'}\right)\\
&\times\left\{\zeta^2 r_o^2(N_r^T + N_r^P) + 0.5A_{11}\zeta^2\left(\frac{w_{,r}}{\zeta'}\right)^2 + 0.5A_{12}\left(\frac{w_{,\theta}}{\Theta}\right)^2\right.\\
&\left.+A_{16}\zeta\left(\frac{w_{,r}}{\zeta'}\right)\left(\frac{w_{,\theta}}{\Theta}\right)\right\} + \frac{w_{,\theta\theta}}{\Theta^2}\left\{\zeta^2 r_o^2(N_\theta^T + N_\theta^P) + 0.5A_{12}\zeta^2\left(\frac{w_{,r}}{\zeta'}\right)^2\right.\\
&\left.+0.5A_{22}\left(\frac{w_{,\theta}}{\Theta}\right)^2 + A_{26}\zeta\left(\frac{w_{,r}}{\zeta'}\right)\left(\frac{w_{,\theta}}{\Theta}\right)\right\} + \left(2\zeta\frac{w_{,r\theta}}{\zeta'\Theta} - \frac{w_{,\theta}}{\Theta}\right)
\end{aligned}
$$

$$\times \left\{ 0.5A_{16}\zeta^2 \left(\frac{w_{,r}}{\zeta'}\right)^2 + 0.5A_{26}\left(\frac{w_{,\theta}}{\Theta}\right)^2 + A_{66}\zeta\left(\frac{w_{,r}}{\zeta'}\right)\left(\frac{w_{,\theta}}{\Theta}\right)\right\}$$
$$+ \zeta^4 r_o^4 q = 0 \tag{8.3}$$

$$\begin{aligned}
&B_{11}\frac{\zeta^3 r_o}{\zeta'^2}u_{,rr} + 2B_{16}\frac{\zeta^2 r_o}{\zeta'\Theta}u_{,r\theta} + B_{66}\frac{\zeta r_o}{\Theta^2}u_{,\theta\theta} + B_{11}\frac{\zeta^2 r_o}{\zeta'}u_{,r} - B_{22}\zeta r_o u \\
&+B_{16}\frac{\zeta^3 r_o}{\zeta'^2}v_{,rr} + (B_{12}+B_{66})\frac{\zeta^2 r_o}{\zeta'\Theta}v_{,r\theta} + B_{26}\frac{\zeta r_o}{\Theta^2}v_{,\theta\theta} - B_{26}\frac{\zeta^2 r_o}{\zeta'}v_{,r} \\
&-(B_{22}+B_{66})\frac{\zeta r_o}{\Theta}v_{,\theta} - B_{26}\zeta r_o v - k^2 A_{55}\frac{\zeta^3 r_o^2}{\zeta'}w_{,r} - k^2 A_{45}\frac{\zeta^2 r_o^2}{\Theta}w_{,\theta} \\
&+D_{11}\frac{\zeta^3 r_o}{\zeta'^2}\phi_{r,rr} + 2D_{16}\frac{\zeta^2 r_o}{\zeta'\Theta}\phi_{r,r\theta} + D_{66}\frac{\zeta r_o}{\Theta^2}\phi_{r,\theta\theta} + D_{11}\frac{\zeta^2 r_o}{\zeta'}\phi_{r,r} - D_{22}\zeta r_o\phi_r \\
&-k^2 A_{55}\zeta^3 r_o^3\phi_r + D_{16}\frac{\zeta^3 r_o}{\zeta'^2}\phi_{\theta,rr} + (D_{12}+D_{66})\frac{\zeta^2 r_o}{\zeta'\Theta}\phi_{\theta,r\theta} \\
&+D_{26}\frac{\zeta r_o}{\Theta^2}\phi_{\theta,\theta\theta} - D_{26}\frac{\zeta^2 r_o}{\zeta'}\phi_{\theta,r} - (D_{22}+D_{66})\frac{\zeta r_o}{\Theta}\phi_{\theta,\theta} - D_{26}\zeta r_o\phi_\theta \\
&-k^2 A_{45}\zeta^3 r_o^3\phi_\theta + 0.5(B_{11}-B_{12})\zeta^2\left(\frac{w_{,r}}{\zeta'}\right)^2 \\
&+0.5(B_{12}-B_{22})\left(\frac{w_{,\theta}}{\Theta}\right)^2 + (B_{16}-B_{26})\zeta\left(\frac{w_{,r}}{\zeta'}\right)\left(\frac{w_{,\theta}}{\Theta}\right) \\
&+B_{11}\zeta^3\left(\frac{w_{,r}}{\zeta'}\right)\left(\frac{w_{,rr}}{\zeta'^2}\right) + B_{12}\left\{\zeta\left(\frac{w_{,\theta}}{\Theta}\right)\left(\frac{w_{,r\theta}}{\zeta'\Theta}\right) - \left(\frac{w_{,\theta}}{\Theta}\right)^2\right\} \\
&+B_{16}\zeta\left\{\zeta\left(\frac{w_{,\theta}}{\Theta}\right)\left(\frac{w_{,rr}}{\zeta'^2}\right) + \zeta\left(\frac{w_{,r}}{\zeta'}\right)\left(\frac{w_{,r\theta}}{\zeta'\Theta}\right) - \left(\frac{w_{,r}}{\zeta'}\right)\left(\frac{w_{,\theta}}{\Theta}\right)\right\} \\
&+B_{16}\zeta^2\left(\frac{w_{,r}}{\zeta'}\right)\left(\frac{w_{,r\theta}}{\zeta'\Theta}\right) + B_{26}\left(\frac{w_{,\theta}}{\Theta}\right)\left(\frac{w_{,\theta\theta}}{\Theta^2}\right) \\
&+B_{66}\zeta\left\{\left(\frac{w_{,\theta}}{\Theta}\right)\left(\frac{w_{,r\theta}}{\zeta'\Theta}\right) + \left(\frac{w_{,r}}{\zeta'}\right)\left(\frac{w_{,\theta\theta}}{\Theta^2}\right)\right\} \\
&+\zeta^2 r_o^2\left(M_r^T + M_r^P - M_\theta^T - M_\theta^P\right) = 0
\end{aligned} \tag{8.4}$$

$$\begin{aligned}
&B_{16}\frac{\zeta^3 r_o}{\zeta'^2}u_{,rr} + (B_{12}+B_{66})\frac{\zeta^2 r_o}{\zeta'\Theta}u_{,r\theta} + B_{26}\frac{\zeta r_o}{\Theta^2}u_{,\theta\theta} + (2B_{16}+B_{26})\frac{\zeta^2 r_o}{\zeta'}u_{,r} \\
&+(B_{22}+B_{66})\frac{\zeta r_o}{\Theta}u_{,\theta} - B_{26}\zeta r_o u + b_{66}\frac{\zeta^3 r_o}{\zeta'^2}v_{,rr} + 2B_{26}\frac{\zeta^2 r_o}{\zeta'\Theta}v_{,r\theta} + B_{22}\frac{\zeta r_o}{\Theta^2}v_{,\theta\theta} \\
&-B_{66}\frac{\zeta^2 r_o}{\zeta'}v_{,r} - B_{66}\zeta r_o v - k^2 A_{45}\frac{\zeta^3 r_o^2}{\zeta'}w_{,r} - k^2 A_{55}\frac{\zeta^2 r_o^2}{\Theta}w_{,\theta} + D_{16}\frac{\zeta^3 r_o}{\zeta'^2}\phi_{r,rr} \\
&+(D_{12}+D_{66})\frac{\zeta^2 r_o}{\zeta'\Theta}\phi_{r,r\theta} + D_{26}\frac{\zeta r_o}{\Theta^2}\phi_{r,\theta\theta} + (2D_{16}+D_{26})\frac{\zeta^2 r_o}{\zeta'}\phi_{r,r} \\
&+(D_{22}+D_{66})\frac{\zeta r_o}{\Theta}\phi_{r,\theta} - D_{26}\zeta r_o\phi_r - k^2 A_{45}\zeta^3 r_o^3\phi_r + D_{66}\frac{\zeta^3 r_o}{\zeta'^2}\phi_{\theta,rr}
\end{aligned}$$

$$
\begin{aligned}
&+ 2D_{26}\frac{\zeta^2 r_o}{\zeta'\Theta}\phi_{\theta,r\theta} + D_{22}\frac{\zeta r_o}{\Theta^2}\phi_{\theta,\theta\theta} - D_{66}\frac{\zeta^2 r_o}{\zeta'}\phi_{\theta,r} - D_{66}\zeta r_o\phi_\theta - k^2 A_{44}\zeta^3 r_o^3\phi_\theta \\
&+ 2\left\{B_{16}\zeta^2\left(\frac{w_{,r}}{\zeta'}\right)^2 + B_{26}\left(\frac{w_{,\theta}}{\Theta}\right)^2 + B_{66}\zeta\left(\frac{w_{,r}}{\zeta'}\right)\left(\frac{w_{,\theta}}{\Theta}\right)\right\} \\
&+ B_{16}\zeta^3\left(\frac{w_{,r}}{\zeta'}\right)\left(\frac{w_{,rr}}{\zeta'^2}\right) + B_{26}\left\{\zeta\left(\frac{w_{,\theta}}{\Theta}\right)\left(\frac{w_{,r\theta}}{\zeta'\Theta}\right) - \left(\frac{w_{,\theta}}{\Theta}\right)^2\right\} \\
&+ B_{66}\zeta\left\{\zeta\left(\frac{w_{,\theta}}{\Theta}\right)\left(\frac{w_{,rr}}{\zeta'^2}\right) + \zeta\left(\frac{w_{,r}}{\zeta'}\right)\left(\frac{w_{,r\theta}}{\zeta'\Theta}\right) - \left(\frac{w_{,r}}{\zeta'}\right)\left(\frac{w_{,\theta}}{\Theta}\right)\right\} \\
&+ B_{12}\zeta^2\left(\frac{w_{,r}}{\zeta'}\right)\left(\frac{w_{,r\theta}}{\zeta'\Theta}\right) + B_{22}\left(\frac{w_{,\theta}}{\Theta}\right)\left(\frac{w_{,\theta\theta}}{\Theta^2}\right) \\
&+ B_{26}\zeta\left\{\left(\frac{w_{,\theta}}{\Theta}\right)\left(\frac{w_{,r\theta}}{\zeta'\Theta}\right) + \left(\frac{w_{,r}}{\zeta'}\right)\left(\frac{w_{,\theta\theta}}{\Theta^2}\right)\right\} = 0
\end{aligned}
\tag{8.5}
$$

An iterative incremental approach based on Newton-Raphson technique is used for the solution of the resulting non-linear algebraic equations. All the three loads - transverse pressure q, potential gradients $E_z^{(k)}$ and the temperature gradients $T_k(z)$ can be applied simultaneously.

8.3 Results and Discussions

Moderately thick laminated sector plates made up of cylindrically orthotropic layers and piezoelectric layers undergoing moderately large deflections are analyzed. The plates are subjected to uniformly distributed lateral mechanical load Q, thermal load caused by prescribed uniform surface temperatures (T_0 and T_n), and, electrical load in the form of uniform electrical fields $E_z^{(k)}$'s applied across the piezoelectric layers. The effects of electrical and thermal fields on the non-linear mechanical response, and, the effects of boundary conditions and geometrical parameters on piezothermomechanical response are studied.

The laminated plates are assumed to be made up of G1195N piezoelectric layers and graphite/epoxy layers with the fiber orientation being either radial (R) or

circumferential (C). The required non-zero material properties are as follows unless otherwise specified.

For graphite/Epoxy layers (with radial fiber orientation) (Kapuria et al., 1997): $E_r = 181$ GPa, $E_\theta = E_0 = 10.3$ GPa, $\nu_{r\theta} = 0.28$, $G_{r\theta} = G_{rz} = 7.17$ GPa, $G_{\theta z} = 2.87$ GPa, $\alpha_r = 0.02 \times 10^{-6}\,/^o$C, $\alpha_\theta = 22.5 \times 10^{-6}\,/^o$C, $\kappa = 0.96$ W/m-^{o}C. For G1195N layers (Yang et al., 2004): $E_r = E_\theta = 63$ GPa, $\nu_{r\theta}$=0.3, $\alpha_r = \alpha_\theta = 120 \times 10^{-6}\,/^o$C, $\kappa = 5$ W/m-^{o}C, $d_{31} = d_{32} = 254 \times 10^{-12}$ m/V.

A plate made up of four layers of cross-ply antisymmetric plate denoted in rectangular domain by $(0^o/90^o)_2$ and a piezoelectric layer bonded on either surface is represented here by $(P(RC)_2P)$ or $(PRCRCP)$, where, R and C represent radial and circumferential orientations of the fibers in orthotropic layers. Unless otherwise stated, the lamination scheme used in the present study is $PRCP$.

The values of various parameters (unless otherwise specified) are: $n = 4$, $h = 0.015$ m, $T_0 = 50$ K, $T_n = 0$ K, $-E_z^{(1)} = E_z^{(n)} = E_z = 2 \times 10^6$ V/m, $r_i = 0.003$ m, $r_o = 0.003$ m, $\Theta = \pi/3$, $M = 13$, $N = 9$ and $(r = 0.65,\ \theta = 0.5)$. Convergence study depicted in Table 8.1 reveals that $(M = 13)$ and $(N = 9)$ yield quite accurate results. Results for thermal and piezoelectric loadings are in excellent agreement with small deflection results of Kapuria et al. (1997) and Jonnalagadda et al. (1994) (refer Table 8.2).

Effect of electric potential on the response in terms of non-dimensional displacement w' and moment resultant M_r' at $(r = 0.65,\ \theta = 0.5)$ of piezolaminated sector plates $(PRCP)$ with $SSSS$ edge conditions is shown in Figs. 8.1 and 8.2 respectively for $(\lambda = 0.1,\ 0.05)$. It can be seen that the effect is more pronounced for thin plates. The effect on w' decreases with load whereas on M_r', the effect increases with

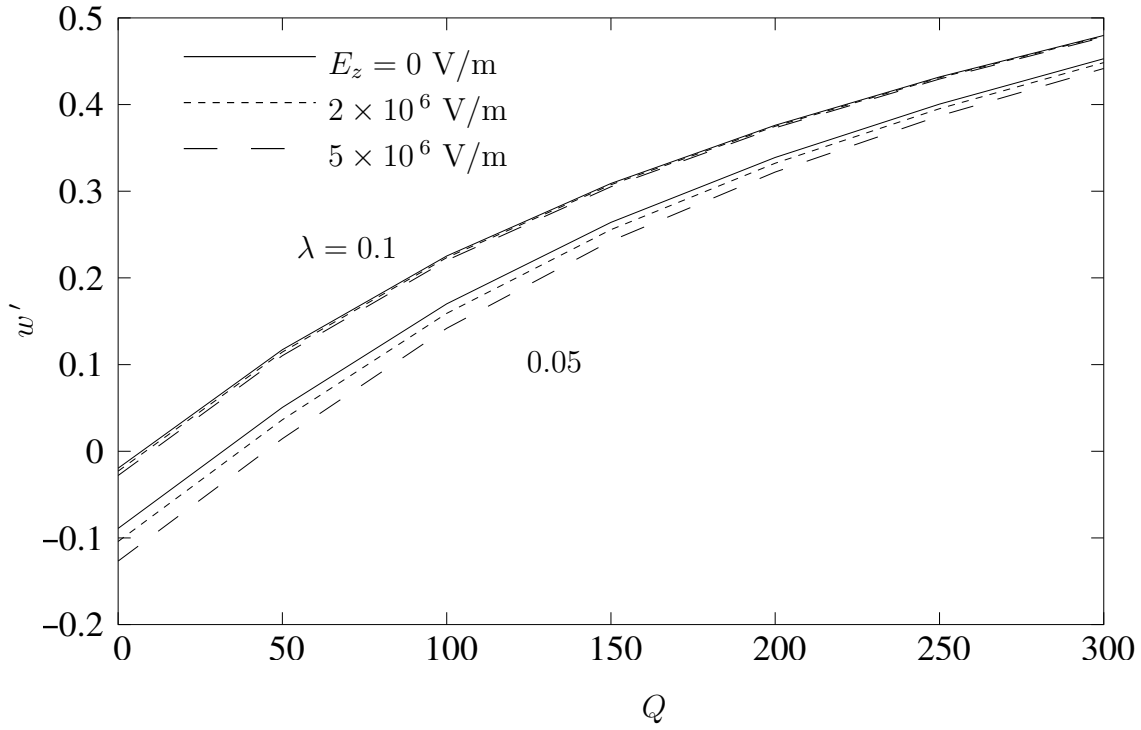

Fig. 8.1 Effect of electrical actuation potential and plate thickness on deflection w'.

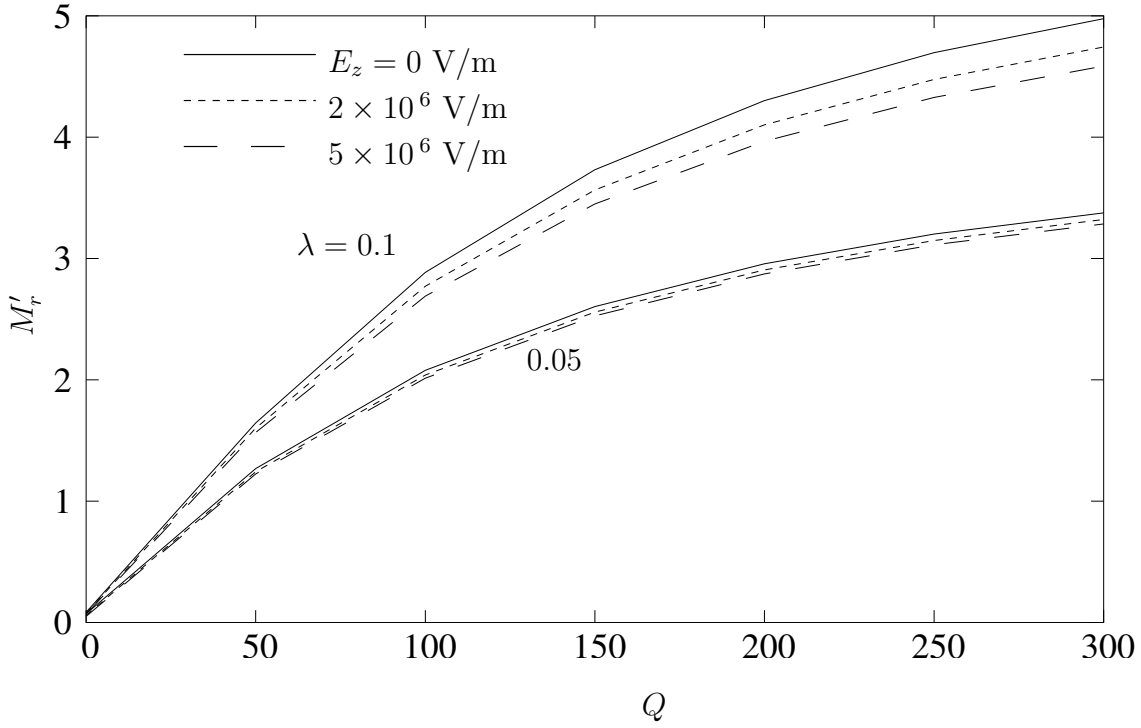

Fig. 8.2 Effect of electrical actuation potential and plate thickness on moment M_r'.

Table 8.1 Convergence of results in terms of M and N with $Q = 100$ and $E_z = 5 \times 10^6$ V/m.

Boundary Condition	$M \times N$	w'	M_r'
$SSSS$	9×5	0.151524	2.83076
	11×7	0.142185	2.87811
	13×9	0.141797	2.88523
	15×11	0.141616	2.89658
$SSFS$	9×5	0.325521	0.375182
	11×7	0.318096	0.485748
	13×9	0.31793	0.485843
	15×11	0.317937	0.491712
$CFSF$	9×5	0.68655	-2.07349
	11×7	0.796403	1.68224
	13×9	0.814417	2.38229
	15×11	0.816517	3.19614
	17×13	0.814313	3.82457

load. As mentioned earlier, these plots suggest the application of this study in a micro-positioning application where mechanical actuation is used for causing most of the displacement, and, electrical actuation is used for finer positioning. Figures 8.3 and 8.4 and show the effect of boundary conditions on the actuation capabilities of piezoelectric layers. The effect of electrical potential is very small on the deflection for all the boundary conditions. The effect of electrical potential is more on M_r' than on w'. It may further be noted that the electrical actuation is lesser for more constrained boundary conditions. This effect is not clearly noticeable in the these plots in which electrical actuation is forming a very small part of the total electro-mechanical actuation.

Effects of temperature rise on the deflection and moment stress resultant is depicted in Figs. 8.5 and 8.6 for plates having $CCSS$ edge conditions. It can be seen from the results that the effect of temperature on w' decreases with load whereas on

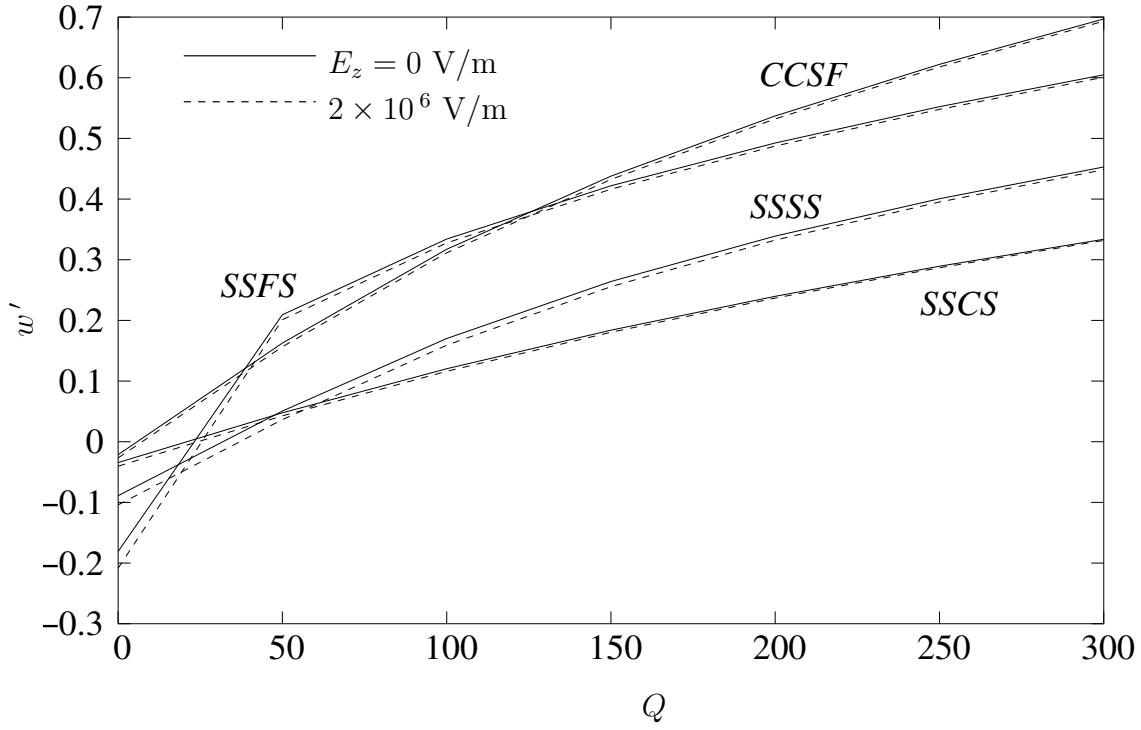

Fig. 8.3 Effect of boundary conditions on deflection w'.

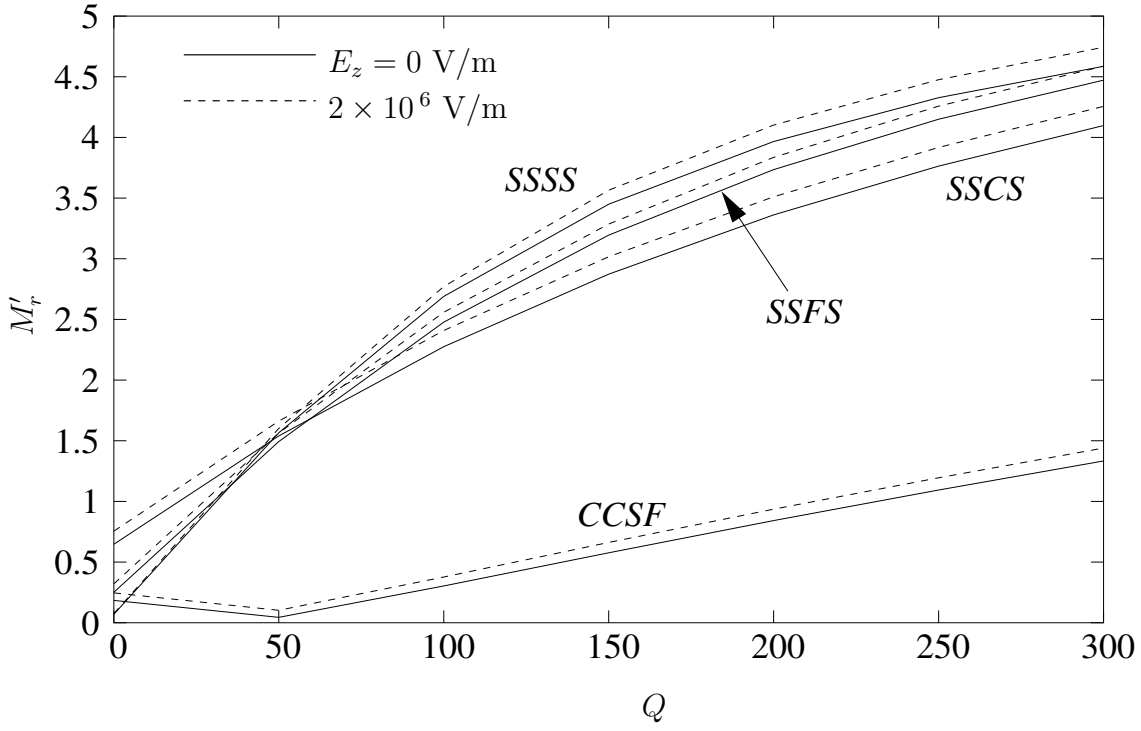

Fig. 8.4 Effect of boundary conditions on moment M_r'.

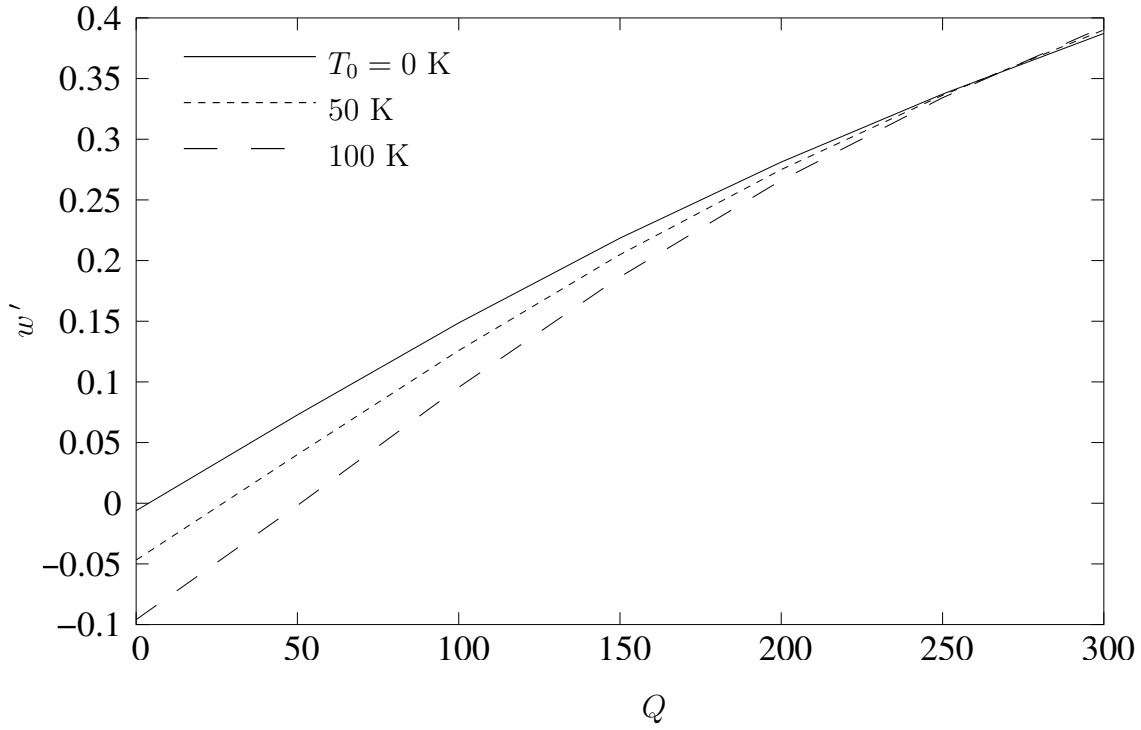

Fig. 8.5 Effect of electrical actuation potential and plate thickness on deflection w'.

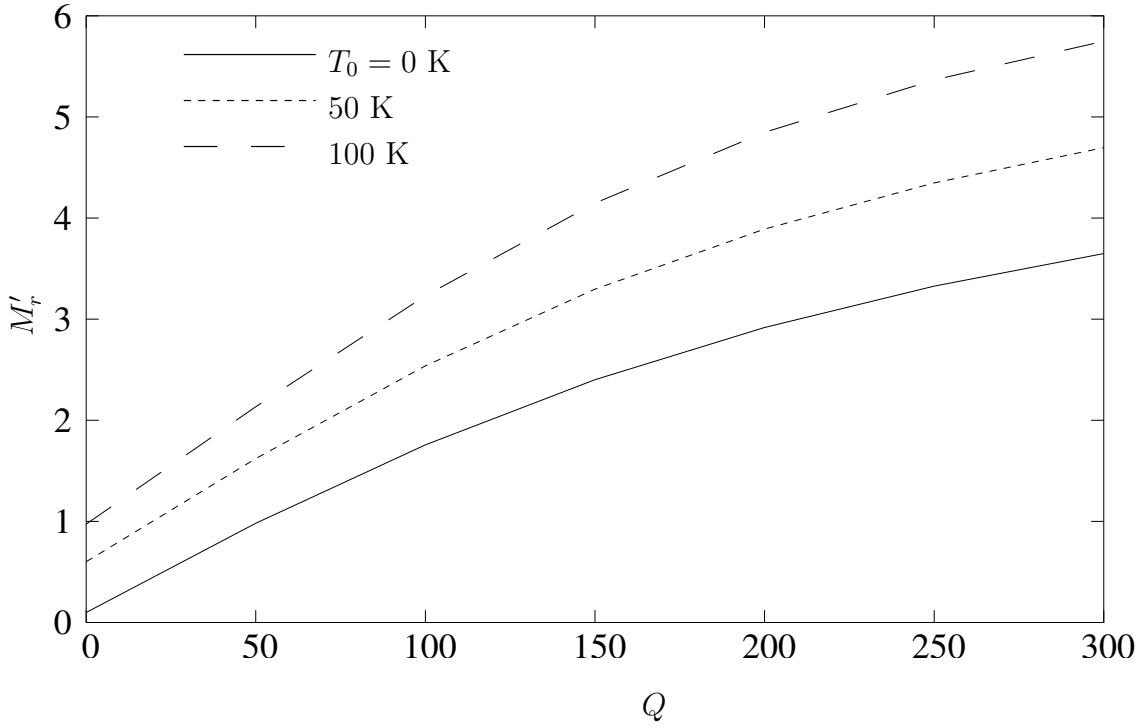

Fig. 8.6 Effect of electrical actuation potential and plate thickness on moment M_r'.

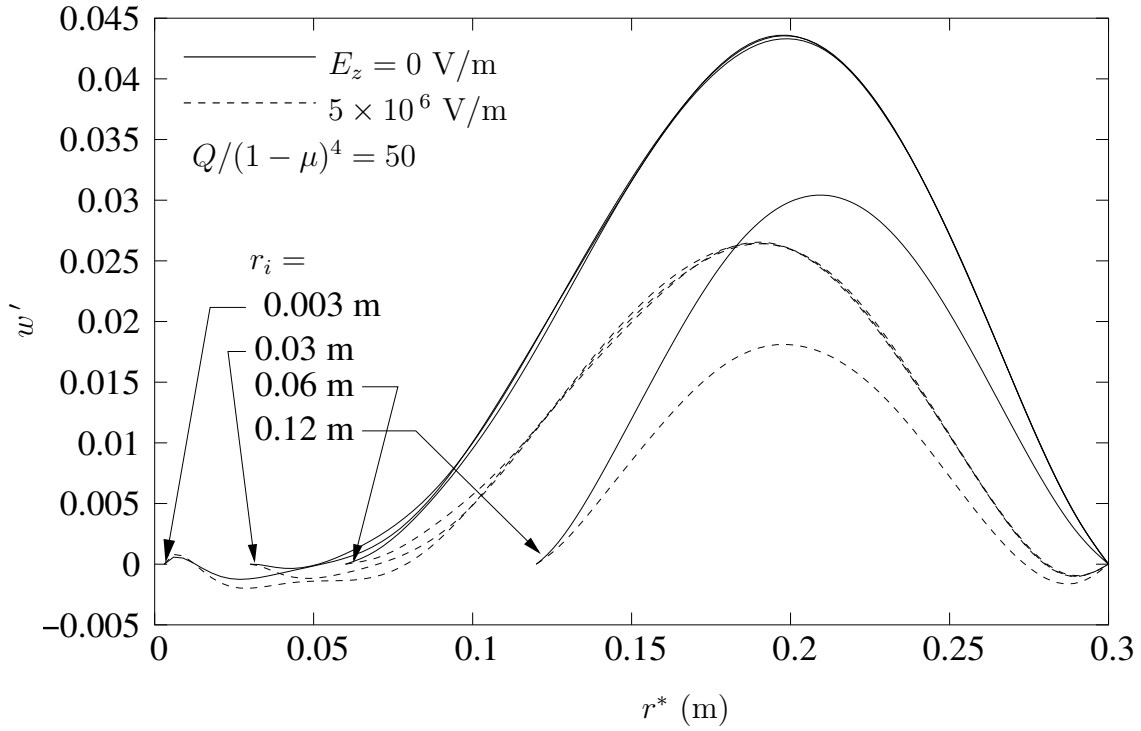

Fig. 8.7 Effect of annularity on electro-mechanical response.

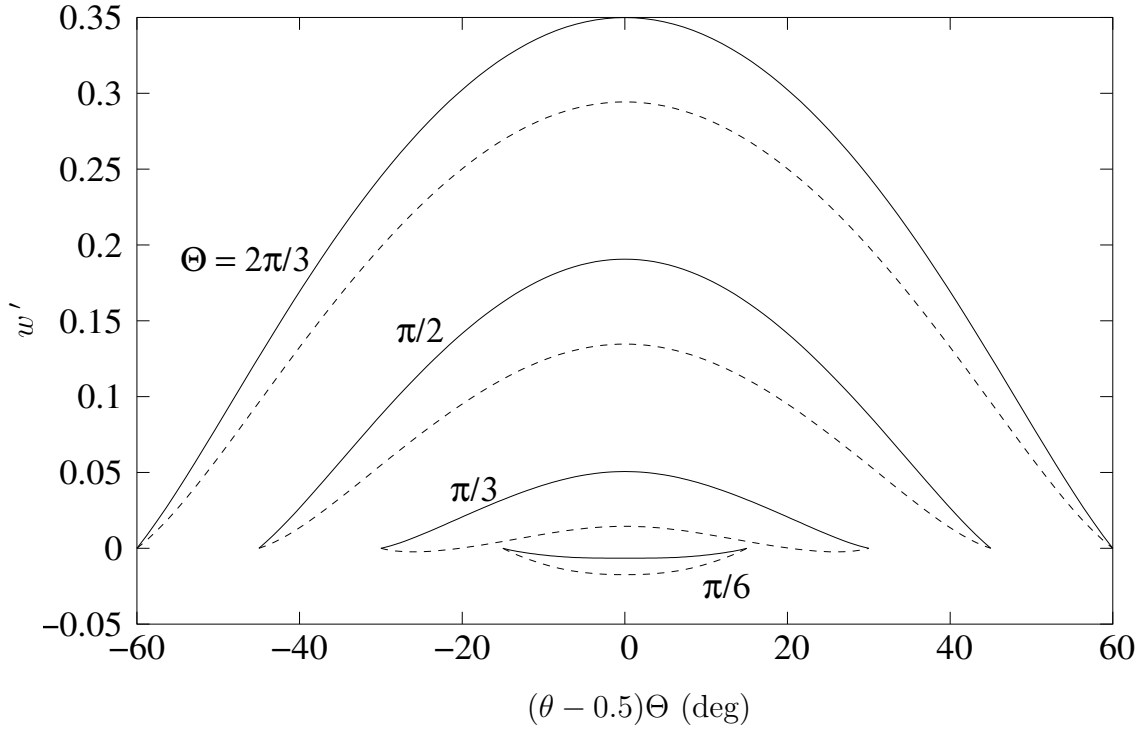

Fig. 8.8 Effect of total included angle Θ on electro-mechanical response with $Q = 50$. ——— : $E_z = 0$ V/m, - - - - - : $E_z = 5 \times 10^6$ V/m.

Table 8.2 Comparison of small deflection results of piezolaminated $((RCRC)_2P)$ almost square plate results with Kapuria et al. (1997) and Jonnalagadda et al. (1994) under thermal and electrical loads. ($q = 0$, $E_z = 0$ V/m, $T_0 = 50\,^oC$), and, under electrical load ($q = 0$, $E_z = 30 \times 10^6$ V/m, $T_0 = 0\,^oC$) . The orthotropic layers are of graphite/epoxy and the piezoelectric layer is of PVDF. For PVDF layer $E_r = E_\theta = 2.0$ GPa, $\nu_{r\theta} = 0.33$, $G_{r\theta} = G_{rz} = G_{\theta z} = 0.752$ GPa, $r_o = 10^6$ m, $r_i = (10^5 - 0.3)$ m, $\Theta = 0.3 \times 10^{-6}$ rad, $\alpha_r = \alpha_\theta = 120 \times 10^{-6}\,/^oC$, $d_{31} = d_{32} = 23 \times 10^{-12}$ m/V, $d_{33} = 33 \times 10^{-12}$ m/V and $T_1 = 0\ ^oC$. Thermal conductivity of PVDF in transverse direction was taken to be same as that for the orthotropic layers (Kapuria et al., 1997). Graphite/epoxy layers are all of equal thickness and PVDF layer is of double thickness.

			$\frac{-1000wh}{(r_0 - r_i)^2\alpha_e T_0}$ for thermal load, or, $\frac{100wh}{(r_0 - r_i)^2 d_{33} E_z}$ for electrical load		
Edge Conditions	Load	side to thickness ratio	Present	Present	(a)	(b)
$S'S'S'S'$	Thermal	4	0.9417	0.9400	0.9395
		10	0.8824	0.8802	0.8797
	Electrical	4	0.6370	0.6360	0.6357
		10	0.6215	0.6205	0.6202
$S'CS'C$	Thermal	4	0.1788	0.1784	0.1784
		10	0.1400	0.1392	0.1393
	Electrical	4	0.2103	0.2099	0.2099
		10	0.1633	0.1628	0.1628

(a) Kapuria et al. (1997) (b) Jonnalagadda et al. (1994)

M_r', the effect increases with load.

Finally, Figures 8.7 and 8.8 show the effects of annularity μ and the total included angle Θ on electro-mechanical actuation of plates having $CSSC$ and $CSSS$ edge conditions respectively. In Fig. 8.7 the mechanical load is specified as $Q/(1-\mu)^4 = 50$ in order to make it independent of μ. It can be seen that the fraction of electrical actuation is almost unaffected by μ whereas it increases with Θ.

8.4 Conclusions

The piezolaminated sector plates undergoing moderately large deflections are analyzed. The methodology based on two-dimensional Chebyshev polynomial approximation was found to be quite efficient. The fundamental advantage of this methodology was found in modeling a wide variety of boundary conditions including clamped, simply supported and free edges. Chebyshev polynomials of degree ($M = 13$) in r-dimension and of degree ($N = 9$) in θ-dimension were found to satisfactory results for all situations. It is found that the effectiveness of piezoelectric actuation depends upon boundary conditions. Electrical actuation is more effective for larger spans.

CHAPTER 9
CONCLUSIONS AND SUGGESTIONS FOR FUTURE WORK

9.1 Conclusions

The fast converging Chebyshev polynomials have been employed for the analysis of moderately thick Mindlin sector plates. Using the first order shear deformation theory, the problems solved in this thesis are:

1. Buckling and free vibration response of isotropic sector plates.

2. Buckling and free vibration analysis of laminated composite sector plates.

3. Non-linear static response of isotropic sector plates taking into account the von-Kármán type geometric non-linearities.

4. Non-linear static response of laminated composite sector plates.

5. Non-linear dynamic response of moderately thick laminated composite sector plates.

6. Non-linear static response of piezolaminated composite sector plates with von-Kármán type geometric non-linearities. In addition to uniform transverse pressure, the plates are also subjected to thermal loading with prescribed uniform in-plane surface temperatures and electrical loadings with electrical potential applied across the thickness direction of piezoelectric layers.

In all the the above studies, following observations can be made:

i. **Boundary Conditions:** The boundary conditions were applied using a method of interpolation between corners. This resulted in a square left hand side matrix in contrast to redundancy produced in the formulations of earlier researchers. This facilitates application of arbitrary combinations of clamped and simply supported edge conditions. The edge conditions having two opposite edges free and the other two having arbitrary combinations of clamped and simply supported edges were also successfully analyzed.

ii. **Convergence:** Detailed convergence study with respect to the number of terms in the series expansions is carried out for each problem. Following observations can be made:

   - In general, 14 terms for radial dimension and 10 terms for circumferential direction for each field variable were found to generate satisfactory results for the non-linear formulations.
   - For the linear eigenvalue problems expansion of size (10×8) yielded the converged results.
   - Problems involving free edge conditions needed (16×12) expansions for the non-linear cases, and, (14×10) expansions for the linear eigenvalue models.
   - The square plate results generated for the purpose of comparison with literature were converged at size (9×9).

iii. **Comparison:** The obtained results were validated by comparison with the results available in the literature. Due to unavailability of results, the results of laminated composite sector plates were compared with the available square plates results. Reasonably good agreements were achieved among the results.

iv. **Parametric studies:** The effects of material properties, sector angle, annularity, thickness ratio and boundary conditions were studied. The exact effects could seen from tabular and graphical results. In general, displacements, static or dynamic, were lower for stiffer systems in terms of boundary conditions, orthotropy and lamination schemes. With increasing non-homogeneity in terms of number of layers as well as orthotropy, the free vibration frequencies and the critical buckling loads were found to be increasing.

    The most significant contribution of these parametric studies could be appreciated in the field of mechatronic devices where accurate motion control could lead to better design of micropositioning devices.

Chebyshev polynomials used for spatial discretization are found to be capable of modeling complicated field variable problems. Their property of being most efficient approximators of zero automatically minimizes the error in transforming the differential equations in to algebraic equations.

9.2 Future scope

The present study concludes that following efforts could be made for better understanding of the problems of laminated composite plates and for better modeling and analysis of similar problems:

- Non-axisymmetric problems of circular plates can be solved.
- Chebyshev polynomials can be used to construct more economical and efficient finite element codes.
- A simple and unified approach for modeling of problems in rectangular and cylindrical domains could be done.
- The developed methodologies could lead to economical design and simulation tools for micropositioning mechatronic devices.
- Arbitrarily increasing the number of layers, the methods developed for laminated plates can be used for analysis of functionally graded materials, the grading being in thickness direction.
- The robustness of the methodology could be utilized to analyze materially non-linear behavior.

REFERENCES

Argyris, N. and Tenek, L. (1997). Recent advances in computational thermostructural analysis of composite plates and shells with strong nonlinearities. *Applied Mechanics Review*, 50(5):285–307.

Auricchio, F. and Sacco, E. (1999). A mixed enhanced finite element for the analysis of laminated composite plates. *International Journal for Numerical Methods in Engineering*, 44:1481–1504.

Ben-Amoz, M. (1959). Note on deflections and flexural vibrations of clamped sectorial plates. *Journal of Applied Mechanics*, 26(1):136–137.

Benjeddou, A. (2000). Advances in piezoelectric finite element modeling of adaptive structural elements: a survey. *Computers and Structures*, 76(1–3):347–363.

Benson, P. R. and Hinton, E. (1976). A thick finite strip solution for static, free vibration and stability problems. *International Journal for Numerical Methods in Engineering*, 10(3):665–678.

Bisegna, P., Caruso, G., and Maceri, F. (2001). A layer-wise Reissner-Mindlin-type model for the vibration analysis and suppression of piezoactuated plates. *Computers and Structures*, 79(26–28):2309–2319.

Cheung, M. S. and Chan, M. Y. T. C. (1981). Static and dynamic analysis of

thin and thick sectorial plates by the finite strip method. *Computers and Structures*, 14(1):79–88.

Chia, C. Y. (1988). Geometrically non-linear behavior of composite plates. *Applied Mechanics Review and ASME*, 41(12):439–451.

Clenshaw, C. W. and Norton, H. J. (1963). The solution of nonlinear ordinary differential equations in Chebyshev series. *The Computer Journal*, 6(1):88–92.

Evans, D. J. and Murphy, C. P. (1981). The solution of the biharmonic equation in a rectangular region by chebyshev series. *Computer Methods in Applied Mechanics and Engineering*, 27(1):81–99.

Fox, L. and Parker, I. B. (1968). *Chebyshev Polynomials in Numerical Analysis*. Oxford University Press London.

Guruswamy, P. and Yang, T. Y. (1979). A sector finite element for dynamic analysis of thick plates. *Journal of Sound and Vibration*, 62(4):505–516.

Harik, I. E. (1985). Stability of annular sector plates with clamped radial edges. *Journal of Applied Mechanics*, 52:971–972.

Houbolt, J. C. (1950). A recurrence matrix solution for the dynamic response of elastic aircraft and. *Journal of Aeronautical Sciences*, 17:540–550.

Huang, X.-L. and Zheng, J.-J. (2003). Nonlinear vibration and dynamic response of simply supported shear deformable laminated plates on elastic foundations. *Engineering Structures*, 25(8):1107–1119.

Irie, T., Yamada, G., and Ito, F. (1979). Free vibration of polar–orthotropic sector plates. *Journal of Sound and Vibration*, 67(1):89–100.

Jain, R. K. (1985). *Some studies on nonlinear axisymmetric deformation of cylindrically orthotropic circular plates and shallow spherical shells on elastic foundations*. PhD thesis, I. I. T. Delhi.

Jonnalagadda, D., K., Blandford, E., G., Tauchert, and R., T. (1994). Piezothermoelastic composite plate analysis using first-order shear deformation theory. *Computers and Structures*, 51(1):79–89.

Kadiri, M. E., Benamar, R., and White, R. G. (1999). The nonlinear free vibration of fully clamped rectangular plates: second order nonlinear model for various plate aspect ratio. *Journal of Sound and Vibration*, 228(2):333–358.

Kapania, R. K. and Raciti, S. (1989). Recent advanced in analysis of laminated beams and plates. *AIAA Journal*, 27(7):923–946.

Kapuria, S., Dube, G. P., Dumir, P. C., and Sengupta, S. (1997). Levy–type piezothermoelastic solution for hybrid plate by using first-order shear deformation theory. *Composites Part B: Engineering*, 28(5–6):535–546.

Khdeir, A. A. (1989). Free vibration and buckling of unsymmetric cross-ply laminated plates using a refined theory. *Journal of Sound and Vibration*, 128(3):377–395.

Khdeir, A. A. and Librescu, L. (1988). Analysis of symmetric cross-ply elastic

plates using a higher-order theory, Part II: Buckling and free vibration. *Composite Structures*, 9(4):259–277.

Kim, C. S. and Dickinson, S. M. (1989). On the free transverse vibration of annular and circular, thin, sectorial plates subject to certain complicating effects. *Journal of Sound and Vibration*, 134(3):407–421.

Kirby, R. M. and Yosibash, Z. (2004). Solution of von-Kármán dynamic non-linear plate equations using pseudo–spectral method. *Computer Methods in Applied Mechanics and Engineering*, 193(6–8):575–599.

Kumar, S. (1997). *Some studies on static and dynamic response of polar orthotropic, layered, moderately thick circular plates and shallow spherical shells*. PhD thesis, I. I. T. Delhi.

Librescu, L. and Marzocca, P. (2005). Advances in the linear/nonlinear control of aeroelastic structural systems. *Acta Mechanica*, 178(3–4):147–186.

Liew, K. M. and Lam, K. Y. (1993). On the use of 2-d orthogonal polynomials in the rayleigh-ritz method for flexural vibration of annular sector plates of arbitrary shape. *International Journal of Mechanical Sciences*, 35(2):129–139.

Liew, K. M. and Liu, F.-L. (2000). Differential quadrature method for vibration analysis of shear deformable annular sector plates. *Journal of Sound and Vibration*, 230(2):335–356.

Loja, M. A. R., Barbosa, J. I., Soares, C. M. M., and Soares, C. A. M. (2001).

Analysis of piezolaminated plates by the spline finite strip method. *Computers and Structures*, 79(26–28):2321–2333.

Mackerle, J. (2001). Smart materials and structures: Fem and bem simulations and a bibliography (1997–1999). *Finite Elements in Analysis and Design*, 37(1):71–83.

McGee, O. G., Huang, C. S., and Leissa, A. W. (1995). Comprehensive exact solutions for free vibrations of thick annular sectorial plates with simply supported radial edges. *International Journal of Mechanical Sciences*, 37(5):537–566.

Mindlin, R. D. (1951). Influence of rotary inertia and shear and shear in flexural motion of isotropic, elastic plates. *Journal of Applied Mechanics*, 18:31–38.

Nath, Y. (1977). *Some studies on nonlinear response and buckling of isotropic and orthotropic spherical shells*. PhD thesis, I. I. T. Madras.

Nath, Y. and Kumar, S. (1995). Chebyshev series solution of non-linear boundary value problem in rectangular domain. *Computer Methods in Applied Mechanics and Engineering*, 125(1–4):41–52.

Nath, Y. and Kumar, S. (1998). Effect of transverse shear on static and dynamic buckling of antisymmetric laminated polar orthotropic shallow spherical shells. *Composite Structures*, 40(1):67–72.

Nath, Y. and Kumar, S. (2000). Nonlinear dynamic response of axisymmetric

thick laminated shallow spherical shells. *International Journal of Nonlinear Mechanics and Numerical Simulation*, 1(3):225–223.

Nath, Y., Sharda, H. B., and Sharma, A. (2005). Non-linear analysis of moderately thick sector plates. *Communications in Nonlinear Science and Numerical Simulation*, 10(7):765–778.

Nath, Y. and Shukla, K. K. (2001a). Analytical solution for buckling and postbuckling of angle-ply laminated plates under thermomechanical loading. *International Journal of Non-Linear Mechanics*, 36(7):1097–1108.

Nath, Y. and Shukla, K. K. (2001b). Non–linear transient analysis of moderately thick laminated composite plates. *Journal of Sound and Vibration*, 247(3):509–526.

Noor, A. K. and Burton, W. S. (1989). Assessment of shear deformation theories for multilayered composite plates. *Applied Mechanics Review*, 42(1):1–13.

Noor, A. K. and Burton, W. S. (1992). Computational models for high temperature multilayered composite plates and shells. *Applied Mechanics Review*, 45(10):419–446.

Noor, A. K., Burton, W. S., and Bert, C. W. (1996). Computational models for sandwich panels and shells. *Applied Mechanics Review*, 49(3):155–199.

Oh, I. K., Han, J. H., and Lee, I. (2000). Postbuckling and vibration characteristics of piezolaminated composite plate subject to thermo-piezoelectric loads. *Journal of Sound and Vibration*, 233(1):19–40.

Oh, S.-Y., Librescu, L., and Song, O. (2003). Vibration of turbomachinery rotating blades made-up of functionally graded materials and operating in a high temperature field. *Act Mechanica*, 166(1–4):69–87.

Ozakca, M., Tay, N., and Kolcu, F. (2003a). Buckling analysis and shape optimization of elastic variable thickness circular and annular plates Part I: Finite element formulation. *Engineering Structures*, 25(2):181–192.

Ozakca, M., Tay, N., and Kolcu, F. (2003b). Buckling analysis and shape optimization of elastic variable thickness circular and annular plates Part II: Shape optimization. *Engineering Structures*, 25(2):193–199.

Park, S. and Kapania, R. K. (1998). Comparison of various orthogonal polynomials in hp-version time finite element method. *AIAA Journal*, 36(4):651–655.

Qatu, M. S. (2002). Recent research advances in the dynamic behavior of shells: 1989-2000, Part 1: Laminated composite shells. *Applied Mechanics Reviews*, 55(4):325–350.

Ramakrishnan, R. and Kunukkasseril, V. X. (1973). Free vibration of annular sector plates. *Journal of Sound and Vibration*, 30(1):127–129.

Rao, M. N. B., Guruswamy, P., and Kumaran, K. S. S. (1977). Finite element analysis of thick annular and sector plates. *Nuclear Engineering and Design*, 41(2):247–255.

Reddy, B. S. (1980). *Some studies on the nonlinear dynamics of annular plates and spherical shells*. PhD thesis, I. I. T. Madras.

Reddy, J. N. (1997). *Mechanics of Laminated Composite Plates*. CRC Press, New York.

Reddy, J. N. and Chandrashekhara, K. (1985). Geometrically nonlinear transient analysis of laminated doubly curved shells. *International Journal of Nonlinear Mechanics*, 20:79–80.

Reddy, J. N. and Robbins Jr. , D. H. (1994). Theories and computational models for composite laminates. *Applied Mechanics Review*, 47(6):147–169.

Reissner, E. (1945). The effect of transverse shear deformation on the bending of elastic plates. *Journal of Applied Mechanics*, 12:69–77.

Rivlin, T. J. (1974). *The Chebyshev Polynomials*. John Wiley & Sons, New York.

Rubin, C. (1978). Stability of polar orthotropic sector plates. *Journal of Applied Mechanics*, 45:448–450.

Salehi, M. and Shahidi, A. (1994). Large deflection analysis of elastic Mindlin sector plates. *Computers and Structures*, 52(5):987–998.

Salehi, M. and Sobhani, A. R. (2004). Elastic linear and non-linear analysis of fiber–reinforced symmetrically laminated sector Mindlin plate. *Composite Structures*, 65(1):65–79.

Sathyamoorthy, M. (1987). Nonlinear vibration analysis of plates: a review and survey of current developments. *Applied Mechanics Review*, 40:1553–1561.

Sekouri, E. M., Hu, Y.-R., and Ngo, A. D. (2004). Modeling of a circular plate with piezoelectric actuators. *Mechatronics*, 14(9):1007–1020.

Sharma, A., Sharda, H. B., and Nath, Y. (2005). Stability and vibration of thick laminated composite sector plates. *Journal of Sound and Vibration*, 287(1–2):1–23.

Shen, H.-S. (2004). Nonlinear bending analysis of unsymmetric cross-ply laminated plates with piezoelectric actuators in thermal environments. *Composite Structures*, 63(2):167–177.

Shi, Y., Lee, R. Y. Y., and Mei, C. (1997). Finite element method for non-linear free vibration of composite plates. *AIAA Journal*, 35(1):159–166.

Shukla, K. K. and Nath, Y. (2000). Nonlinear analysis of moderately thick laminated rectangular plates. *Journal of Engineering Mechanics*, 126(8):831–838.

Sinha, S. C. and Butcher, E. A. (1996). Solution and stability of a set of pth order linear differential equations with periodic coefficients via chebyshev polynomials. *Mathematical Problems in Engineering*, 2(2):165–190.

Srinivasan, R. S. and Thiruvenkatachari, V. (1985). Free vibration of transverse isotropic annular sector Mindlin plates. *Journal of Sound and Vibration*, 101(2):193–210.

Tanriover, H. and Senocak, E. (2004). Large deflection analysis of unsymmetri-

cally laminated composite plates analytical–numerical type approach. *International Journal of Non–Linear Mechanics*, 39(8):1385–1392.

Tauchert, T. R. (1991). Thermally induced flexure, buckling and vibration of plates. *Applied Mechanics Review*, 44(8–9):347–360.

Timoshenko, S. P. and Woinowsky-Krieger, S. (1970). *Theory of plates and shells*. McGraw Hill Book Co., Auckland.

Turvey, G. J. and Marshall, I. H. (1995). *Buckling and postbuckling of composite plates*. Chapman & Hall., London.

Turvey, G. J. and Salehi, M. (1990). Dr large deflection analysis of sector plates. *Computers and Structures*, 34(1):101–112.

Turvey, G. J. and Salehi, M. (1998). Large deflection analysis of eccentrically stiffened sector plates. *Computers and Structures*, 68(1–3):191–205.

Varadan, T. K. and Bhaskar, K. (1997). Review of different laminate theories for the analysis of composites. *Journal of the Aeronautical Society of India*, 49(4):202–208.

Vinson, J. R. (1999). *Behavior of Sandwich Structures of Isotropic and Composite Materials*. Technomic Publishing Company, Inc., Lancaster, Pennsylvania.

Vinson, J. R. (2001). Sandwich structures. *Applied Mechanics Reviews*, 54(3):201–214.

Wang, C. M. and Xiang, Y. (1999). Deducing buckling loads of sectorial Mindlin plates from kirchhoff plates. *Journal of Engineering Mechanics and ASCE*, 125(5):596–598.

Wang, C. M., Xiang, Y., Kitipornchai, S., and Liew, K. M. (1994). Buckling solutions of Mindlin plates of various shapes. *Engineering Structures*, 16(2):119–127.

Wang, J., Vinson, J. R., and Glancey, J. L. (2004). Geometrical nonlinear deformation effects in composite sandwich plates subjected to in-plane shear loads. *Journal of Sandwich Structures and Materials*, 6(5):167–194.

Wilkinson, J. H. and Reinsch, C. (1971). *Handbook for Automatic Computation*, volume II. Springer–Verlag, New York.

Woo, K. S., Hong, C. H., and Basu, P. K. (2003). Materially and geometrically nonlinear analysis of laminated anisotropic plates by p–version fem. *Computers and Structures*, 81(16):1653–1662.

Xiang, Y., Liew, K. M., and Kitipornchai, S. (1993). Transverse vibration of thick annular sector plates. *Proceedings of the American Society of Civil Engineers, Journal of Engineering Mechanics*, 119:1579–1599.

Xiang, Y. and Wei, G. W. (2002). Exact solution for vibration of multi-span rectangular Mindlin plates. *Journal of Vibration and Acoustics*, 124(4):545–551.

Yamada, G. and Irie, T. (1987). Plate vibration research in japan. *Applied Mechanical Review*, 40:879–892.

Yang, J., Kitipornchai, S., and Liew, K. M. (2004). Non-linear analysis of the thermo-electro-mechanical behavior of shear deformable fgm plates with piezoelectric actuators. *International Journal of Numerical Methods in Engineering*, 59(12):1605–1632.

Yonezawa, H. (1962). Moments and free vibrations in curved girder bridges. *Journal of Engineering Mechanics ASCE*, 88(1):1–21.

Yosibash, Z., Kirby, R. M., and Gottlieb, D. (2004). Collocation methods for the solution of von-Kármán dynamic non-linear plate systems. *Journal of Computational Physics*, 200(2):432–461.

HOUBOLT ACCELERATION COEFFICIENTS FOR SINUSOIDAL AND STEP FUNCTION LOADS

					β_5	
Time step	β_1	β_2	β_3	β_4	Sinusoidal load	Step load
$J = 1$	6	0	0	0	0	$-2Q\Delta\tau^2$
$J = 2$	2	-5	0	0	0	$-Q\Delta\tau^2$
$J = 3$	2	-5	4	0	0	0
$J > 3$	2	-5	4	-1	0	0

Brief bio-data of the author

Ashish Sharma, son of Shree Siya Ram Sharma, was born on 29^{th} June 1971 at Indore and his native place is Gwalior in the state of Madhya Pradesh in India. He completed his B.E. in Mechanical Engineering from Madhav Institute of Technology and Science, Gwalior in 1993 and M.E. in Machine Design from the Government Engineering College, Jabalpur in 1996. He taught for a semester in the MITS, Gwalior in the year 1996-'97. Thereafter, he joined the Thapar Institute of Engineering and Technology (Deemed University), Patiala in March 1997 and is working there as Lecturer in the Mechanical Engineering Department. He has taught various subjects like Mechanics of Deformable Bodies, Mechanical Vibrations, Industrial Automation, Mechatronics and Robotics. He has guided ten number of M.E. theses.